Agrociencia

eISSN: 2521-9766

VOLUME 58, NUMBER 3 | APRIL 1 - MAY 15, 2024 | MEXICO

AGRICULTURA
SECRETARÍA DE AGRICULTURA

COPYRIGHT AND RELATED RIGHTS, **Volume 58, Number 3, April 1 - May 15, 2024**, Agrociencia is a semi-monthly publication edited by Colegio de Postgraduados. Carretera Mexico-Texcoco, Km 36.5, Montecillo, Texcoco, State of Mexico. CP 56264. Phone: 5959284427. www.colpos.mx. Editor in chief: Dr. Fernando Carlos Gómez Merino. Reservations of Rights to Exclusive Use 04-2021-031913431800-203. eISSN: 2521-9766, granted by the National Copyright Institute. Last modification date, **April 15, 2024**.

All correspondence (subscription information, sales, advertising, author contributions, etc.) should be addressed to:

Central Office:

Agrociencia
Guerrero #9, Esquina Avenida Hidalgo.
56220. San Luis Huexotla. Texcoco,
State of Mexico

Phone: 595 92 84427

https://agrociencia-colpos.org/index.php/agrociencia

Cover: *Trigona nigerrima* and *Agapanthus africanus*
Photography and credits: Dr. Miguel Ignacio Delgado Blancas

Contents

Volume 58, Number 3 | April 1 - May 15, 2024

Food Science

Water-Soil-Climate

Agrociencia

HIVE TEMPERATURE REGULATION BY HONEYBEES IN RESPONSE TO EXTREME CONDITIONS

Samantha **Rodríguez-Vásquez**[1], Alfonso A. **Gardea-Béjar**[1*], Alejandro **Romo-Chacón**[2], Jaqueline **García-Hernández**[1], Humberto **González-Ríos**[3], Jesús Antonio **Orozco-Avitia**[4]

[1]Centro de Investigación en Alimentación y Desarrollo A.C. Coordinación Regional Guaymas. Carretera al Varadero Nacional km 6.6, Las Playitas, Guaymas, Sonora, Mexico. C. P. 85480.
[2]Centro de Investigación en Alimentación y Desarrollo A.C. Coordinación Regional Cuauhtémoc. Avenida Río Conchos S/N, Parque Industrial, Cuauhtémoc, Chihuahua, Mexico. C. P. 31570.
[3]Centro de Investigación en Alimentación y Desarrollo A.C. Coordinación de Tecnología de Alimentos de Origen Animal. Carretera Gustavo Enrique Astiazarán Rosas 46, La Victoria, Hermosillo, Sonora, Mexico. C. P. 83304.
[4]Centro de Investigación en Alimentación y Desarrollo A.C. Coordinación de Alimentos de Origen Vegetal. Carretera Gustavo Enrique Astiazarán Rosas 46. La Victoria, Hermosillo, Sonora, Mexico. C. P. 83304.
* Author for correspondence: gardea@ciad.mx

ABSTRACT

Honeybees are considered the primary pollinators of agricultural crops. However, climate change, pesticide use, disease transmission and pests all have an impact on their survival. Temperature is an important consideration, especially when bees are subjected to harsh conditions as a result of the effort required to regulate them within their hives. The brood chamber should be kept between 33 and 35 °C. The recognized temperature thresholds are 6 and 38 °C; deviations above or below these values cause metabolic damage in honeybees; the larger the difference, the greater the stress. These eusocial insects have developed thermoregulating mechanisms in response to adverse environmental conditions; the colony compensates for this difference by either fanning their wings to create air circulation and cause evaporative cooling or raising the temperature by generating endothermic heat to raise the temperature of the breeding chamber. This review brings together the most important and updated references on how to improve colony thermoregulation and its relationship to climate change.

Keywords: *Apis mellifera* L., thermoregulation, extreme temperatures.

Citation: Rodríguez-Vásquez S, Gardea-Béjar AA, Romo-Chacón A, García-Hernández J, González-Ríos H, Orozco-Avitia JA. 2024. Hive temperature regulation by honeybees in response to extreme conditions. **Agrociencia** 58(3): 273-287. https://doi.org/ 10.47163/agrociencia.v58i3.3082

Editor in Chief:
Dr. Fernando C. Gómez Merino

Received: October 05, 2023.
Approved: February 02, 2024.
Published in Agrociencia: May 06, 2024.

INTRODUCTION

Honeybees (*Apis mellifera* L.) are the most valuable pollinators in agriculture around the world. However, devastating colony losses have recently occurred due to synergistic factors. Climatic conditions are an important factor in the bee colony's well-being. Within the hive, the brood chamber must be strictly controlled within the range of 33 to 35 °C; maintaining such a narrow range is critical for proper brood development (Eouzan *et al*., 2019). As a result, if the temperature exceeds this range, bee physiology and behavior are affected.

Currently, conventional Langstroth chambers are the most popular among beekeepers due to their low cost and ease of operation. They are constructed with softwood from various timber species with a thickness of approximately 23 mm. This design has a deficient isolating factor, which causes an unstable hive microclimate (Mitchell, 2019). This is critical in areas where temperatures reach extreme levels, resulting in declining colony populations, death, and the unexplainable disappearance of colonies. Beekeepers have traditionally suffered from winter losses, but in recent years, summer losses have increased, posing a new threat. Steinhauer *et al*. (2021) studied colony losses in the USA from 2020 to 2021 and discovered losses of up to 32.2 % during the winter and 31.3 % during the summer.

Worldwide colony losses are increasing year after year, which has been linked to global climate change (IPCC, 2023). Although many threats affect the honeybee industry, the occurrence of extreme temperatures is linked to colony losses (Alattal and Alghamdi, 2015). Nonetheless, honeybees have an outstanding capacity to adapt to different environments. Beekeeping is extended worldwide in very different climates, though resilience is somewhat limited. Fast global warming is threatening genetic variability, making it a limiting factor because the accelerated pace of environmental change outpaces honeybees' natural adaptation mechanisms. Should this trend persist, it could lead to the disappearance of several subspecies that are not genetically equipped to cope with such rapid and intense changes (Table 1). This, in turn, would have a cascading impact on pollination ecosystems and, consequently, agriculture on a broader scale.

Table 1. Critical and lethal high temperatures for five *Apis mellifera* subspecies (Abou-Shaara *et al*., 2017; Li *et al*., 2019).

Subespecies	Critical intolerance (°C)	Lethal temperature (°C)
A. mellifera mellifera	54	60
A. mellifera dorsata	38	45
A. mellifera carnica	61	66
A. mellifera jemenitica	66	68
A. mellifera cerana	57	60

There are several studies in the literature reporting accessories and designs for apiaries held in adverse climates. The insulating capacity of Langstroth hives is rather poor when compared to those in wild-dwelling colonies (Mitchel, 2015). In areas where extreme conditions exist, hive structure has resulted in thicker walls and smaller entries to reduce colony stress caused by temperature and humidity fluctuations (Mitchel, 2019). Hence, it is critical to develop hive designs that effectively reduce thermal stress while remaining inexpensive. Based on the foregoing, the goal of this review was to gather the most relevant literature on the efficiency of hive thermoregulating mechanisms in order to identify available alternatives capable of reducing hive thermal stress caused by extreme temperatures.

CONTEXT

To compensate for environmental changes, honeybees have evolved a variety of thermoregulating mechanisms. Endothermic heat production and evaporative cooling by wing fanning are among these mechanisms for either heating or cooling the brood chamber (Heinrich, 1980; Jarimi *et al*., 2020). However, these are not sufficiently effective under extreme conditions, either when exceeding 38 °C or below -6 °C. These strategies require excessive energy inputs during high deviations or prolonged exposures, resulting in a significant decline in worker bees. This, in turn, decreases the overall hive strength and productivity (Li *et al*., 2019).

Former reports have demonstrated increased thermoregulation efficiency in modified hives designed for both hot and cold climates (Abou-Shaara *et al*., 2013; Erdoğan, 2019; Floris *et al*., 2020; Alburaki and Corona, 2021), increasing yield and decreasing mortality rates. Although conventional Langstroth hives have prevailed since 1852, exploring the use of different materials according to the local climate may offer advantages to keeping the hive microclimate within an appropriate physiologic range (Mitchell, 2015). In turn, it may help decrease colony losses and improve productivity in extreme weather. Precision Beekeeping (Zacepins *et al*., 2015) offers accessories and communication devices to maintain hive internal conditions near optimal through cooling and heating. However, they are usually expensive for beekeepers, regardless of their operation scale (Cousin *et al*., 2019). Besides, their handling requires specific know-how and continuous maintenance.

While most beekeeping hangs on traditional practices, the scenario has changed dramatically due to the presence of novel diseases, pests, exposure to new pesticides, and global warming. Because of these factors, the stress caused by synergistic issues and the strong oscillating weather, whether cold or hot, is becoming more dangerous (St. Clair *et al*., 2022). Consequently, the need for developing new hives, as well as new breeds selected for specific climates, is becoming critical.

Microclimate in *Apis mellifera* hives

Temperature and humidity

As poikilothermic organisms, insects lack the capacity to regulate their internal temperature, and their metabolic functions are influenced by abiotic factors. The temperature range within brood chambers is even more narrowly defined, with minimal fluctuations between 34.5±1.5 °C. Given that the developmental stages of larvae and pupae are stenothermal, their immediate surroundings must be maintained within this precise range (Stabentheiner *et al*., 2010). Humidity is another crucial factor, as it is necessary to ensure successful egg hatching. Optimal humidity conditions are 75 % for egg hatching and 90 to 95 % for larvae survival (Ellis *et al*., 2008).

Hive functioning rests on labor assignments such as brood feeding, food collection, wax, propolis, and honey production, hive building and cleaning, and hive defense, among others. Each worker bee is assigned to a particular task according to its temporal polyethism, which is influenced by its life stage (Tautz *et al*., 2003). Temperature regulation is achieved through a series of mechanisms according to brood demands. Under cold temperatures (below 6 °C), heat production by bees does not reach efficient levels, causing death within exposure for less than one hour. When temperature remains between 9 and 12 °C, they may survive for several hours if appropriate thermoregulation is achieved, which, in turn, will depend on workers abundance and available resources, among other factors (Jarimi *et al*., 2020). Honeybees are more resilient in high-temperature conditions, and their heat tolerance has been reported to be close to 54 °C.

The adaptation to high or low temperatures is also subspecies-dependent, as different genotypes can adapt to different climates (Abou-Shaara *et al*., 2017) (Table 1). Subspecies tolerance capacity is explained by the presence of heat shock proteins, whose role is to reduce oxidative stress; differences in heat tolerance are also attributed to body size and setae abundance (Li *et al*., 2019). As a result, it is critical to select the appropriate subspecies based on the local climate.

Social thermoregulation

Honeybee colonies in the wild are often sedentary, making them vulnerable to seasonal changes. They have responded to such challenges by establishing collective mechanisms to deal with thermal stress. The strategies used to regulate hive temperature can be passive or active.

Passive thermoregulation is based upon the proper location of brood chambers within the hive, as well as hive orientation, architecture, and building material (Jones and Oldroyd, 2006). To minimize microclimatic fluctuations, hive inner walls are isolated with propolis in a circular fashion to reduce any heat input or output and avoid undesirable air flow (Jarimi *et al*., 2020). Propolis is made by collecting sap and resins from plants. It works as a water-proofing varnish to seal the hive. Also, it serves as a barrier to avoid the entrance of invaders, besides offering a sanitary effect, given the antimicrobial nature of resins. Therefore, passive mechanisms work by buffering the temperature differential between the hive interior and its immediate surroundings, facilitating active temperature regulation. This is an important consideration when designing hives.

Temperature fluctuations are also influenced by changes in bee density as they stay in and out of the hive. In places where temperatures drop below 15 °C, honeybees are forced to thermoregulate and warm the hive (Stabentheiner *et al*., 2003). Thermoregulation consists of clustering together compact bee agglomerates in layers oriented towards the hive interior to reduce the air volume close to the brood chamber (Figure 1). Bees in the external layer connect their legs to create a barrier, blocking heat dissipation towards the exterior. Consequently, this conglomerate formation reduces

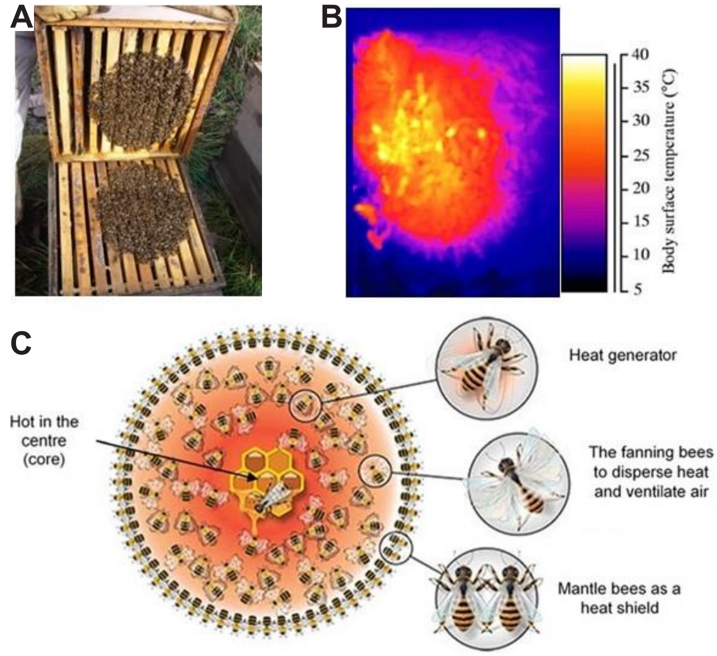

Figure 1. Hive thermoregulation system. A: bee winter conglomerates to generate and maintain heat; B: representative figure of endothermic heat and the winter bee cluster providing heat for the brood chamber; C: conglomerate infrared thermogram, temperature gradient showing how temperature decreases towards the outer layers of bees; sidebar shows the temperature corresponding to each color. Adapted from Stabentheiner *et al*. (2003).

bee body surface, which in turn minimizes heat loss by convection (Stabentheiner *et al*., 2003; Jones and Oldroyd, 2006; Stabentheiner *et al*., 2010).

As far as hive low-temperature exposure is concerned, bee survival is strongly compromised in the hive (Table 2). The thermal isolating mechanism becomes efficient through the release of endothermic heat by individuals within the conglomerate nuclei

Table 2. Effect of temperature and exposure on survival of Italian honeybee (*Apis mellifera L.*) colonies (Southwick and Heldmaier, 1987).

Temperature	Effect
9–12 °C	Bees may survive for several hours if their temperature matches that of the surrounding environment.
Between -2 and -6 °C	Bees die in less than one hour.
External temperature *ca*. -25 °C	A hive with 17 500 bees survived for more than 300 hours.
External temperature *ca*. -28 °C	A hive was capable to maintain an internal temperature of 31 °C for a short time.

(Stabentheiner *et al*., 2003). Bees generate heat by unintentional quick movements contracting and releasing their chests (shaking chills), which is energetically expensive (Abou-Shaara *et al*., 2013). When temperatures fall below this threshold, colonies face population decline due to mortality from excessive individual energy consumption.

In hot weather, brood chambers are exposed to overheating; therefore, bees use evaporative mechanisms to keep temperatures down. When temperatures reach peak maximum daily values, most foragers are working outside the hive, collecting food. At night, should excess heat accumulate, most bees will remain outside the hive. This behavior helps reduce internal temperature, as long as conditions are not extreme (Zeaiter and Myerscough, 2020). However, if above threshold, bees rely on wing fanning by placing themselves in the correct formation to favor input of outside fresh air and expelling of internal CO_2-enriched hot air through the hive entrance (Peters *et al*., 2019). This underlies the importance of keeping entrances free of obstructions to improve air circulation (Figure 2A). Evaporative cooling is another means to regulate hive internal conditions. To achieve results, bees collect and bring water to the hive to be used for lowering temperatures by wing fanning (Figure 2B).

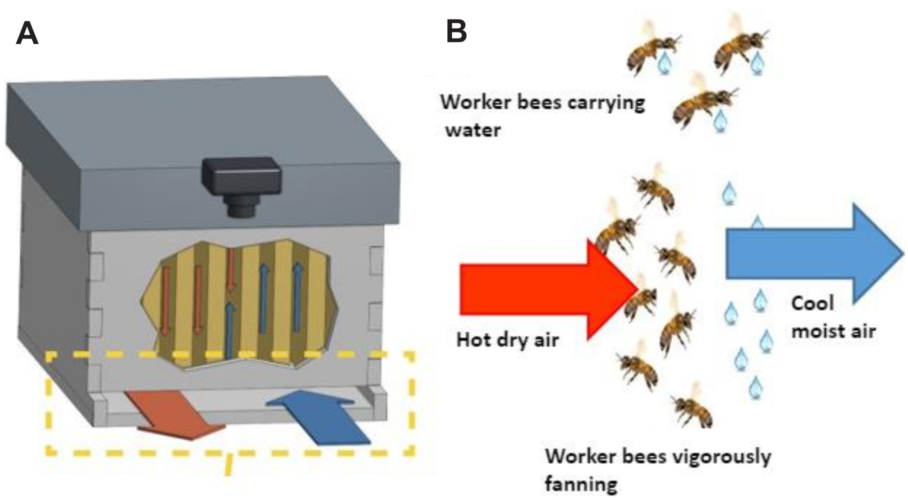

Figure 2. Hive temperature regulation in hot weather. A: Hot air expelled from the hive is replaced or exchanged by external fresh air passively entering the hive; B: evaporative cooling created by bees. Adapted from Peters *et al*. (2019) and Jarimi *et al*. (2020).

Adverse microclimate conditions

Alterations in physiology, morphology, and behavior.

A. mellifera bees developed adaptations to diverse climatic conditions through thermoregulating mechanisms as well as quick responses to microclimatic changes within the hive. However, keeping such conditions near optimum is not always achieved. Under suboptimal conditions below 31 and above 37 °C, diverse negative effects may occur, like morphological malformations in the abdomen and legs and size changes in the proboscis, tergum, and wings (Wang *et al*., 2016).

Groh *et al*. (2004) reported that temperature during brood influences larvae brain development; even small changes during the pupae stage dictate alterations in the development of the nervous system synaptic maturation, causing neuronal deficiencies. Concomitantly, memory and orientation are compromised, affecting exploration and foraging since their capacity to associate smells with food is fundamental, warranting success in nectar search as well as finding the way back to the hive. The same authors found that bees bred at 35 to 36 °C developed less efficient memory and orientation than those bred at 33 °C. Besides, prolonged exposure to such temperatures causes deficiencies in the waggle dance, whose function is to communicate about potential nectar and pollen source locations. A misperformed waggle dance prevents worker bees from locating food sources, given deficient communication (Tautz *et al*., 2003).

The queen is the only female in the hive with reproductive capacity. Once reaching maturity, she goes through a mating period with drones. Mating may occur once or twice in her lifetime, keeping their sperm in a specialized organ, the spermatheca, for up to five years. Temperatures below 15 and above 38 °C cause significant reductions in sperm viability (Preston *et al*., 2019; McAfee *et al*., 2020). Semen viability and abundance directly affect the reproductive capacity of laying-egg queens, thus reducing hive productivity. High temperatures cause stress in queens, which in turn reduces the quantity and quality of eggs destined to become workers (Stürup *et al*., 2013).

Thermal stress caused by cold decreases egg hatching and delays worker development; therefore, queen wellbeing impacts hive health and resilience (Preston *et al*., 2019; McAfee *et al*., 2020). Evidently, temperature is one factor affecting diverse physiological aspects and behavior, affecting hive productivity. However, these are just some examples of repercussions caused by thermal stress.

Global warming impact on beekeeping

Beekeeping relies heavily on stable climatic conditions for the proper development and productivity of apiaries. It has a direct impact on an essential benefit beyond honey production, as pollination is a crucial service in food production. Indirectly, it influences the socio-economic impacts of this activity. The economic value of *A. mellifera* becomes much more significant when considering crop pollination, since approximately 75 % of consumed crops depend on biotic pollination (Sosenski and Domínguez, 2018). The latest estimate calculates the global economic value of this service to be around 217 billion USD per year (Gallai *et al*., 2008).

Global warming simulation models predict effects on food distribution, interaction, and scarcity, as well as increases in diseases and diminishing populations of pollinators, including honeybees (Menzel and Feldmeyer, 2021). Because of global warming, beekeepers have adopted new practices, increasing investment and management expenses, resulting in reduced profits and leading to bankruptcy. Furthermore, the presence of Africanized bees in North America must be considered since they are more susceptible to changing environmental conditions, responding with migration when that occurs. Surveys in Mexico show that from 30 to 100 % of European honeybee colonies have some degree of hybridization (Alaniz-Gutiérrez *et al*., 2016), forcing beekeepers to replace queens on a yearly basis. Most of them (56 %) point towards global warming as the main cause of colony losses in later years (Medina-Flores *et al*., 2018).

Climate change and irregular vegetation development negatively impact beekeeping socioeconomics, forcing changes in apiary management that increase costs and affect rentability. Although studies on pesticides linked to colony collapse disorder have been under study for a long time, they focus on other threats like global warming and its relation to biological invasions and the spreading of diseases (Decourtye *et al*., 2019).

Stress-combined factors act synergistically, causing severe damage in apiaries (Goulson *et al*., 2015). Temperature fluctuations affect bee chemical detoxication and excretion (Kena *et al*., 2023). Hence, temperature modulates pesticide impact in diverse contexts, depending upon exposure dosages. Previous studies have determined that exposure to neonicotinoids under cold conditions affects orientation and foraging (Monchanin *et al*., 2019). Tosi *et al*. (2016) found that exposure to extreme temperatures (below 4 and above 33 °C) and tiametoxam affect thermoregulation capacity just one hour after exposure in Africanized bees. Medrzycki *et al*. (2010) found increased susceptibility to pesticide poisoning when the brood chamber fell 2 °C from optimum, such as in the case of dimethoate. When an appropriate thermoregulation is not achieved, many other functions are affected, such as foraging, waggle dancing, food discharge, work assignment, and flight efficiency, which decrease hive productivity and eventually lead to the loss of colonies. While many studies focus on the effect of global warming on honeybees, this review found that little attention has been directed to alternatives to help them thrive in this new situation.

A solution to increase hive thermoregulating efficiency

Hive design is of paramount importance since it serves as the home for bees. They adopt it and adapt it according to their own necessities, but to maximize thermoregulation, hive design must consider the local climate. Langstroth hives are extensively used in commercial beekeeping because of their accessible cost (Mitchel, 2019), even though their isolating capacities do not favor thermoregulation under extreme weather (Cook *et al*., 2021). Synergic factors influence thermal stress in bees. Climatic oscillation, hard winters, and hot summer spells are creating dangerous conditions; therefore, there is a need to develop alternative, specific designs according to the local climate as well as the bee subspecies used. Because of the above, it is important to acknowledge the need for direct efforts to contribute with novel strategies to improve beehives efficiency in their thermoregulation.

Hive designs for cold climate conditions.

During winter or in regions characterized by predominantly low temperatures, colony losses are frequently observed. This situation is often aggravated by the limited availability or poor quality of floral resources, including low-quality nectar. Unlike some other species, honeybees do not hibernate. In regions with short vegetation growth seasons, bees must work diligently to accumulate sufficient food for winter preparation (Stabentheiner *et al*., 2003; Steinhauer *et al*., 2021). In winter, resources are used for the reproduction cycle, primarily to feed the queen and worker bees, while drones are not fed and consequently perish. This halt in hive productivity during winter makes this season the largest risk to hive sustainability (Döke *et al*., 2015).

Winter mortality is among the main causes of beehive losses in the world. The Bee Informed Partnership monitors hive losses in the USA every year to identify causes and establish management strategies. During the 2020–2021 winter season, 32.2 % of losses were estimated. It represented an important increase as compared to the 22.6 % reported the previous winter, becoming the highest loss in the last 14 years (Steinhauer *et al*., 2021). In Mexico, there are no official records of winter mortality; however, independent studies have reported losses of 16.4 % in the temperate sub-humid zone (Brodschneider *et al*., 2018). Nonetheless, since climate effects may vary according to a particular region, such figures are not representative of the whole country.

Recent technologies have been implemented to face the detrimental effects of extreme temperatures, such as thermoregulating hives and intelligent hives, or so-called Precision Beekeeping (Zacepins *et al*., 2015). These systems are based on remote monitoring to achieve the most efficient use of the available resources and improve hive productivity. They consist of a series of sensors constantly collecting data that shows the hive's condition, allowing beekeepers to access information through a mobile device. Such developments have improved beekeeping significantly since direct control over hive microclimate can be achieved by monitoring different variables all together, such as hygiene, bee population, temperature, and humidity, among many others. Despite being a very efficient management tool, their prohibitive cost, requiring costly maintenance and care, affects rentability, which may prevent their widespread adoption (IEEE, 2019).

Another economically viable alternative is designing components to improve Langstroth hives thermoregulating capacity, regardless of weather. It may be low-cost, requiring simple changes in structure and materials, bringing the best possible results (Mitchell, 2019). During the winter, it is important to insulate hives with protective materials to avoid heat loss. Since there is scarce information regarding thermoregulation efficiency in modified hives, this review shows some examples from previous studies.

It has been demonstrated that hives insulated with polyurethane improve winter insulation by maintaining temperature and humidity within small oscillations. The brood chamber temperature was 10.2±0.04 °C, while in non-isolated controls it was only 9.7±0.05 °C. Although this temperature range is still far from an ideal 35–36 °C, it represents an important forward advance for not-so-extreme conditions. This study was done at mean temperatures around 0 °C. Under such conditions, achieving efficient thermoregulation is costly; however, using extra insulation helps bees improve temperature and humidity conditions and leads to less energy wear. Brood chamber humidity with and without polyurethane insulation remained at 52.2 and 62.5 %, respectively (Alburaki and Corona, 2021).

Such a response may result from wood differential absorption capacity since humidity increases during the daytime. Decreasing humidity has beneficial effects because, in winter, internal humidity rises in wooden hives, which creates an optimum condition for disease dispersal. Working in a temperate climate, St. Clair *et al*. (2022) evaluated the effects of insulating Langstroth hive upper lids with polypropylene plates. Warmer temperatures were achieved in insulated hives; even though no significant differences were found in the hive average temperatures, food consumption diminished significantly, resulting in a higher winter survival rate.

Cork was used by Floris *et al*. (2020) to evaluate its insulation capacity. It has been documented that cork has a higher insulation index than wood, and their data corroborated that. Significant improvements in hive temperature were found, averaging 34.7 °C in cork-insulated hives against 31.5 °C in controls. Since the ambient temperature was 25 °C, no significant stress was caused; however, cork-insulated hives remained at optimum temperatures for longer periods.

Although these studies showed promising alternatives when hives are modified for cold climates, the bee subspecies was not considered, and that is an important factor in temperature regulation. Materials like polystyrene and cork have low thermal conductivity as compared to conventional wood hives. Modifying hives suggests that a combination of materials may offer a synergistic effect (Wolfslehner *et al*., 2019; Floris *et al*., 2020).

Hive designs for hot climate conditions

Until recently, the threat posed by hot temperatures has been of little concern for beekeeping (Decourtye *et al*., 2019). Consequently, fewer reports are available on hive design and materials to fight internal temperature increases, even though negative reports are increasing year after year (Steinhauer *et al*., 2021). Thermoregulating mechanisms under hot temperatures bring along yield declines because of the excessive energetic wear required to cool down the hive. Besides, in arid regions, hot conditions go hand in hand with very low relative humidity. Scarce designs have been documented specifically for hot regions, although closer attention should be paid due to heat waves and global warming effects in beekeeping (Marshall *et al*., 2020; Menzel and Feldmeyer, 2021).

Abou-Shaara *et al*. (2013) evaluated distinct types of hives for *A. mellifera carnica* and *A. mellifera jemenitica*, two subspecies native to Yemen in the Arabic peninsula, under temperatures around 37±1.2 °C. Hives showed significant results as far as collecting activity, disease presence, and average temperature, all depending on bee subspecies.

Considering both genotypes, the most efficient design was the thermoregulated hive, which was equipped with cooling and ventilation features to create a 9.8 °C reduction in internal hive temperatures. This was the most efficient model, since mellifera bees did not need to thermoregulate. However, this technology demands a high energy input, increasing production costs in an activity with marginal profits.

Erdoğan (2019) evaluated the design proposed by Abou-Shaara *et al*. (2013), although excluding the water box. The summer season reached an average of 31.2±4 °C. Neither insulating wall thickness nor bee subspecies were specified, but this was the hive with the best performance as compared with polyurethane and wood. Besides better insulation, lower temperature oscillation was recorded, and a 27.9 % increment in yield was obtained, well above the 19.8 % found in the other treatments. Another model included an external box filled with water covering the back side of the hive, which reduced the hive temperature by 8.3 °C. This design consisted of a wooden hive surrounded by insulation material and the box described above. Such a box provides not only insulation but a water source as well, therefore offering a double advantage, not only thermoregulating but also minimizing the critical search for water, crucial in deserts. Nonetheless, it´s worth mentioning that humid conditions may cause sanitary issues (Eouzan *et al*., 2019).

Although previous experiences have shown promising alternatives regarding modifications to hive components, there is plenty of room for other improvements, which must include specific climatic conditions and bee genotype since they are closely related to adaptation (Abou-Shaara *et al*., 2017). Precision Beekeeping represents a promising and sophisticated alternative, although expensive; therefore, research and development on simple, affordable, and profitable designs are required to improve conditions for beekeepers thriving in hot, dry climates. Considering the rural nature of this economic activity, viable options are necessary (Magaña-Magaña *et al*., 2016). Simple actions such as using above-ground structures and not placing the hives directly on the ground decrease heat gain, as well as choosing shady places for the apiary. Criteria like that rely mostly on care and interest, which have little impact on costs.

Component design perspectives for extreme condition beekeeping

It is evident that research on hive design and components is required, particularly when facing the present threats and their synergistic effects with the extreme conditions brought by global warming (Abou-Shaara *et al*., 2013; Alatta and Alghamdi, 2015; Erdoğan, 2019; Floris *et al*., 2020; Alburaki and Corona, 2021). Beekeeping is a sustainable livestock activity, and given the multiple benefits bees offer to ecosystems, its preservation requires important modifications to traditional management (Mitchell, 2019). Critical issues such as hive design and adaptations linked to local climate and bee genetics are to be included, should appropriate thermoregulation be considered.

The joint use of wood and polystyrene as insulation is a combination of materials leading to improvements in thermal properties, reducing heat transfer and kinetic oscillations in the hive (Erdoğan, 2019). Wood's porous nature and thermal properties are well documented, but it is also hygroscopic, implying that it retains or exudes moisture depending on environmental conditions (Mitchell, 2015). On the other hand, expandible polyurethane features low thermal conductivity, low humidity absorption, and notable buffering properties, which become important when sharp environmental changes occur. A synergistic effect of these materials can be expected, resulting in improved hive thermoregulation efficiency when extreme weather is present (Erdoğan, 2019; Wolfslehner *et al*., 2019). Its low cost is another factor to consider.

CONCLUSIONS

This comprehensive literature review highlights the crucial importance of thermoregulation in honeybee (*Apis mellifera* L.) colonies, particularly in the context of climate change and extreme temperatures. Bees have developed ingenious mechanisms to cope with adverse environmental conditions, but it is essential to consider additional measures to enhance hive productivity while minimizing thermal stress, given its physiological and behavioral consequences. This review contributes to improving our understanding of how bees confront thermal challenges and underscores the need for concrete measures, such as hive modifications, to safeguard these valuable pollinators in an ever-changing world and promote their resilience in the face of climate change and other stressors.

The modification of hives to reduce thermal stress includes the use of insulating materials and ventilation systems to maintain a more constant temperature inside the hive, protect bees from extreme temperature fluctuations, and facilitate their thermoregulatory efforts. Due to the increased thermal buffering, bees do not waste energy attempting to regulate temperature, redirecting this energy toward food collection, which results in increased egg laying, worker population, and hive productivity. Furthermore, these modifications must be tailored to local conditions, since what works in one environment may not be effective in another.

REFERENCES

Abou-Shaara HF, Al-Ghamdi AA, Mohamed AA. 2013. Honey bee colonies performance enhance by newly modified beehives. Journal of Apicultural Science 57 (2): 45–57. https://doi.org/10.2478/jas-2013-001Abou-Shaara HF, Owayss AA, Ibrahim YY, Basuny NK. 2017. A review of impacts of temperature and relative humidity on various activities of honey bees. Insectes Sociaux 64 (4): 455–463. https://doi.org/10.1007/s00040-017-0573-8

Alaniz-Gutiérrez L, Torres-Salado N, Ail-Catzim CE, Velazco-López JL. 2016. Frecuencia de morfotipos africanizados y europeos de *Apis mellifera* en Ensenada y Mexicali, Baja California. Ecosistemas y Recursos Agropecuarios 3 (9): 421–426.

Alattal Y, Alghamdi A. 2015. Impact of temperature extremes on survival of indigenous and exotic honey bee subspecies, *Apis mellifera*, under desert and semiarid climates. Bulletin of Insectology 68 (2): 219–222.

Alburaki M, Corona M. 2021. Polyurethane honey bee hives provide better winter insulation than wooden hives. Journal of Apicultural Research 61 (2): 190–196. https://doi.org/10.1080/00218839.2021.1999578

Brodschneider R, Gray A, Adjlane N, Ballis A, Brusbardis V, Charrière JD, Chlebo R, Coffey MF, Dahle B, de Graaf DC *et al*. 2018. Multi-country loss rates of honey bee colonies during winter 2016/2017 from the COLOSS survey. Journal of Apicultural Research 57 (3): 452–457. https://doi.org/10.1080/00218839.2018.1460911

Cook D, Blackler A, McGree J, Hauxwell C. 2021. Thermal impacts of apicultural practice and products on the honey bee colony. Journal of Economic Entomology 114 (2): 538–546. https://doi.org/10.1093/jee/toab023

Cousin P, Căuia E, Siceanu A, de Cledat J. 2019. The development of an efficient system to monitor the honeybee colonies depopulations. 2019 Global IoT Summit: Aarhus, Denmark. https://doi.org/10.1109/giots.2019.8766435

Decourtye A, Alaux C, le Conte Y, Henry M. 2019. Toward the protection of bees and pollination under global change: present and future perspectives in a challenging applied science. Current Opinion in Insect Science 35: 123–131. https://doi.org/10.1016/j.cois.2019.07.008

Döke MA, Frazier M, Grozinger CM. 2015. Overwintering honey bees: biology and management. Current Opinion in Insect Science 10: 185–193. https://doi.org/10.1016/j.cois.2015.05.014

Ellis MB, Nicolson SW, Crewe RM, Dietemann V. 2008. Hygropreference and brood care in the honeybee (*Apis mellifera*). Journal of Insect Physiology 54 (12): 1516–1521. https://doi.org/10.1016/j.jinsphys.2008.08.011

Eouzan I, Garnery L, Pinto MA, Delalande D, Neves CJ, Fabre F, Lesobre J, Houte S, Estonba A, Montes I *et al.* 2019. Hygroregulation, a key ability for eusocial insects: Native western European honeybees as a case study. PLoS ONE 14 (2): e0200048. https://doi.org/10.1371/journal.pone.0200048

Erdoğan Y. 2019. Comparison of colony performances of honeybee (*Apis mellifera* L.) housed in hives made of different materials. Italian Journal of Animal Science 18 (1): 934–940. https://doi.org/10.1080/1828051X.2019.1604088

Floris I, Pusceddu M, Raccimolo E, Casula A, Patteri G, Satta A. 2020. The use of cork in the thermoregulation of the hive: An innovation attempt to enhance non-wood products and beekeeping in Mediterranean forests. Annals of Silvicultural Research 45 (1): 99–104. https://doi.org/10.12899/asr-2116

Gallai N, Salles J, Settele J, Vaissière BE. 2008.Economic valuation of the vulnerability of world agriculture confronted with pollinator decline. Ecological Economics 68 (3): 810–821. https://doi.org/10.1016/j.ecolecon.2008.06.014

Goulson D, Nicholls E, Botías C, Rotheray EL. 2015. Bee declines driven by combined stress from parasites, pesticides, and lack of flowers. Science 347 (6229): 1255957. https://doi.org/10.1126/science.1255957

Groh C, Tautz J, Rössler W. 2004. Synaptic organization in the adult honey bee brain is influenced by brood-temperature control during pupal development. Proceedings of the National Academy of Sciences 101 (12): 4268–4273. https://doi.org/10.1073/pnas.0400773101

Heinrich B. 1980. Mechanisms of body-temperature regulation in honeybees, *Apis mellifera* II. Regulation of thoracic temperature at high air temperatures. Journal of Experimental Biology 85 (1): 73–87. https://doi.org/10.1242/jeb.85.1.73

IEEE (Institute of Electrical and Electronics Engineers). 2019 IEEE International Conference on Automatic Control and Intelligent Systems. IEEE Control System Society Malaysian Chapter. Shah Alam, Malaysia.

IPCC (Intergovernmental Panel on Climate Change). 2023. Climate Change 2023: Synthesis Report. A report of the intergovernmental panel on climate change. Contribution of Working Groups I, II and III to the Sixth Assessment Report of the Intergovernmental Panel on Climate Change. Geneva, Switzerland. https://doi.org/10.59327/ipcc/ar6-9789291691647.001

Jarimi H, Tapia-Brito E, Riff S. 2020. A review on thermoregulation techniques in honey bees' (*Apis mellifera*) beehive microclimate and its similarities to the heating and cooling management in buildings. Future Cities and Environment 6 (1): 1–8. https://doi.org/10.5334/fce.81

Jones JC, Oldroyd BP. 2006. Nest thermoregulation in social insects. Advances in Insect Physiology 33: 153–191. https://doi.org/10.1016/S0065-2806(06)33003-2

Kena D, Graystock P, Gil RJ. 2023. Toxic temperatures: Bee behaviours exhibit divergent pesticide toxicity relationships with warming. Global Change Biology 29 (11): 2981–2998. https://doi.org/10.1111/gcb.16671

Li X, Ma W, Shen J, Long D, Feng Y, Su W, Xu K, Du Y, Jiang Y. 2019. Tolerance and response of two honeybee species *Apis cerana* and *Apis mellifera* to high temperature and relative humidity. PLoS ONE 14 (6): e0217921. https://doi.org/10.1371/journal.pone.0217921

Magaña-Magaña MA, Tavera-Cortés ME, Salazar-Barrientos LL, Sanginés-García JR. 2016. Productividad de la apicultura en México y su impacto sobre la rentabilidad. Revista Mexicana de Ciencias Agrícolas 7 (5): 1103–1115. https://doi.org/10.29312/remexca.v7i5.235

Marshall KE, Gotthard K, Williams CM. 2020. Evolutionary impacts of winter climate change on insects. Current Opinion in Insect Science 41: 54–62. https://doi.org/10.1016/j.cois.2020.06.003

McAfee A, Chapman A, Higo H, Underwood R, Milone J, Foster LJ, Guarna MM, Tarpy DR, Pettis JS. 2020. Vulnerability of honey bee queens to heat-induced loss of fertility. Nature Sustainability 3 (5): 367–376. https://doi.org/10.1038/s41893-020-0493-x

Medina-Flores CA, Esquivel-Marín NH, López-Carlos M, Medina-Cuellar SE, Aguilera-Soto JI. 2018. Estimación de la pérdida de colonias de abejas melíferas en el altiplano y el norte de México. Ecosistemas y Recursos Agropecuarios 5 (14): 365–371. https://doi.org/10.19136/era.a5n14.1459

Medrzycki P, Sgolastra F, Bortolotti L, Bogo G, Tosi S, Padovani E, Porrini C, Sabatini AG. 2010. Influence of brood rearing temperature on honey bee development and susceptibility to poisoning by pesticides. Journal of Apicultural Research 49 (1): 52–59. https://doi.org/10.3896/ibra.1.49.1.07

Menzel F, Feldmeyer B. 2021. How does climate change affect social insects? Current Opinion in Insect Science 46: 10–15. https://doi.org/10.1016/j.cois.2021.01.005

Mitchell D. 2019. To save honey bees we need to design them new hives. The Conversation. 9 September 2019. https://theconversation.com/to-save-honey-bees-we-need-to-design-them-new-hives-121792 (Retrieved: February 2024).

Mitchell D. 2015. Ratios of colony mass to thermal conductance of tree and man-made nest enclosures of *Apis mellifera*: Implications for survival, clustering, humidity regulation and *Varroa destructor*. International Journal of Biometeorology 60 (5): 629–638. https://doi.org/10.1007/s00484-015-1057-z

Monchanin C, Henry M, Decourtye A, Dalmon A, Fortini D, Bœuf E, Dubuisson L, Aupinel P, Chevallereau C, Petit J, Fourrier J. 2019. Hazard of a neonicotinoid insecticide on the homing flight of the honeybee depends on climatic conditions and *Varroa* infestation. Chemosphere 224: 360–368. https://doi.org/10.1016/j.chemosphere.2019.02.129

Peters JM, Peleg O, Mahadevan L. 2019. Collective ventilation in honeybee nests. Journal of the Royal Society Interface 16 (150): 2018056. https://doi.org/10.1098/rsif.2018.0561

Preston SR, Palmer JH, Harrison JW, Carr HM, Rittschof CC. 2019. The impacts of maternal stress on worker phenotypes in the honey bee. Apidologie 50 (5): 704–719. https://doi.org/10.1007/s13592-019-00680-1

St. Clair AL, Beach NJ, Dolezal AG. 2022. Honey bee hive covers reduce food consumption and colony mortality during overwintering. PLoS ONE 17 (4): e0266219. https://doi.org/10.1371/journal.pone.0266219

Sosenski P, Domínguez CA. 2018. The value and risks of pollination as an ecosystem service. Revista Mexicana de Biodiversidad 89 (3): 961–970. https://doi.org/10.22201/ib.20078706e.2018.3.2168

Southwick EE, Heldmaier G. 1987. Temperature control in honey bee colonies. BioScience 37 (6): 395–399. https://doi.org/10.2307/1310562

Stabentheiner A, Kovac H, Brodschneider R. 2010. Honeybee colony thermoregulation - Regulatory mechanisms and contribution of individuals in dependence on age, location and thermal stress. PLoS ONE 5 (1): e8967. https://doi.org/10.1371/journal.pone.0008967

Stabentheiner A, Pressl H, Papst T, Hrassnigg N, Crailsheim K. 2003. Endothermic heat production in honeybee winter clusters. Journal of Experimental Biology 206 (2): 353–358. https://doi.org/10.1242/jeb.00082

Steinhauer N, Aurell AD, Bruckner S, Wilson M, Rennich K, van Engelsdrop D, Williams G. 2021. United States honey bee colony losses 2020-2021: Preliminary results. The Bee Informed. 21 June 2021. https://beeinformed.org/2021/06/21/united-states-honey-bee-colony-losses-2020-2021-preliminary-results/ (Retrieved: February 2024).

Stürup M, Baer-Imhoof B, Nash DR, Boomsma JJ, Baer B. 2013. When every sperm counts: Factors affecting male fertility in the honeybee *Apis mellifera*. Behavioral Ecology 24 (5): 1192–1198. https://doi.org/10.1093/beheco/art049

Tautz J, Maier S, Groh C, Rössler W, Brockmann A. 2003. Behavioral performance in adult honey bees is influenced by the temperature experienced during their pupal development. Proceedings of the National Academy of Sciences 100 (12): 7343–7347. https://doi.org/10.1073/pnas.1232346100

Tosi S, Démares FJ, Nicolson SW, Medrzycki P, Pirk CW, Human H. 2016. Effects of a neonicotinoid pesticide on thermoregulation of African honey bees (*Apis mellifera scutellata*). Journal of Insect Physiology 93–94: 56–63. https://doi.org/10.1016/j.jinsphys.2016.08.010

Wang Q, Xu X, Zhu X, Chen L, Zhou S, Huang ZY, Zhou B. 2016. Low-temperature stress during capped brood stage increases pupal mortality, misorientation and adult mortality in honey bees. PLoS ONE 11 (5): e0154547. https://doi.org/10.1371/journal.pone.0154547

Wolfslehner B, Prokofieva I, Mavsar R. 2019. Non-wood forest products in Europe seeing the forest around the trees. European Forest Institute: Joensuu, Finland. 116 p.

Zacepins A, Brusbardis V, Meitalovs J, Stalidzans E. 2015. Challenges in the development of Precision Beekeeping. Biosystems Engineering 130: 60–71. https://doi.org/10.1016/j.biosystemseng.2014.12.001

Zeaiter Z, Myerscough MR. 2020. Poor hive thermoregulation produces an Allee effect and leads to colony collapse. Journal of Theoretical Biology 503: 11036. https://doi.org/10.1016/j.jtbi.2020.110361

METABOLITE CONTENT AND ANTIOXIDANT ACTIVITY OF SPENT COFFEE GRAIN FERMENTED WITH *Pleurotus pulmonarius* MYCELIUM

Rosa Isela **Castillo-Zamudio**[1], Rey David **Vargas-Sánchez**[2], Armida **Sánchez-Escalante**[2], Martín **Esqueda-Valle**[2], Brisa del Mar **Torres-Martínez**[2], Gastón Ramón **Torrescano-Urrutia**[2*]

[1]Colegio de Postgraduados Campus Veracruz. Carretera Xalapa-Veracruz km 88.5, Xalapa, Veracruz, Mexico. C. P. 91690.

[2]Centro de Investigación en Alimentación y Desarrollo A.C. Carretera Gustavo Enrique Astiazarán Rosas 46, La Victoria, Hermosillo, Sonora, Mexico. C. P. 83304.

* Author for correspondence: gtorrescano@ciad.mx

ABSTRACT

Spent coffee beans are agro-industrial waste that contain nutrients and bioactive compounds that can be recovered by fungal fermentation-assisted extraction using edible fungal strains. In this study, the metabolite content and antioxidant activity of the aqueous extract of spent coffee beans fermented in a submerged culture using the mycelium of *Pleurotus pulmonarius* were evaluated. The total carbohydrate, phenol, flavonoid, and caffeoylquinic acid contents of the extract were determined, as well as the antioxidant activity by free radical and cation inhibition, reducing power, and lipid oxidation inhibition. The experimental design was completely randomized using a factorial arrangement, with three independent experimental replicates. The data were examined using analysis of variance (ANOVA) and the Tukey-Kramer mean comparison test ($p \leq 0.05$). To determine the association between variables and parameters evaluated, a principal component analysis was used. The results showed that the aqueous extract obtained by submerged culture fermentation using *P. pulmonarius* and different levels of spent coffee beans presented a high content of metabolites such as carbohydrates (70.2 %), phenols (64.5 %), flavonoids (61.9 %), and caffeoylquinic acid (90.8 %), as well as a higher antioxidant activity by inhibiting the formation of 2,2-diphenyl-1-picrylhydrazyl (DPPH$^{\bullet}$) and 2,2′-azino-bis(3-ethylbenzothiazoline-6-sulfonic acid) (ABTS$^{\bullet+}$) radicals (31.6 and 31.9 %, respectively), lipid oxidation (70 %), reducing power (14.9 %), and Ferric Reducing Antioxidant Power (FRAP) (89.4 %), compared to the control. Furthermore, the first two main components explained 91.3 % of the variation, revealing that fermented samples with and without mycelium differed in terms of metabolite content and antioxidant activity, which were dependent on the proportion of wasted coffee beans. In conclusion, the fungal fermentation of spent coffee beans is a potential strategy for the recovery of antioxidant ingredients.

Keywords: coffee residues, fungal fermentation, chemical composition, bioactivity.

Citation: Castillo-Zamudio RI, Vargas-Sánchez RD, Sánchez-Escalante A, Esqueda-Valle M, Torres-Martínez B del M, Torrescano-Urrutia GR. 2024. Metabolite content and antioxidant activity of spent coffee grain fermented with *Pleurotus pulmonarius* mycelium. **Agrociencia** 58(3): 288-300. https://doi.org/ 10.47163/ agrociencia.v58i3.3030

Editor in Chief:
Dr. Fernando C. Gómez Merino

Received: June 11, 2023.
Approved: February 18, 2024.
Published in Agrociencia:
May 13, 2024.

INTRODUCTION

Coffee is a perennial plant belonging to the *Coffea* genus of the Rubiaceae family. The processing of its fruit into liquid coffee is the main commercial use of this plant. Coffee is considered one of the most consumed beverages in the world and is classified as the second most commercialized product after petroleum. Dispensing coffee generates large quantities of by-products such as pulp, husk, silver skin, and spent coffee beans (Murthy and Naidu, 2012).

Spent coffee beans are the residue obtained in the process of making "instant coffee," a beverage prepared by the extraction in boiling water of the soluble material from roasted and ground coffee beans (Mussatto *et al*., 2011). This by-product is an important source of nitrogenous components (proteins, free amino acids, and caffeine), fat and fatty acids (palmitic acid and linoleic acid), carbohydrates (fructose, glucose, and galactose), and fiber (cellulose and hemicellulose), as well as bioactive compounds such as melanoidins and phenolic acids (Mussatto *et al*., 2011; Campos-Vega *et al*., 2015). Coffee by-products are used in limited applications such as livestock feed, composts, and fertilizers. However, the recovery of these compounds with antioxidant potential through chemical and biotechnological processes can be considered a strategy for obtaining new additives for the pharmaceutical or food industry (Ozuna *et al*., 2020).

Fermentation in solid or liquid/submerged culture of various substrates (agro-industrial waste), using bacteria and fungi, is reported to be a useful tool for the production (secondary metabolic pathway) and procurement of antioxidant compounds (extracellular enzymatic release), compared to conventional methods that use organic solvents that do not allow the complete release of bioactive compounds bound to plant tissues (Dey *et al*., 2016). In addition, some of these solvents cannot be used in food production. Fermentation in submerged culture presents potential advantages over solid-state culture by allowing uniformity in the dispersion of the inoculum in the substrate and a considerable reduction in time. However, this will depend on the species of microorganisms used, culture conditions (pH, temperature, aeration, among others), and substrate (Dey *et al*., 2016; Xu *et al*., 2015).

In this context, Zerva *et al*. (2021) reported obtaining aqueous-methanolic extracts (1:1) with the capacity to inhibit free radicals ($DPPH^•$) from agro-industrial wastes (oil mill wastewater and corn cobs) fermented in a submerged culture with *Pleurotus citrinopileatus*. Ogidi *et al*. (2020) reported the antiradical capacity ($DPPH^•$, $HO^•$, and $NO^•$) of polysaccharides obtained from fruit skins (pineapple, banana, and mango) and peels (walnut and peanut) fermented in a submerged culture with *P. pulmonarius*. However, information on the recovery of antioxidant compounds from spent coffee beans by fermentation in a submerged culture using *Pleurotus* spp. is still limited. Therefore, the objective of the present work was to evaluate the metabolite content and antioxidant activity of the aqueous extract of spent coffee beans fermented in a submerged culture using the mycelium of *P. pulmonarius*.

MATERIALS AND METHODS

Plant material

Spent coffee bean residues were collected from local commercial suppliers (CAFFENIO®; Hermosillo, Mexico) and dried at 60 °C in a drying oven (Yamato DX402; Tokyo, Japan) to a moisture content of 10 %. Subsequently, these residues were sterilized at 121 °C for 20 min in an autoclave (Yamato SM300; Tokyo, Japan).

Mycelium collection and fermentation medium

The strain of *P. pulmonarius* (IE-115) used belongs to the fungal collection of the Coordination of Food Technology of Plant Origin (CIAD A.C., Hermosillo, Mexico). The strain was cultivated on Petri dishes with potato dextrose agar at 25 °C for 5 d in an incubator (Yamato IC602; Tokyo, Japan), ensuring that the mycelium covered the entire surface of the plate. The fermentation medium for substrate wetting was sterilized at 121 °C for 20 min using the following composition: glucose (20 g L^{-1}), yeast extract (5 g L^{-1}), potassium phosphate (1 g L^{-1}), magnesium sulfate (0.5 g L^{-1}), and ascorbic acid (0.05 g L^{-1}). The pH was adjusted to 5.4 by the addition of hydrochloric acid (0.1 N) or sodium hydroxide (2.5 M).

The fermentation process was carried out in 250 mL Erlenmeyer flasks with 100 mL of fermentation medium and different proportions of spent coffee beans (0, 5, and 10 %, w/v), which were fermented with or without the addition of 1.5 mg of *P. pulmonarius* mycelium, which was collected aseptically from the surface of the plates with culture. Flasks were incubated at 28 °C and 150 rpm in a rotary incubator (MaxQTM 5000, Fisher Scientific; Nepean, Canada) for 10 d in the dark (Vargas-Sánchez *et al*., 2023).

Extract preparation

The fermented culture medium was homogenized at 10 000 rpm for 30 s (Ultraturrax T25, IKA®; Staufen, Germany), filtered using Whatman 1 filter paper under vacuum (MVP 6 pump, Soosung Vacuum Co. Ldt.; Jeju, South Korea), and dried (Yamato DC401 freeze dryer; Tokyo, Japan). The resulting aqueous extract was stored at -20 °C in the dark until analysis (Liu *et al*., 2018).

Qualitative metabolite profile

The metabolites in the aqueous extract were analyzed qualitatively using standard methods (Griffiths *et al*., 1992; Samejo *et al*., 2013). To extract the metabolites, 0.5 g of the aqueous extract was homogenized with 10 mL of distilled water at 10 000 rpm for 1 min (vortex mixer, Fisher Scientific; CA, USA) and filtered through Whatman 1 filter paper (stock solution).

For carbohydrate analysis (phenol-sulfuric acid test), 2 mL of the stock solution was mixed with 1 mL of aqueous phenol (1 %, v/v) and 1 mL of concentrated sulfuric acid. After mixing, it was incubated at 100 °C for 5 min in the dark. The formation of a brown precipitate indicated a positive result. For phenol analysis (ferric chloride test), the stock solution (2 mL), previously incubated at 100 °C for 10 min (Yamato BM510 water bath; Tokyo, Japan) and filtered, was mixed with 2 mL of iron chloride solution (0.1 %, w/v). The formation of a blue-black precipitate indicated a positive result.

For flavonoid analysis (Shinoda test), a few pieces of magnesium tape and 0.1 mL of concentrated hydrochloric acid were carefully added to 1 mL of the stock solution. The appearance of a red color indicated a positive result. Finally, for chlorogenic acid analysis (sodium nitrite test), 1 mL of the stock solution was mixed with 1 mL of urea (0.17 M), 1 mL of glacial acetic acid (0.1 M), and 2.5 mL of distilled water. Subsequently, 2.5 mL of sodium nitrite (0.14 M) and 2.5 mL of sodium hydroxide (0.5 M) were added. The appearance of a red color indicated a positive result.

Total metabolite content

Total carbohydrate content was determined using the phenol-sulfuric acid method (Albalasmeh *et al*., 2013). The aqueous extract (50 μL, 5 mg mL^{-1}) was placed in a 96-well microplate and homogenized with 25 μL of aqueous phenol solution (5 %, v/v) and 125 μL of concentrated sulfuric acid. The reaction mixture was incubated at room temperature (25 °C) for 10 min in the dark. Subsequently, absorbance was measured at 490 nm in a spectrophotometer (Multiskan FC UV-Vis, Thermo Scientific; Vantaa, Finland). The results were expressed as mg glucose equivalents per g of dry extract (mg GE g^{-1}).

The Folin-Ciocalteu technique was used to measure total phenol content (Ainsworth and Gillespie, 2007). The aqueous extract (20 μL, 5 mg mL^{-1}) was homogenized with 160 μL of distilled water, 60 μL of sodium carbonate (7 %, w/v), and 40 μL of Folin-Ciocalteu reagent (2 M). The reaction mixture was incubated at 25 °C for 1 h in the dark. Subsequently, the absorbance was measured at 750 nm. The results were expressed as mg of gallic acid equivalents per g of dry extract (mg GAE g^{-1}).

The total flavonoid content was determined using the procedure described by Zhishen *et al*. (1999). An aliquot of the aqueous extract (500 μL, 5 mg mL^{-1}) was mixed with 1 mL of sodium nitrite (5 %, w/v), 1 mL of aluminum chloride (10 %, w/v), and 10 mL of sodium hydroxide (1 M). The resulting mixture was adjusted to 25 mL with 70 % ethanol and incubated at 25 °C for 15 min in the dark. The absorbance was measured at 510 nm, and the results were expressed as mg of quercetin equivalents per g of dry extract (mg EQ g^{-1}).

Total caffeoylquinic acid content was determined by the method previously described (Griffiths *et al*., 1992). The aqueous extract (100 μL, 5 mg mL^{-1}) was homogenized with 200 μL of urea (0.17 M), 200 μL of glacial acetic acid (0.1 M), and 500 μL of sodium hydroxide (0.5 M). The reaction mixture was centrifuged at 2250 ×g at 4 °C for 10 min (Sorvall ST18R, Thermo Scientific; Waltham, USA). Subsequently, the absorbance was measured at 510 nm. The results were expressed as mg of chlorogenic acid equivalents per g of dry extract (mg CAE g^{-1}).

Antioxidant activity

Free radical inhibition was determined by the method described by Molyneux (2004). The aqueous extract (100 μL, 100 μg mL^{-1}) was homogenized with 100 μL of 2,2-diphenyl-1-picrylhydrazyl (DPPH$^{\bullet}$) solution (300 μM) and incubated at 25 °C for 30 min in the dark. Absorbance was measured at 517 nm. Ascorbic acid (70 μM) was used as a standard. The ability of the extract to inhibit the radical was calculated as follows:

$$DPPH \bullet (\%) = AbsA - \frac{Abs\ B}{Abs\ A} \times 100$$

where Abs A is the absorbance of the control (t = 0) and Abs B is the absorbance of the antioxidant (t = 30 min).

Cation radical inhibition was determined by the method described by Re *et al*. (1999). Prior to analysis, equal parts of ethanolic solution of 2,2′-azino-bis(3-ethylbenzothiazoline-6-sulfonic acid) (ABTS$^{\bullet+}$) (7 mM) and potassium persulfate (2.45 M) were homogenized at 10 000 rpm for 1 min. The resulting solution was stored at 25 °C for 16 h in the dark. The radical formed was adjusted to an absorbance of 0.8 with ethanol, mixed with the aqueous extract (100 μg mL^{-1}) in a 99:1 ratio, and incubated for 10 min. The absorbance was measured at 734 nm, using ascorbic acid (70 μM) as a standard. The ability of the extract to inhibit the cation radical was calculated as follows:

$$ABTS^{\bullet+} (\%) = AbsA - \frac{Abs\ B}{Abs\ A} \times 100$$

where Abs A is the absorbance of the control (t = 0) and Abs B is the absorbance of the antioxidant (t = 10 min).

The reducing power was determined using the ferricyanide/Prussian blue method (Berker *et al*., 2010). An aliquot of aqueous extract (100 μL, 100 μg mL^{-1}) was homogenized with 300 μL of phosphate buffer (0.2 M, pH 6.6) and 300 μL of potassium ferricyanide (1 %, w/v). The resulting solution was incubated at 50 °C for 20 min in a water bath in the dark. After cooling at 25 °C for 10 min, the mixture was homogenized with 300 μL of trichloroacetic acid (10 %, w/v) and centrifuged at 4200 ×g at 4 °C for 10 min. Then, 100 μL of the supernatant was mixed with 100 μL of distilled water and 250 μL of ferric chloride (0.1 %, w/v). The absorbance was measured at 700 nm, and the results were expressed as an increase in absorbance at the same wavelength.

Ferric-reducing antioxidant power was determined using the method described by Berker *et al*. (2010). An aliquot of aqueous extract (20 μL, 100 μg mL^{-1}) was homogenized with 150 μL of Ferric Reducing Antioxidant Power (FRAP) solution (10:1:1, 300 mM of sodium acetate buffer in glacial acetic acid at pH 3.6 and 4,4,6-tripyridyl-S-triazine in 40 nM of hydrochloric acid and 20 mM of iron chloride). The reaction mixture was incubated at 25 °C for 8 min in the dark. The absorbance was measured at 595 nm, and the results were expressed as mg iron ion equivalents per g of dry extract (mg Fe^{2+} g^{-1}).

Lipid oxidation was determined using the Thiobarbituric Acid Reactive Substances (TBARS) assay (Kim *et al*., 2016) with slight modifications. Pork (semimembranosus muscle, 48 h *postmortem*) was homogenized with 10 mL of water and 1 mL of each aqueous extract at 500 ppm at 4500 rpm at 4 °C for 1 min. The homogenate obtained was mixed with a 1:2 ratio of trichloroacetic acid solution (10 %, w/v). Subsequently, the sample was centrifuged at 2300 ×g at 4 °C for 10 min and filtered through Whatman paper 1. The resulting solution was homogenized with 2-thiobarbituric acid solution (0.02 M) at a 1:1 ratio and placed in a water bath (97 °C for 20 min). The absorbance was measured at 531 nm, expressing the results as mg of malondialdehyde per kg of meat (mg MDA kg^{-1}).

Statistical analysis

Values were expressed as the mean ± standard deviation. All data were obtained from three independent experimental trials (with three replicates). The data on metabolite content and antioxidant activity were subjected to a two-way analysis of variance (ANOVA), considering as factors the level of addition of spent coffee beans to the culture medium and the use or non-use of the fungal mycelium. Additionally, a Tukey-Kramer multiple comparison test was performed to determine the statistical differences between treatments ($p \leq 0.05$). To evaluate the relationship between the variables analyzed, a principal component analysis (SPSS version 21, IBM Statistics) was performed.

RESULTS AND DISCUSSION

The metabolite content of aqueous extracts was affected by the level of addition of spent coffee beans fermented with *P. pulmonarius* mycelium (Table 1). The highest content of carbohydrates (> 100 mg g^{-1}), phenols (> 20 mg g^{-1}), flavonoids (> 10 mg g^{-1}), and caffeoylquinic acid (> 300 mg g^{-1}) was presented by the aqueous extract obtained from the culture medium added with 10 % spent coffee beans fermented with mycelium, compared to the extracts obtained from fermented samples without the addition of residue and mycelium.

In a study by Xu *et al*. (2014), the ability of *Inonotus obliquus* mycelium to degrade peanut shell biomass (substrate/carbon source) and the recovery of bioactive compounds during submerged culture fermentation were evaluated. These authors demonstrated that more than 60 % of the cellulose, hemicellulose, and lignin in the shell were degraded after 12 d of fermentation. They also reported an increase in the content of polysaccharides and total phenols when using this residue as a substrate and *I. obliquus* mycelium. The increase in total phenol content was attributed to the degradation of

Table 1. Total metabolite composition of aqueous extracts of spent coffee beans fermented in a submerged culture with and without *Pleurotus pulmonarius* mycelium.

Parameters	Residue	Quality profile		Quantity profile	
		Without mycelium	With mycelium	Without mycelium	With mycelium
Carbohydrates (mg GE g^{-1})	0 %	+	+	21.19 ± 0.97 a	30.81 ± 2.35 c
	5 %	+	++	23.86 ± 0.31 b	92.40 ± 2.19 d
	10 %	+	+++	23.85 ± 0.32 b	103.54 ± 3.30 e
Phenols (mg GAE g^{-1})	0 %	-	+	0.91 ± 0.19 a	7.82 ± 0.09 b
	5 %	+	++	7.69 ± 1.35 b	17.63 ± 2.01 c
	10 %	+	+++	7.86 ± 1.53 b	22.03 ± 1.69 d
Flavonoids (mg EQ g^{-1})	0 %	-	+	0.72 ± 0.02 a	4.50 ± 0.12 b
	5 %	+	++	4.03 ± 0.75 b	10.25 ± 0.24 c
	10 %	+	++	3.72 ± 0.90 b	11.81 ± 0.39 d
Caffeoylquinic acid (mg CAE g^{-1})	0 %	-	+	1.65 ± 0.04 a	30.71 ± 3.82 b
	5 %	+	++	51.99 ± 2.70 c	216.49 ± 3.64 e
	10 %	+	+++	88.22 ± 2.70 d	333.15 ± 4.76 f

(-): absent; (+): slight presence; (++): moderate presence; (+++): high presence; 0 %: culture medium without addition of spent coffee beans; 5 %: culture medium with 5 % spent coffee beans; 10 %: culture medium with 10 % spent coffee beans. EG: glucose equivalents; GAE: gallic acid equivalents; EQ: quercetin equivalents; CAE: chlorogenic acid equivalents. Metabolite content values are expressed as mean ± standard deviation. Means with different superscripts (a-f) between samples indicate significant differences ($p \leq 0.05$).

lignocellulose because it showed a stimulatory effect on the yield of extracellular and intracellular flavonoids such as epigallocatechin-3-gallate, epicatechin-3-gallate, feligidrin G, davallialactone, and inoscavin B. However, the content of phenolic acids, such as gallic and ferulic, was reduced by the effect of lignocellulose degradation.

Likewise, in a study conducted by Choi *et al*. (2010), the optimal conditions to produce *Cordypces sinensis* by fermentation in a submerged medium for 7 d using citrus peel as a substrate were evaluated. The results showed an increase in the total content of polysaccharides, phenols, and flavonoids after fermenting citrus peel with *C. sinensis*. In another study, Vargas-Sánchez *et al*. (2023) evaluated the qualitative profile and metabolite content of the aqueous extract of spent coffee beans fermented in a submerged culture using the mycelium of *P. ostreatus*. According to their results, an increase in the content of carbohydrates, phenols, flavonoids, and caffeoylquinic acid was reported after the fermentation process (10 d) in a submerged culture with the use of mycelium from this species.

Based on the studies described above, the increase in the content of these metabolites may be associated with the degradation of the lignocellulosic material of agro-industrial wastes during the fermentation process. The increased release of these compounds is associated with their bioactivity, which is mainly antioxidant and antimicrobial (Xu *et al*., 2014; Ogidi *et al*., 2020). The evaluation of antioxidant activity makes it possible to determine the ability of certain compounds to scavenge or reduce free radicals, as well as to yield electrons to reduce an oxidizing agent. This evaluation can be carried out by different methods or reaction mechanisms, such as oxygen radical scavenging capacity, hydroxyl radical prevention capacity, ferric ion reducing power, inhibition of peroxyl and hydroxyl radicals, as well as inhibition of $DPPH^{•}$ and $ABTS^{•+}$ radicals (Echegaray *et al*., 2021).

The antioxidant activity of the extracts was affected by the level of addition of spent coffee beans fermented with *P. pulmonarius* mycelium (Table 2). The highest antiradical activity was presented by the aqueous extract obtained from the culture medium added with 5 and 10 % of spent coffee beans fermented with mycelium, compared to the extracts obtained from the samples in which no mycelium and spent coffee beans were used. On the other hand, the highest reducing power (> 1.5 absorbance and 30 mg Fe^{2+} g^{-1}) was presented by the aqueous extract obtained from the culture medium added with 10 % of spent coffee beans fermented with *P. pulmonarius* mycelium, in relation to the extracts obtained from samples fermented without the addition of residue and mycelium.

Table 2. Antioxidant activity of aqueous extract of spent coffee beans fermented in a submerged culture with and without *Pleurotus pulmonarius* mycelium.

Parameters	Residue	Without mycelium	With mycelium
$DPPH^{•}$ (% inhibition)	0 %	28.57 ± 0.32 a	44.26 ± 1.48 b
	5 %	58.06 ± 0.32 c	64.30 ± 0.69 e
	10 %	61.39 ± 0.94 d	64.74 ± 0.93 e
$ABTS^{•+}$ (% inhibition)	0 %	49.64 ± 1.18 a	60.47 ± 2.37 b
	5 %	88.29 ± 0.79 c	89.58 ± 0.64 c
	10 %	88.35 ± 0.89 c	88.77 ± 0.88 c
Reducing power (absorbance)	0 %	0.42 ± 0.01 a	1.31 ± 0.01 c
	5 %	0.51 ± 0.01 b	1.31 ± 0.01 c
	10 %	0.51 ± 0.01 b	1.54 ± 0.04 d
FRAP (mg Fe^{2+} g^{-1})	0 %	3.13 ± 0.10 a	3.19 ± 0.92 a
	5 %	9.97 ± 0.10 b	12.44 ± 0.66 c
	10 %	11.73 ± 0.82 c	30.04 ± 1.63 d

Values are expressed as mean ± standard deviation. 0 %: culture medium without addition of spent coffee beans; 5 %: culture medium with 5 % spent coffee beans; 10 %: culture medium with 10 % spent coffee beans. FRAP: ferric reducing antioxidant power; $DPPH^{•}$: 2,2-diphenyl-1-picrylhydrazyl; $ABTS^{•+}$: 2,2′-azino-bis(3-ethylbenzothiazoline-6-sulfonic acid). Means with different superscripts (a-e) between samples indicate significant differences ($p \leq 0.05$).

In this regard, Ogidi *et al*. (2020) extracted antioxidant compounds by assisted extraction with fungal fermentation for 7 d, using *P. pulmonarius* mycelium and different agro-industrial residues as carbon sources (banana peel, pineapple, mango, peanut, walnut, and coconut fiber). These authors reported activity against free radicals (DPPH$^•$), hydroxyl (HO$^•$), and nitric oxide (NO$^•$) (> 70 % inhibition) in the extracts after fermentation in a submerged medium with mycelium, comparable to the evaluated commercial antioxidant butylated hydroxytoluene (BHT). In addition, these extracts showed a reduction capacity (> 70 %) to chelate metal ions such as iron (Fe^{+2}), as did the commercial antioxidant.

In another study, Xu *et al.* (2014) reported increased activity against DPPH$^•$ and HO$^•$ radicals (> 40 and 50 % inhibition, respectively) by subjecting peanut shells to fermentation for 12 d in a submerged culture with *I. obliquus*, which was associated with an increase in flavonoid content (epigallocatechin-3-gallate and epicatechin-3-gallate) during fermentation with the mycelium. Meanwhile, Choi *et al*. (2010) demonstrated an increase in ABTS$^{•+}$ antiradical activity (approximately 400 mg of ascorbic acid equivalents per 100 g) by fermenting citrus peel in a submerged culture for 7 d using *C. sinensis* mycelium. In addition, increased activity has been demonstrated against DPPH$^•$ and ABTS$^{•+}$ radicals (> 40 and 50 % inhibition, respectively), reducing power (0.4–0.9 absorbance), and metal ion chelation (> 60 %) of the extract obtained by fermentation in a submerged culture for 5 d, using the mycelium of *P. ostreatus*, whose bioactivity was associated with metabolite formation (Vamanu, 2012).

In turn, Vargas-Sánchez *et al*. (2023) evaluated the antioxidant activity of the aqueous extract of spent coffee beans fermented in a submerged culture using the mycelium of *P. ostreatus*. In that study, an increase in the inhibition values of DPPH$^•$ and ABTS$^{•+}$ radicals, as well as reducing power and FRAP values, was achieved after the fermentation process (10 d) in a submerged culture with the use of mycelium from this species. Also, the activity shown in the controls is reported to be attributed to the use of ascorbic acid in the formulation of the culture medium. On the other hand, it has been demonstrated that food matrices, such as meat and meat products, are susceptible to oxidative deterioration due to their main components, such as proteins and lipids. These components can serve as targets for different radicals such as hydroxyl (HO$^•$), peroxyl (ROO$^•$), hydroperoxyl ($HO_2^•$), and alkoxy (RO$^•$), which favor the oxidative process of proteins and lipids (Echegaray *et al*., 2021). In this context, the formation of thiobarbituric acid-reactive substances is a widely used method to measure the formation of lipid oxidation by-products, such as MDA, and consequently, to measure the oxidative stability of extracts from natural sources in foods (Kim *et al*., 2016; Shah *et al*., 2014).

Based on the above, the oxidative stability of meat homogenates subjected to heat treatment was affected by time and the inclusion of aqueous extracts obtained from spent coffee beans fermented in a submerged culture with or without *P. pulmonarius* mycelium (Figure 1).

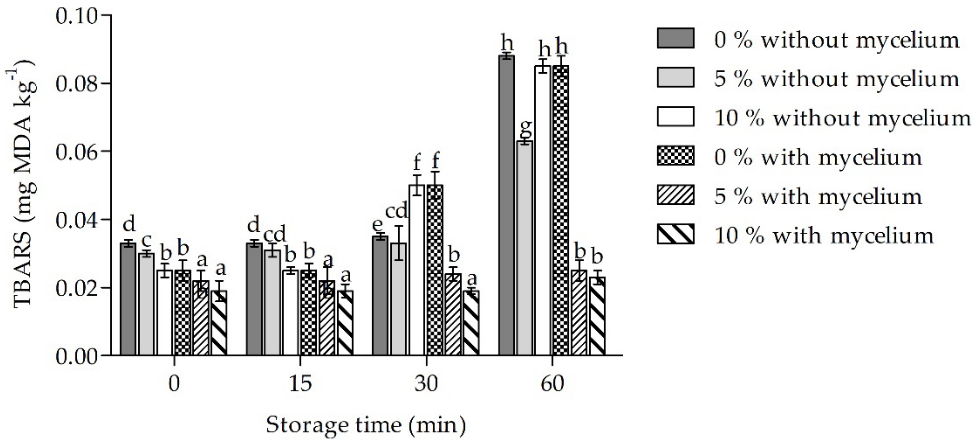

Figure 1. Oxidative stability of meat homogenate added with aqueous extract of spent coffee beans fermented in a submerged culture with and without *Pleurotus pulmonarius* mycelium.

At the beginning of storage, the results showed that the lowest lipid oxidation values (< 0.02 mg MDA kg^{-1}) were presented by the aqueous extracts obtained from the culture medium added with 5 and 10 % of spent coffee beans fermented with mycelium of *P. pulmonarius*, in comparison to the aqueous extracts obtained from fermented samples without the addition of residue and mycelium ($p \leq 0.05$). Lipid oxidation values increased during storage time ($p \leq 0.05$), with no changes observed in the oxidation values of meat extracts treated with an aqueous extract of spent coffee beans fermented with mycelium. At the end of storage (60 min), a reduction of lipid oxidation (> 70 % inhibition) was observed in the meat extract treated with aqueous extracts obtained from the culture medium added with 5 and 10 % spent coffee beans fermented with mycelium, compared to the rest of the treatments ($p \leq 0.05$).

Information related to the use of extracts obtained by fungal fermentation to increase oxidative stability in foods is limited. However, the antioxidant effect of extracts obtained from spent coffee beans on raw and cooked chicken meat during storage has been demonstrated (Kim *et al*., 2016). In a recent study, Vargas-Sánchez *et al*. (2023) evaluated the oxidative stability of pork meat treated with the aqueous extract of spent coffee beans fermented in a submerged culture using *P. ostreatus* mycelium. They proved that lipid oxidation values showed a reduction in meat samples treated with aqueous extracts fermented using the mycelium of this species.

Additionally, the principal component analysis showed that 91.3 % of the variation among treatments and parameters evaluated was due to two main components (76.7 and 14.6 %, respectively) (Figure 2).

The results showed a separation of treatments of fermented samples with and without *P. pulmonarius* mycelium compared to chemical composition and antioxidant activity, in dependence on the level of addition of spent coffee beans ($p \leq 0.05$) during fermentation.

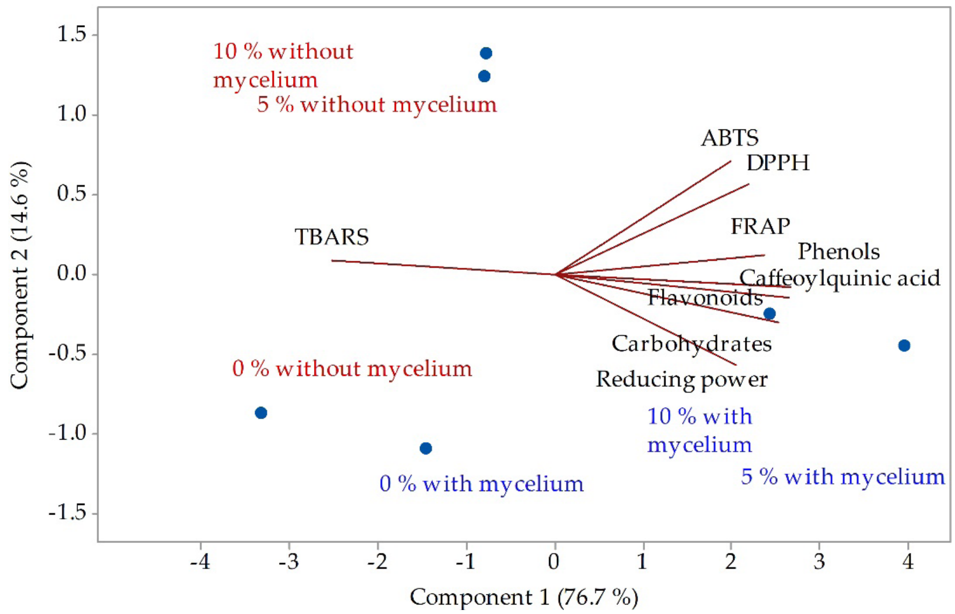

Figure 2. Principal component analysis of the parameters evaluated. TBARS: thiobarbituric acid reactive substances; DPPH: 2,2-diphenyl-1-picrylhydrazyl radicals; ABTS: 2,2′-azino-bis(3-ethylbenzothiazoline-6-sulfonic acid radicals; FRAP: ferric reducing antioxidant power.

CONCLUSIONS

The aqueous extract obtained by submerged culture fermentation using *Pleurotus pulmonarius* mycelium and spent coffee beans as substrate showed an increase in the content of metabolites (carbohydrates, phenols, flavonoids, and caffeoylquinic acid), as well as greater antioxidant activity by inhibiting the formation of free radicals and lipid oxidation while increasing the reducing power, compared to the fermented aqueous extracts without mycelium.

ACKNOWLEDGEMENTS

Rey David Vargas-Sánchez is grateful for the support received from CONAHCYT "Investigadoras e Investigadores por México" program.

REFERENCES

Ainsworth EA, Gillespie KM. 2007. Estimation of total phenolic content and other oxidation substrates in plant tissues using Folin-Ciocalteu reagent. Nature Protocols 2 (4): 875–877. https://doi.org/10.1038/nprot.2007.102

Albalasmeh AA, Berhe AA, Ghezzehei TA. 2013. A new method for rapid determination of carbohydrate and total carbon concentrations using UV spectrophotometry. Carbohydrate Polymers 97 (2): 253–261. https://doi.org/10.1016/j.carbpol.2013.04.072

Berker KI, Güçlü K, Tor İ, Demirata B, Apak R. 2010. Total antioxidant capacity assay using optimized ferricyanide/Prussian blue method. Food Analytical Methods 3 (3): 154–168. https://doi.org/10.1007/s12161-009-9117-9

Campos-Vega R, Loarca-Pina G, Vergara-Castaneda HA, Oomah BD. 2015. Spent coffee grounds: A review on current research and future prospects. Trends in Food Science and Technology 45 (1): 24–36. https://doi.org/10.1016/j.tifs.2015.04.012

Choi JW, Ra KS, Kim SY, Yoon TJ, Yu KW, Shin KS, Lee SP, Suh HJ. 2010. Enhancement of anti-complementary and radical scavenging activities in the submerged culture of *Cordyceps sinensis* by addition of citrus peel. Bioresource Technology 101 (15): 6028–6034. https://doi.org/10.1016/j.biortech.2010.02.083

Dey TB, Chakraborty S, Jain KK, Sharma A, Kuhad RC. 2016. Antioxidant phenolics and their microbial production by submerged and solid-state fermentation process: A review. Trends in Food Science and Technology 53: 60–74. https://doi.org/10.1016/j.tifs.2016.04.007

Echegaray N, Pateiro M, Munekata PE, Lorenzo JM, Chabani Z, Farag MA, Domínguez R. 2021. Measurement of antioxidant capacity of meat and meat products: methods and applications. Molecules 26 (13): 3880. https://doi.org/10.3390/molecules26133880

Griffiths DW, Bain H, Dale MFB. 1992. Development of a rapid colorimetric method for the determination of chlorogenic acid in freeze-dried potato tubers. Journal of the Science of Food and Agriculture 58 (1): 41–48. https://doi.org/10.1002/jsfa.2740580108

Kim JH, Ahn DU, Eun JB, Moon SH. 2016. Antioxidant effect of extracts from the coffee residue in raw and cooked meat. Antioxidants 5 (3): 21. https://doi.org/10.3390/antiox5030021

Liu SR, Zhang WR, Kuang YB. 2018. Production of stalk spawn of an edible mushroom (*Pleurotus ostreatus*) in liquid culture as a suitable substitute for stick spawn in mushroom cultivation. Scientia Horticulturae 240: 572–577. https://doi.org/10.1016/j.scienta.2018.06.068

Molyneux P. 2004. The use of the stable free radical diphenylpicrylhydrazyl (DPPH) for estimating antioxidant activity. Songklanakarin Journal of Science and Technology 26 (2): 211–219.

Murthy PS, Naidu MM. 2012. Sustainable management of coffee industry by-products and value addition-A review. Resources, Conservation and Recycling 66: 45–58. https://doi.org/10.1016/j.resconrec.2012.06.005

Mussatto SI, Machado EM, Martins S, Teixeira JA. 2011. Production, composition, and application of coffee and its industrial residues. Food and Bioprocess Technology 4 (5): 661–672. https://doi.org/10.1007/s11947-011-0565-z

Ogidi CO, Ubaru AM, Ladi-Lawal T, Thonda OA, Aladejana OM, Malomo O. 2020. Bioactivity assessment of exopolysaccharides produced by *Pleurotus pulmonarius* in submerged culture with different agro-waste residues. Heliyon 6 (12): e05685. https://doi.org/10.1016/j.heliyon.2020.e05685

Ozuna, LC, Mulík S, Valdez-Rodríguez B, Abraham-Juárez M del R, Fernández-López CL. 2020. The effect of organic farming on total phenols, total flavonoids, brown compounds, and antioxidant activity of spent coffee grounds from Mexico. Biological Agriculture and Horticulture 36 (2): 107–118. https://doi.org/10.1080/01448765.2019.1704876

Re R, Pellegrini N, Proteggente A, Pannala A, Yang M, Rice-Evans C. 1999. Antioxidant activity applying an improved ABTS radical cation decolorization assay. Free Radical Biology and Medicine 26 (9–10): 1231–1237. https://doi.org/10.1016/s0891-5849(98)00315-3

Samejo MQ, Sumbul A, Shah S, Memon SB, Chundrigar S. 2013. Phytochemical screening of *Tamarix dioica* Roxb. ex Roch. Journal of Pharmacy Research 7 (2): 181–183. https://doi.org/10.1016/j.jopr.2013.02.017

Shah MA, Bosco SJD, Mir SA. 2014. Plant extracts as natural antioxidants in meat and meat products. Meat Science 98 (1): 21–33. https://doi.org/10.1016/j.meatsci.2014.03.020

Vamanu E. 2012. Biological activities of the polysaccharides produced in submerged culture of two edible *Pleurotus ostreatus* mushrooms. Journal of Biomedicine and Biotechnology 565974: 1–8. https://doi.org/10.1155/2012/565974

Vargas-Sánchez RD, Esqueda M, Torres-Martínez BM, Torrescano-Urrutia GR, Sánchez-Escalante A. 2023. Antioxidant activity of the aqueous extract from spent coffee grounds fermented with *Pleurotus ostreatus*. Scientia Fungorum 54: e1433.

Xu XQ, Hu Y, Zhu LH. 2014. The capability of *Inonotus obliquus* for lignocellulosic biomass degradation in peanut shell and for simultaneous production of bioactive polysaccharides and polyphenols in submerged fermentation. Journal of the Taiwan Institute of Chemical Engineers 45 (6): 2851–2858. https://doi.org/10.1016/j.jtice.2014.08.029

Xu X, Shen M, Quan L. 2015. Stimulatory agents simultaneously improving the production and antioxidant activity of polyphenols from *Inonotus obliquus* by submerged fermentation. Applied Biochemistry and Biotechnology 176 (5): 1237–1250. https://doi.org/10.1007/s12010-015-1642-y

Zerva A, Tsafantakis N, Topakas E. 2021. Evaluation of basidiomycetes wild strains grown in agro-industrial residues for their anti-tyrosinase and antioxidant potential and for the production of biocatalysts. Fermentation 7 (1): 19. https://doi.org/10.3390/fermentation7010019

Zhishen J, Mengcheng T, Jianming W. 1999. The determination of flavonoid contents in mulberry and their scavenging effects on superoxide radicals. Food Chemistry 64 (4): 555–559. https://doi.org/10.1016/S0308-8146(98)00102-2

Agrociencia

YIELD STABILITY OF PURPLE CORN HYBRIDS (*Zea mays* L.) IN SOUTHERN SONORA, MEXICO

Gilberto **Rodríguez-Pérez**[1*], Alejandro **García-Ramirez**[1], Felipe de Jesús **Reynaga-Franco**[1], Jaime Edzael **Mendívil-Mendoza**[1], Francisco **Cervantes-Ortiz**[2], Enrique **Andrio-Enriquez**[2], Mariano **Mendoza-Elos**[2]

[1]Tecnológico Nacional de México, Campus Valle del Yaqui. Avenida Tecnológico Calle 600, Block 611, Bácum, Sonora, Mexico. C. P. 85276.
[2]Tecnológico Nacional de México, Campus Roque. Carretera Celaya-Juventino Rosas km 8, Celaya, Guanajuato, Mexico. C. P. 38110.
*Author for correspondence: gilberto.rp@vyaqui.tecnm.mx

ABSTRACT

Corn (*Zea mays* L.) production in Mexico is in deficit despite generating 27 million Mg. In southern Sonora, the planted area has grown significantly over the last four years, from 544 to 680 thousand Mg produced in 2018 and 2021, respectively. Ninety-seven percent of the production corresponds to improved white-colored maize from transnational companies; however, there are no commercial plantings of colored maize. The objective of this research was to estimate grain yield and its agronomic components in improved purple corn hybrids in southern Sonora, Mexico, over three years using the additive main effects and multiplicative interaction method (AMMI). A randomized, complete-block experimental design with three replications was used. The plots were two 4 m long furrows with a stocking density of 100 000 plants ha^{-1}. The variables recorded were: grain yield (RG), thousand-kernel weight (PMG), ear length (LM), grains per row (GH), rows per ear (HM), and hectoliter weight (PH). The results showed statistical differences among years, hybrids, and their interaction (AxH) in all variables. The AMMI model was highly effective, allowing the identification of hybrids 1, 2, 7, and 10 with greater stability in the year 2021 associated with RG, PH, and LM, obtaining outstanding averages in all variables and being more appropriate for the climatic conditions of southern Sonora. On the contrary, the most sensitive hybrid with the highest interaction was 4, associated with GH and HM; hybrids 3, 5, 6, 8, 9, 11, and 12 were stable with negative values in 2019 and 2020.

Keywords: purple hybrids, adaptability.

Citation: Rodríguez-Pérez G, García-Ramirez A, Reynaga-Franco F de J, Mendívil-Mendoza JE, Cervantes-Ortiz F, Andrio-Enriquez E, Mendoza-Elos M. 2024. Yield stability of purple corn hybrids (Zea *mays* L.) in southern Sonora, Mexico. **Agrociencia** 58(3): 301-313. https://doi.org/ 10.47163/ agrociencia.v58i3.2980

Editor in Chief: Dr. Fernando C. Gómez Merino

Received: February 24, 2023.
Approved: January 07, 2024.
Published in Agrociencia: April 24, 2024.

INTRODUCTION

In the last four years, corn (*Zea mays* L.) cultivation in southern Sonora has expanded from 48 967 to 785 860 ha, yielding 544 to 680 thousand Mg in 2018 and 2021, respectively. Ninety-seven percent of production corresponds to improved white corn produced with appropriate technologies and economic resources for crop development. An adequate average grain yield of 13.7 Mg ha^{-1} was obtained (SIAP, 2022).

Although improved hybrids from transnational companies with excellent yield stability are being planted (Vázquez-Carrillo *et al*., 2020), there are no records or breeding programs for pigmented corn such as purple corn, which represents an alternative to be established due to its yield and antioxidant properties. For this reason, it is important to promote planting and carry out agricultural management innovations for purple corn that can improve productivity in the local and state markets, in addition to adapting to the edaphoclimatic conditions present in southern Sonora. These are important measures to bring competitive materials in yield, stability, and price to significantly enhance grain production in corn (Acevedo-Barona *et al*., 2019).

Grain yield is the most important trait to consider when evaluating maize in different environments, since environmental effects (E) have a greater impact on this crop than genotypes (G) and genotype-environment interaction (IGA) (López-Morales *et al*., 2019). IGA is the differential relative behavior shown by genotypes when evaluated in different environments (Ponce-Encinas *et al*., 2022). Therefore, when plant breeders seek genotypes with superior yields for different locations or environmental conditions, they face challenges such as stability and adaptability (Fayeun *et al*., 2018). Stability is the genotype's ability to behave at high or low levels of performance across settings, whereas adaptability is the genotype's ability to display optimal development under varied environmental conditions (Neisse *et al*., 2018). Eberhart and Russell (1966) pointed out that stability is a genetic trait and that genotypes with wide adaptability possess low IGA; therefore, it is important to determine stability and adaptability for selection and recommendation of maize genotypes in specific environments (Ponce-Encinas *et al*., 2022).

The AMMI is a multivariate model that combines analysis of variance (ANDEVA) and principal component analysis (CP) in one. It requires fewer replications, and better captures the variation of the treatments. Gauch (2006) pointed out that effectiveness increases with the size of the trial, which can be increased by establishing trials in different environments. Additionally, it allows the evaluation of a larger number of genotypes without losing precision or increasing the cost of the experiments (Gauch and Zobel, 1996; Crossa *et al*., 1990). Most of the work with AMMI has emphasized grain production for different crops.

The segmented analysis of information in the study of IGA has been carried out in previous works such as that of Eberhart and Russell (1966), who used stability parameters to analyze grain yield. They also separated the environments based on yield, carrying out the corresponding analysis for each group of environments; in addition, they proposed a new classification of genotypes. For this reason, the objective of this research was to estimate grain yield and its agronomic components in southern Sonora in improved purple corn hybrids over three years using the AMMI method.

MATERIALS AND METHODS

Genetic material and experimental site

Twelve improved purple corn hybrids provided by CIMMYT (International Corn and Wheat Improvement Center) were used (Table 1).

Table 1. Genetic material for purple corn hybrids (*Zea mays* L.) evaluated over a three-year period in southern Sonora, Mexico.

Hybrid	Genealogy	Hybrid	Genealogy
1	GUAT1130/CML376//CML321///CML373	7	GUANGP28//CML373///CML376
2	MOR297/CML373//CML312///CML376	8	GUAT1130/CML376///CML373
3	GUAT1130/CML376///CML373	9	MOR297/CML373///CML376
4	LIM88/CML376//CML373	10	GUANGP24/CML313///CML376
5	MOR297/CML373//CML381///CML376	11	LIM88/CML313//CML373///CML311
6	MOR297/CML373//CML360	12	LIM88/CML374//CML312///CML376

The trials were established for three years of evaluation in the experimental field of the National Technological Institute of Mexico, Campus Valle del Yaqui, in Ciudad Obregón, Sonora, Mexico, located in the south of Sonora, between the Sierra Madre Occidental and the Gulf of California (27° 41’ 37” N and 100° 13’ 19” W) at an altitude of 13 m. The predominant climate is BW (h), which is very hot and extreme, with an annual mean temperature of 24 °C and a mean maximum of 31 °C. From July to August, the maximum is 48 °C and in January, the minimum is 16 °C, with an average annual rainfall of 450 mm. Arable soils are fertile, rich in clay, and generally located in sub-humid and arid areas with wet hydration and exposure, cracking when dry (García, 2004).

Agronomic management

Plantings were made on November 15, 2019, December 15, 2020, and January 15, 2021. The fertilization formula 250 N, 100 P, and 00 K was applied in two stages: 50 % of N and total P at the time of planting, and the rest at weeding 30 days after planting. Gravity irrigation was applied, ensuring that there was no lack of moisture in the soil.

Design and experimental unit

A randomized, complete block experimental design with three replications was used. The experimental unit consisted of two 4 m long rows, using spatial arrangements of 0.8 m spacing between rows and 12.5 cm distance between plants, with an expected population of approximately 100 000 plants ha^{-1}.

Response variables

The trials were established and harvested manually in each test environment. To determine the effect of the genotype-environment interaction and the productive potential in the studied hybrids, grain yield (RG) adjusted to 15 % moisture, grains per row (GH), rows per ear (HM), thousand-kernel weight (PMG), ear length (LM), and hectoliter weight (PH) were used.

Statistical analysis

Statistical analysis was performed by individual and combined analysis of variance (ANDEVA) for the mean of each experimental unit, using the GLM procedure of SAS, version 9.4 (SAS Institute, 2012). The combined ANDEVA was performed according to the following model:

$$Y_{ijkl} = \mu + t_i + R_j\,(l) + \beta k\,(R_{jl}) + \lambda l + \tau\lambda il + \varepsilon_{ijkl}$$

which considered the observation obtained in genotype I and evaluated in replicate j within each test year l, in block k; μ was the overall mean; ti was fixed effect of genotype; β*k* (*jl*) the random effect of block within replicate and year; λ*l* the random effect by year; τλ*il* the random effect of the interaction between genotype and year; and ε_{ijkl} the error associated with the observation Y_{ijkl}, according to Steel and Torrie (1988).

Once the presence of the genotype-environment interaction was detected, the multivariate analysis was performed to obtain the singular values of the first significant AMMI terms for the genotypes and environments. The calculation was based on the procedures reported by Vargas and Crossa (2000) using only the adjusted means, so it was necessary to provide the program with the information corresponding to the value of the combined error estimator, the degrees of freedom of this error, and the number of replications, according to the following mathematical model:

$$Y_{ijkl} = \mu + t_i + R_j\,(l) + \beta k\,(R_{jl}) + \lambda l + \tau\lambda il + \varepsilon_{ijkl}$$

where Y_{ij} represented the mean of genotype i in environment (year) j; μ the overall mean; *gi* and aj the effects of genotype and environment, respectively; n the number of principal components (CP) retained in the model; *k* the singular value for each CP; *ik* were values of the genotype vectors for each CP; *jk* the values of the environment vectors for each CP; *ij* the residual of the IGA; and ε_{ij} the mean experimental error.

Genotypic and environmental values were obtained using the PROC GML procedure of SAS. The significance of each CP was measured by Fisher's test at 0.05 probability, comparing the mean square of each CP with the mean square of the experimental error, according to Crossa *et al*. (1990). The number of possible axes (CP) that the model can retain in AMMI is the minimum (G-1; E-1); the axes that were not significant were included in the residual and the values of CP1 and the mean yield of genotypes/environments were used to construct the double biplot representation of the AMMI model (García *et al*., 2020).

RESULTS AND DISCUSSION

Statistical differences ($p \leq 0.01$) were evident in all study variables (Table 2). According to the additive main effects and multiplicative interaction model (AMMI), performed with the routine developed by Vargas and Crossa (2000) that contemplates replications as a main factor, it was observed that in years, hybrids, and the years x hybrids interaction (IGA), the variables PMG and GH obtained higher values in the mean squares, followed by PH and LM. The inequality between maize hybrids and environments (years) manifested a wide genetic difference in the environmental conditions that occurred by year (López-Morales *et al*., 2019). The significant statistical differences for the mean squares of all sources of variation in the analysis of variance coincide in significance with those reported in the two models, AMMI and SREG (Ponce-Encinas *et al*., 2022; García-Mendoza *et al*., 2021).

Table 2. Mean squares and significance of AMMI for grain yield and its agronomic traits of 20 purple corn hybrids (*Zea mays* L.) evaluated in southern Sonora, Mexico.

FV	GL	RG	PMG	PH	LM	HM	GH
Replication	2	0.86	0.09	0.14	0.50	0.50	0.10
Years (A)	2	9.98**	576.69**	38.17**	23.26**	86.40**	330.18**
Hybrids (H)	11	7.98**	36441.01**	61.86**	14.25**	44.79**	139.33**
A*H	22	0.17**	1.68**	0.10*	0.90**	2.20**	0.80*
CP1	12	7.32	33404.67	56.73	13.53	42.47	127.89
CP2	10	0.24	2.36	0.15	0.98	2.69	1.31
Residual	72	0.19	18.66	0.74	1.80	4.35	7.73
CV(%)		6.1	5.14	7.29	9.22	13.7	3.09

*,**Significant at 0.05 and 0.01 probability, respectively. FV: sources of variation; GL: degrees of freedom; RG: grain yield; PMG: thousand-kernel weight; LM: ear length; GH: grains per row; HM: rows per ear; PH: hectoliter weight; CP1: principal component 1; CP2: principal component 2; CV (%): coefficient of variation.

The AMMI analysis explained 98.91 % of the IGA (Figure 1) between grain yield and its components across the three years of evaluation, while hybrids H-1, H-2, H-6, H-7, and H-10 were more stable in RG, PH, and LM in 2021. In these variables, only the first principal component was highly significant, suggesting that the interactions of hybrids with years were more complex, probably due to differences in the maize studied, which undoubtedly influenced the coefficient of variation reported in that

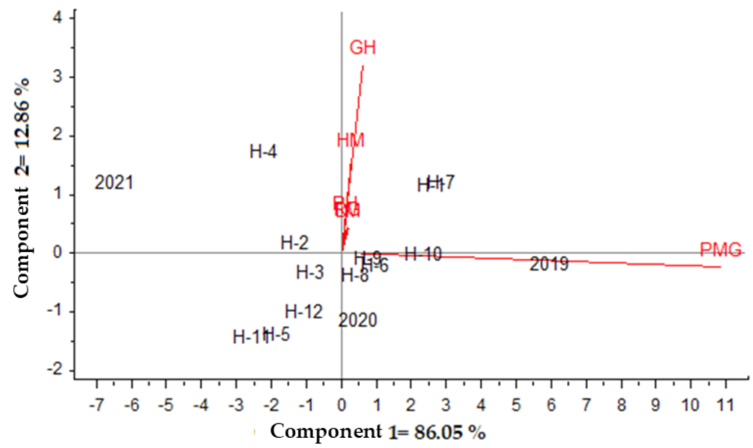

Figure 1. Genotype-environment interaction for grain yield and its components in purple corn hybrids (*Zea mays* L.) evaluated in southern Sonora, Mexico.

variable (Martínez-Gutiérrez *et al*., 2018). On the other hand, hybrids H-3, H-5, H-6, H-8, H-9, H-11, and H-12 in 2019 and 2020 were stable but presented negative values associated with PMG; however, the one with the highest interaction was hybrid H-4, which that had associations with GH and HM for being more distant to the center of origin and had yields lower than the overall mean (6.39 Mg ha^{-1}). These results coincide with those reported by Lozano-Ramírez *et al*. (2015).

Grain yield

The analysis graph for grain yield (Figure 2) shows that two components explained 98.81 % of the total variation in IGA. By plotting a polygon between the hybrids farthest from the origin and perpendicular lines going from the origin to each side of the polygon, the hybrids, and environments with response, it could be identified that hybrid H-6 had better yield in 2019 and 2021, with values higher than the overall average (6.58 Mg ha^{-1}), while the hybrids H-2, H-3, H-4, H-6, H-10, and H-12 were far from the vector, with yields lower than the overall mean, with average values of 6.12, 6.35, 5.78, 7.8, and 5.9 Mg ha^{-1}, respectively (Vázquez-Carrillo *et al*., 2018; López-Morales *et al*., 2019).

Environments (years) with long vectors are known to discriminate better among genotypes; in that sense, if we want to know how a hybrid adapts in the three years, we can trace an imaginary line from the origin where hybrids H-11 and H-8 presented low yields in 2020, having yields below the general average with 6.50, 6.43, and 6.36 Mg ha^{-1}, respectively. In this research, hybrids with high yields were located at the vertices that formed a polygon in the three years of evaluation that were outside the polygon and allowed discrimination among hybrids (Yan *et al*., 2016).

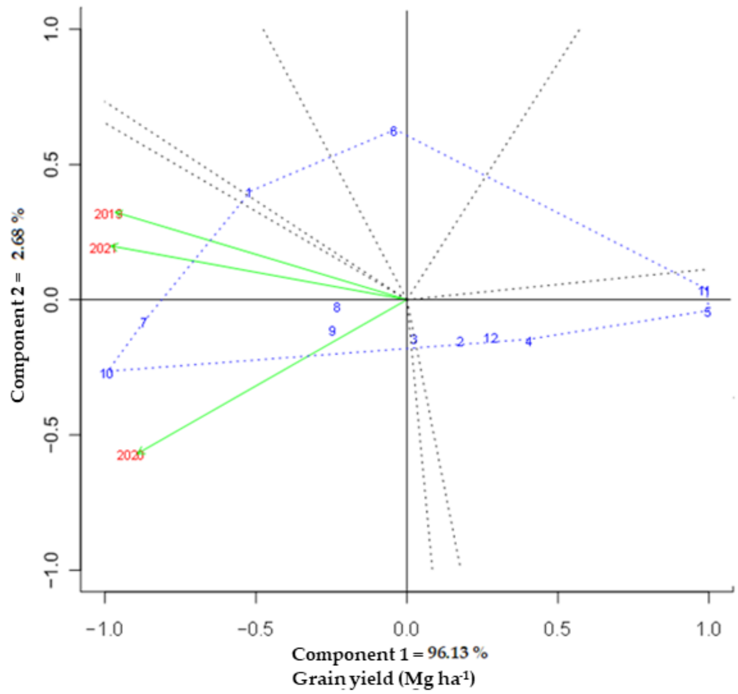

Figure 2. Biplot of the first two components of grain yield in purple hybrids (*Zea mays* L.) evaluated in southern Sonora, Mexico.

This type of classified stability is useful in agriculture, given that producers demand cultivars with desirable agronomic stability that show consistent behavior across environments while also responding favorably to environmental improvements; this means cultivars that present the best performance under any environmental condition (Acevedo-Barona *et al*., 2019).

Thousand-kernel weight

For the thousand-kernel weight, the components explained 99.94 % of the total variation in IGA (Figure 3). The hybrids with the highest weight were H-11, H-4, H-5, H-1, H-7, and H-10, with a sowing date in November 2019, which produced the best yields (7.88 Mg ha^{-1}) and could be considered a suitable environment with outstanding potential in the stability of these hybrids (García *et al*., 2020).

These findings suggest that thousand-kernel weight is the most important direct behavior in indirect yield selection for genotypes. In this sense, it can be inferred that the yields obtained in this research were due to agronomic management during crop development, which was strongly related to thousand-kernel weight. On the other hand, hybrids H-3, H-12, H-6, H-9, H-2, and H-8 obtained lower weights and were concentrated in the most distant vectors, presenting greater interaction.

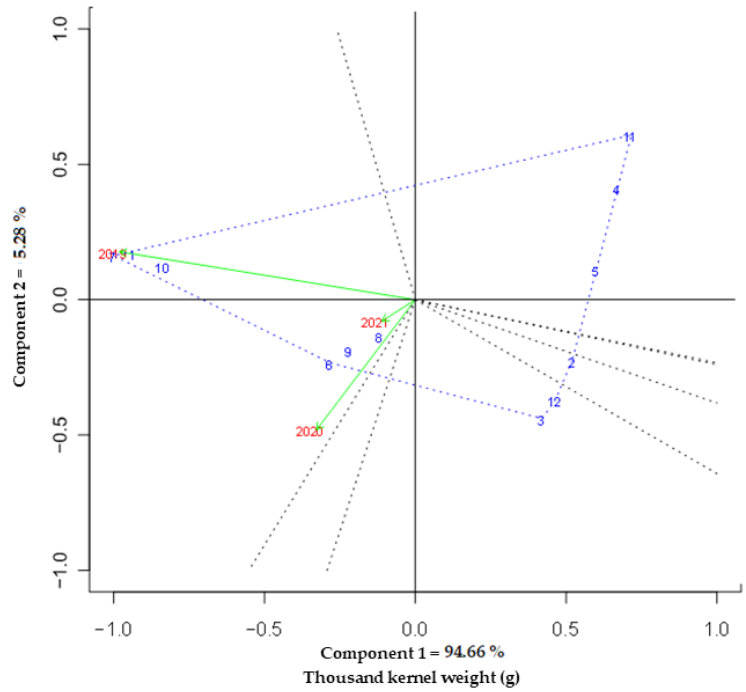

Figure 3. Biplot of the first two components of thousand-kernel weight (g) in purple hybrids (*Zea mays* L.) evaluated in southern Sonora, Mexico.

Salinas-Moreno *et al*. (2010) reported that large kernels have a weight greater than 380 g, medium sizes between 330 and 379 g, and small kernels have values less than 330 g. Based on this classification, only hybrid H-11 had large kernels (384.67 g); hybrids H-16, H-14, H-6, H-19, and H-15 were of medium size, while the rest had small kernels. It was observed that the grains obtained in 2021 were heavier than in 2019 and 2020; this could be a consequence of the sowing date in mid-November, which had a positive influence during the grain filling period. Vázquez-Carrillo *et al*. (2018) observed similar results regarding the positive effect of sowing date on grain filling and its effect on weight.

Hectoliter weight

The hybrids that presented favorable hectoliter weight were H-6, H-10, H-8, and H-4 (Figure 4), which were higher than the general mean with 83.7, 82.13, 80.63, and 80.44 kg hL^{-1}, respectively, being considered with greater stability, while hybrids H-9, H-1, H-3, and H-2 obtained values lower than the general mean (77.69 kg hL^{-1}).

Ninety percent of the hybrids had a hectoliter weight greater than 74 kg hL^{-1}, which is an indicator of grain hardness among the hybrids evaluated. This value indicates that the above hybrids are more crystalline than hybrids H-5, H-7, H-11, and H-12, whose

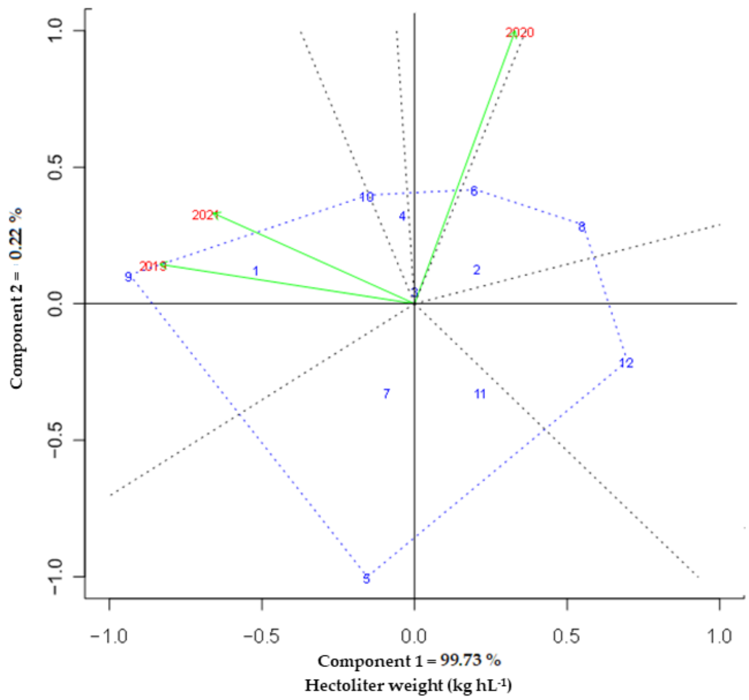

Figure 4. Biplot of the first two components of hectoliter weight in purple hybrids (*Zea mays* L.) evaluated in southern Sonora, Mexico.

values were lower than 74 kg hL^{-1} and negative, so they can be used as processed cereals (Vázquez-Carrillo *et al*., 2018).

Rows per ear

Hybrids H-2, H-8, and H-11 had the highest number of rows per ear in 2019 and 2021 (Figure 5), but hybrids H-4 and H-7 had lower values than the general average. Ponce-Encinas *et al*. (2022) reported that the hybrids standing out for their wide stability and adaptability in the genotype-environment interaction are the most suitable to be considered within a breeding program when they present higher values. On the other hand, the hybrids with the lowest number of rows per ear and negative values were H-12, H-8, H-10, H-6, H-9, and H-1, which contributed less to the number of rows per ear, in the December 2020 planting. This indicates that the selection of superior maize germplasm for grain yield is based on the consideration of traits such as the number of rows per ear, kernel size, or number of ears per plant (Ponce-Encinas *et al*., 2022).

Grains per row

The number of grains per row (Figure 6) shows that hybrids H-6, H-10, H-7, H-9, H-12, and H-8 had greater stability in 2019, which were sown in November. Other hybrids with low responses were H-1, H-2, H-3, H-5, H-4, and H-11. Such behavior could be

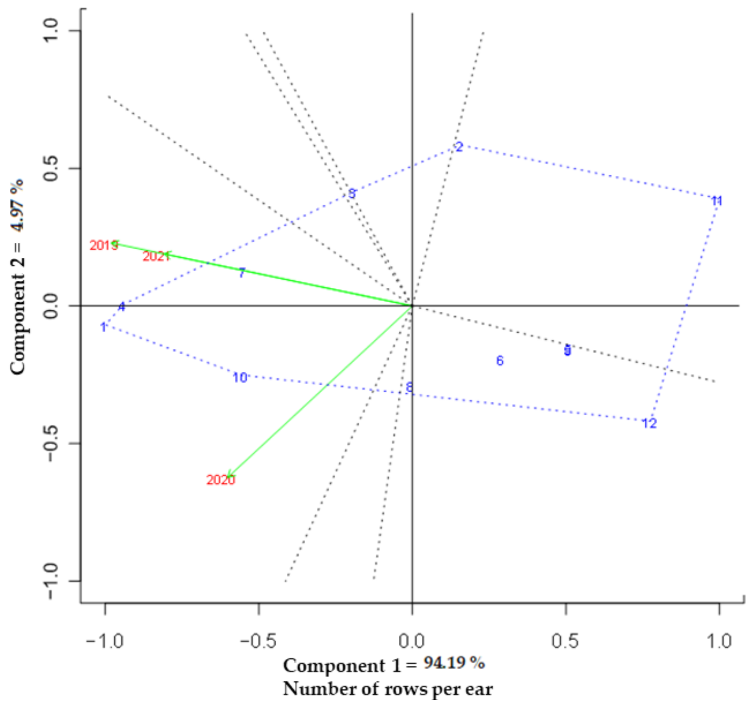

Figure 5. Biplot of the first two components of rows per ear in purple hybrids (*Zea mays* L.) evaluated in southern Sonora, Mexico.

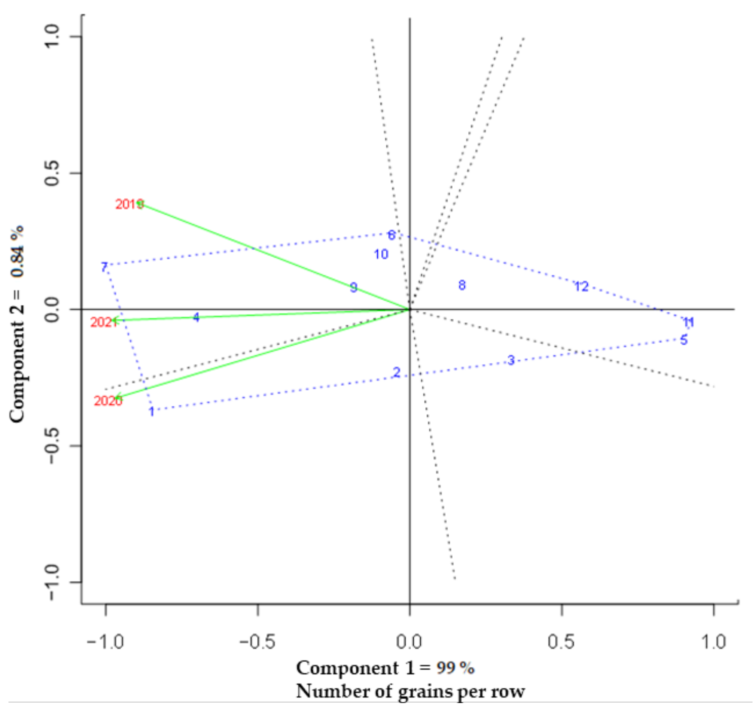

Figure 6. Biplot of the first two components of grains per row in purple hybrids (*Zea mays* L.) evaluated in southern Sonora, Mexico.

due to differences in sowing dates, which were in December and January 2020 and 2021, respectively (López-Morales *et al*., 2019).

Ear length

In terms of ear length (Figure 7), it was possible to identify those hybrids that adapted better, such as H-4 and H-10, which were closer to the vector direction, resulting in lengths greater than the overall average (15.2 cm) in 2019 and 2021. On the other hand, hybrids H-8, H-5, H-9, and H-7 were far from the vector, so their lengths were lower than the general average with values below 13 cm and presenting negative interactions with the first component, which is expected to have lower production. These results indicate that low-length hybrids were highly affected by IGA in the 2020s, which were sown in December.

Yan *et al*. (2016) reported that planting date and climatic conditions present during the crop cycle are factors that negatively influenced grain yield and other agronomic traits, such as thousand-kernel weight, hectoliter weight, ear length, kernels per row, and rows per ear; this was the case in this research, where planting in 2020 affected this variable by its lower values and consequently limited its agronomic utilization. On the contrary, hybrids in which greater lengths were obtained and were more stable may be viable in industrial and agronomic processing, which will allow farmers to

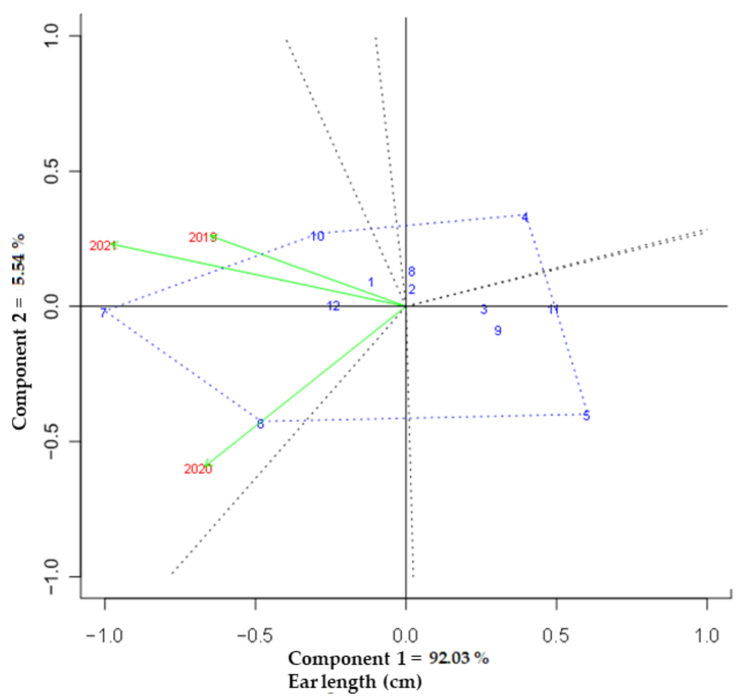

Figure 7. Biplot of the first two components of ear length in purple hybrids (*Zea mays* L.) evaluated in southern Sonora, Mexico.

offer hybrids with potential for the climatic conditions of southern Sonora (Acevedo-Barona *et al*., 2019).

CONCLUSIONS

Hybrids H-1, H-2, H-6, H-7, H-8, H-10, and H-11 were the most outstanding for their wide stability and adaptability in the genotype-environment interaction in 2021, being appropriate for grain production in the present climatic conditions of southern Sonora, Mexico. The additive main effects and multiplicative interaction model was useful to understand the genotype-environment interaction in grain yield and its components in the discrimination of the evaluated hybrids. The biplots allowed the identification of hybrids with higher grain yields and desirable agronomic characteristics.

REFERENCES

Acevedo-Barona M, Álvarez R, Silva R, Torres O, Reyes E. 2019. Interacción genotipo ambiente en arroz para identificar mega-ambientes y ambientes ideales mediante el modelo de regresión por sitios y biplot. Bioagro 31 (1): 35–44.

Crossa J, Gauch HG, Zobel RW. 1990. Additive main effects and multiplicative interaction analysis of two international maize cultivar trials. Crop Science 30 (3): 493–500. https://doi.org/10.2135/cropsci1990.0011183X003000030003x

Eberhart SA, Russel WA. 1966. Stability parameters for comparing varieties. Crop Science 6 (1): 36–40. https://doi.org/10.2135/cropsci1966.0011183X000600010011x

Fayeun LS, Alake CG, Akinlolu OA. 2018. GGE biplot analysis of fluted pumpkin (*Telfairia occidentalis*) landraces evaluated for marketable leaf yield in Southwest Nigeria. Journal of the Saudi Society of Agricultural Sciences 17 (4): 416–423. https://doi.org/10.1016/j.jssas.2016.10.001

García E. 2004. Modificaciones al sistema de clasificación climática de Köppen. Universidad Autónoma de México: Ciudad de México, México. 90 p.

García MPJ, Pérez CAA, Silva DRJ, Álvarez PRM, Monasterio PP, Taramona RLA. 2020. Evaluación del potencial agronómico de híbridos de maíz amarillo basado en el análisis GGE biplot y el modelo AMMI. Bioagro 32 (2): 95–106.

García-Mendoza PJ, Pérez-Almeida IB, Prieto-Rosales GP, Medina-Castro DE, Manayay-Sánchez D, Marín-Rodríguez CA, Ricse-Nestares JC, Ortecho-Llanos R, Medina-Hoyos AE. 2021. Interacción genotipo ambiente y potencial productivo de 25 variedades de maíz amiláceo en la provincia de Tayacaja, Perú. Bioagro 33 (2): 67–78. https://doi.org/10.51372/bioagro332.1

Gauch HG, Zobel RW. 1996. AMMI analysis of yield trials. *In* Kang MS, Gauch HG. (eds.), Genotype-by-Environment interaction. CRC Press: Boca Raton, FL, USA, pp: 85–122. https://doi.org/10.1201/9781420049374.ch4

Gauch HG 2006. Statistical analysis of yield trials by AMMI and GGE. Crop Science 46 (4): 1488–1500. https://doi.org/10.2135/cropsci2005.07-0193

López-Morales F, Chura-Chuquija J, García-Pando G. 2019. Interacción genotipo por ambiente del rendimiento de maíz amarillo en híbridos trilineales, Perú. Revista Mexicana de Ciencias Agrícolas 10 (4): 859–872. https://doi.org/10.29312/remexca.v10i4.1696

López-Morales F, Vázquez-Carrillo MG, García-Zavala JJ, López-Romero G, Reyes-López D, Molina-Galá JD. 2019. Estabilidad y adaptación del rendimiento y calidad de tortilla en maíz Tuxpeño, Valles-Altos. Revista Mexicana de Ciencias Agrícolas 10 (8): 1809–1821. https://doi.org/10.29312/remexca.v10i8.1851

Lozano-Ramírez Á, Santacruz-Varela A, San Vicente-García F, Crossa J, Burgueño J, Molina-Galán JD. 2015. Modelación de la interacción genotipo ambiente en rendimiento de híbridos de maíz blanco en ambientes múltiples. Revista Fitotecnia Mexicana 38 (4): 337–347. https://doi.org/10.35196/rfm.2015.4.337

Martínez-Gutiérrez A, Zamudio-González B, Tadeo-Robledo M, Espinosa-Calderón A, Cardoso-Galvão JC, Vázquez-Carrillo G, Turrent-Fernández A. 2018. Rendimiento de híbridos de maíz grano blanco en cinco localidades de valles Altos de México. Revista Mexicana de Ciencias Agrícolas 7 (9): 1447–1458. https://doi.org/10.29312/remexca.v9i7.1357

Neisse AC, Kirch LJ, Hongyu K. 2018. AMMI and GGE biplot for genotype x environment interaction: a medoid-based hierarchical cluster analysis approach for high dimensional data. Biometrical Letters 55 (2): 97–121. https://doi.org/10.2478/bile-2018-0008

Ponce-Encinas MC, López-Morales F, Chura-Chuquija J, Hernández-Leal E, Hernández-Salinas G, Aragón-García A. 2022. Interacción genotipo-ambiente del rendimiento en híbridos de maíz amarillo mediante AMMI y SREG. Revista Mexicana de Ciencias Agrícolas 13 (7): 1247–1258. https://doi.org/10.29312/remexca.v13i7.3070

SAS Institute. 2012. User's Guide of SAS. SAS Institute Inc. Cary, NC, USA. 550 p. https://doi.org/10.12691/ajbr-5-1-1

Salinas-Moreno Y, Gómez-Montiel NO, Cervantes-Martínez JE, Sierra-Macías M, Palafox-Caballero A, Betanzos-Mendoza E, Coutiño-Estrada B. 2010. Calidad nixtamalera y tortillera en maíces del trópico húmedo y sub-húmedo de México. Revista Mexicana de Ciencias Agrícolas 1 (4): 509–523.

SIAP (Servicio de Información Agroalimentaria y Pesquera). 2022. Avance de siembras y cosechas. Resumen nacional por estado. Gobierno de México. Secretaría de Agricultura y Desarrollo Rural. Servicio de Información Agroalimentaria y Pesquera. Ciudad de México, México. http://infosiap.siap.gob.mx:8080/agricola_siap_gobmx/AvanceNacio-nalCultivo.do (Retrieved: May 2022).

Steel R, Torrie J. 1988. Bioestadística: principios y procedimientos. McGraw-Hill: Ciudad de México, México. 640 p.

Vargas HM, Crossa J. 2000. El análisis AMMI y la gráfica del biplot en SAS. Universidad Autónoma de Chapingo (UACh), Unidad de Biometría y Estadística, Centro Internacional de Mejoramiento de Maíz y Trigo. Ciudad de México, México. 42 p.

Vázquez-Carrillo MG, Preciado-Ortiz RE, Santiago-Ramos D, Palacios-Rojas N, Terrón-Ibarra A, Hernández-Calette A. 2018. Estabilidad del rendimiento y calidad de grano y tortilla de nuevos híbridos de maíz con valor agregado para el subtrópico de México. Revista Fitotecnia Mexicana 41 (4): 509–518. https://doi.org/10.35196/rfm.2018.4-a.509-518

Vázquez-Carrillo MG, Martínez-Gutiérrez A, Zamudio-González B, Espinosa-Calderón A, Tadeo-Robledo M, Turrent-Fernández A. 2020. Estabilidad de rendimiento y características fisicoquímicas de grano de híbridos de maíz en Valles Altos de México. Revista Mexicana de Ciencias Agrícolas 8 (11): 1803–1814. https://doi.org/10.29312/remexca.v11i8.1990

Yan W, Frégeau RJ, Pageau D, Martin R. 2016. Genotype-by-environment interaction and trait associations in two genetic populations of oat. Crop Science 56 (3): 1136–1145. https://doi.org/10.2135/cropsci2015.11.0678

Agrociencia

TREE HEALTH ASSESSMENT IN AN INSTITUTIONAL GREEN SPACE: INAOE CASE STUDY

Luz de Lourdes **Saavedra-Romero**[1], Dionicio **Alvarado-Rosales**[1*]

[1]Colegio de Postgraduados Campus Montecillo. Programa en Fitosanidad-Fitopatología. Carretera Mexico-Texcoco km 36.5, Montecillo, Texcoco, State of Mexico, Mexico. C. P. 56264.
* Author for correspondence: dionicio@colpos.mx

ABSTRACT

Knowledge of the health condition of urban trees is fundamental for making decisions regarding management and resource allocation. The objective of this study was to determine the current health status of the trees at the National Institute of Astrophysics, Optics, and Electronics (INAOE) in San Andres Cholula, Mexico. Five health indicators previously used in urban forests were assessed. The structure and diversity indicator indicated the existence of 2210 trees, mostly (58.8 %) of small size (< 20 cm average diameter at breast height), 20 botanical families, and 32 tree species. The crown condition and its variables indicated high foliage transparency (> 40 %) in some of its species and low percentages of dieback. Live crown ratio and crown density were moderate in eight and six species, respectively. The tree damage indicator showed the existence of 44 damaging agents in 956 trees (43.3 % of the total), highlighting the ball moss (*Tillandsia recurvata*), the felt fungus of evergreen ash (*Septobasidium* sp.) associated with an armored scale, the same fungus also affecting white cedar (*Hesperocyparis lusitanica*) in association with another scale (a new record), and two bark beetles, *Hylesinus aztecus* in evergreen ash, and *Phloesinus* sp. in white cedar. Regarding the mortality indicator, 75 trees (3.3 %) were recorded. Finally, the soil condition indicated that the pH was close to neutral, with electrical conductivity values above 2 dS m^{-1} and a low beneficial mycoflora population. All these factors, together with the imbalance in tree diversity, high planting density, compacted soils, and the presence of risky trees, are negatively affecting the health of INAOE's tree community.

Key words: health indicators, plant diversity, crown condition, damage, soil.

INTRODUCTION

The importance of maintaining the environmental quality and health of forest ecosystems and urban forests is increasing due to the rapid development of urban centers (McDonnell and Kendal, 2018). In this context, and as part of the New Urban Agenda 2030, the United Nations, in its Sustainable Development Goal (ODS) 11, highlights the importance of green spaces to improve living standards and human health, foster social cohesion and inclusion, and ensure the sustainable development of cities. Therefore, some countries were committed to increasing the area of green, accessible, safe, and high-quality spaces (Borelli *et al*., 2018). Given this commitment,

Citation: Saavedra-Romero LL, Alvarado-Rosales D. 2024. Tree health assessment in an institutional green space: INAOE case study. **Agrociencia** 58(3): 314-330. https://doi.org/ 10.47163/agrociencia.v58i3.3034

Editor in Chief:
Dr. Fernando C. Gómez Merino

Received: June 15, 2023.
Approved: January 02, 2024.
Published in Agrociencia:
April 19, 2024.

increasing and/or maintaining the world's forested area is an unprecedented challenge. However, meeting current demands in an equitable manner is not easy. In European cities, for example, the green area per capita distribution varies by country, from 4 m^2 in Macedonia and southern Italy to 200 m^2 in Belgium and Austria (Fuller and Gaston, 2009). In Mexico City, 7.54 m^2 are reported (SEDEMA, 2017), so achieving an acceptable surface of green area per individual requires substantial economic resources, better urban planning (Peckham *et al.*, 2013), and greater environmental education.

Urban trees provide shade, remove pollutants from the atmosphere, capture carbon, reduce noise, and beautify the city, as well as contribute to improving the physical and psychological health of citizens. Their presence alone can increase property values by 9–27 %, depending on their location and health condition (Conway *et al*., 2010; Turner-Skoff and Cavender, 2019). The inclusion of healthy wooded areas is becoming increasingly important in urban development plans (Abebe and Megento, 2017). However, the current health condition of urban green areas must be studied in order to implement timely management strategies to mitigate precarious tree health conditions (Guerra-Hernández *et al*., 2021) and reduce possible tree risk situations (Macías-Muro *et al*., 2022). In this sense, different studies on the health assessment of urban trees using health indicators have been carried out in various parts of the world, including Mexico (Zaragoza-Hernández *et al*., 2015; Saavedra-Romero *et al*., 2021).

Not enough attention has been given to the institutional green areas, which are distinct from other types of green spaces. It is the responsibility of the authorities to offer quality green areas to students, teachers, and employees. Unfortunately, due to a lack of budget and vision, this is becoming increasingly difficult. Therefore, the objective of this study was to determine the current health condition of the trees belonging to the National Institute of Astrophysics, Optics, and Electronics (INAOE), as a prior step to making decisions regarding management, resource allocation, and congruence with the objectives of the New Urban Agenda 2030.

MATERIALS AND METHODS

Study area

The study was conducted in the green areas of INAOE at Santa Maria Tonantzintla, located in the municipality of San Andres Cholula in the state of Puebla, Mexico (19° 01′ 53″ N and 98° 18′ 55″ W), from January 27 to September 23, 2022. According to the points generated through the UTM Geo Map and Google Earth 2022 platforms, the institute has an area of approximately 7.5 ha and a general parking space of 0.53 ha (Figure 1).

Inventory and sampling

All standing trees (living and dead) between the buildings with a diameter at breast height (DBH) of more than 7.5 cm (Saavedra-Romero *et al*., 2016) were inventoried. A sampling was conducted using three 1000 m^2 circular plots (radius = 17.84 m) in the

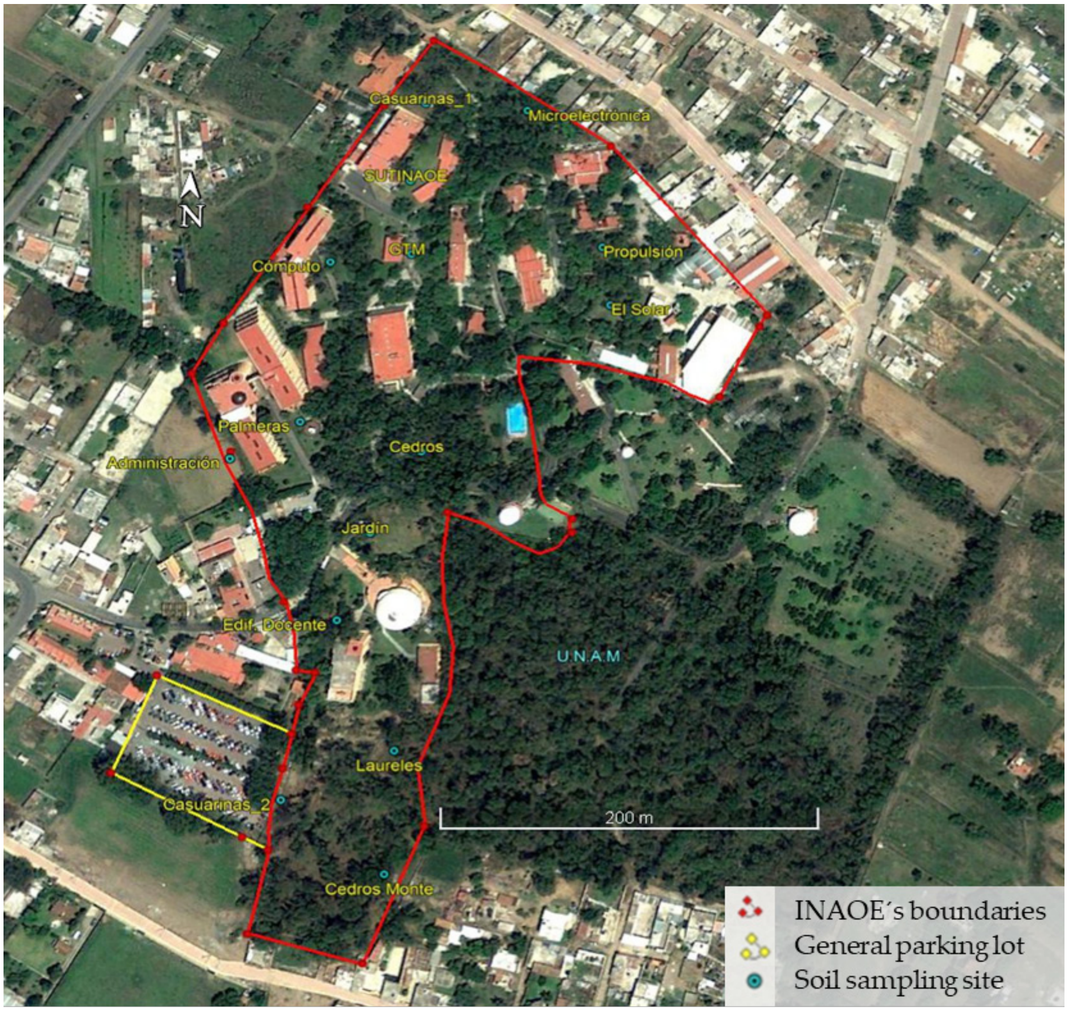

Figure 1. Polygon of the National Institute of Astrophysics, Optics, and Electronics (INAOE) in Santa Maria Tonantzintla, Puebla, Mexico, through UTM Geo-Map and Google Earth 2022 platforms.

"El Monte" portion (based on its topography, similar to a natural forest), located on the southern side (Casuarinas 2, Laureles, and Cedros Monte) (Figure 1).

Health condition assessment

The assessment was performed by recording five health indicators previously used in natural forests (Randolph, 2018) and adapted by Saavedra-Romero *et al*. (2016, 2019b, 2020, 2021) for urban green areas in Mexico City. Additionally, a tree risk assessment was carried out for potential damage to property and human lives (Saavedra-Romero *et al*., 2019a). The assessment description of each indicator is briefly described below.

Tree diversity and structure
Each tree was taxonomically identified. The DBH (calculated at a height of 1.3 m from the base of the tree) was measured using a Haglöf caliper, and the overall tree height was recorded using a Haga altimeter. These data were used to create frequency histograms.

Crown condition
Four absolute crown variables were assessed visually to estimate the amount, condition, and distribution of biomass in the crown of each tree at 5 % intervals (Randolph, 2015): a) live crown ratio (Lcr), b) crown density (CDen), c) foliage transparency (Ftra), and d) crown dieback (CDie). The results were expressed as average values per species.

Damage agents
Two damaging agents per live tree were recorded. In the case of epiphytic plants, the level of severity was recorded using the Hawksworth (1977) six-class system. Samples with symptoms and signs were collected and processed at the Forest Pathology Laboratory of the Postgraduate College in the municipality of Texcoco, State of Mexico, Mexico.

Soil condition
A fractionated auger was used to collect 33 composite soil samples at a depth of 15 cm in 5 cm increments. The laboratory analyses performed were: bulk density (BD) and porous space (PS), pH (soil:water ratio, 1:2.5), electrical conductivity (EC), and associated mycoflora. Fifteen areas of the INAOE were sampled (Figure 1).

Mortality
Previous studies suggest that trees, regardless of age, die as a result of the impact of different additive and interactive stressors (Hilbert *et al*., 2019). Dead trees were identified and, when possible, the probable reason was determined.

Tree risk assessment
The components included in the protocol were: a) probability of tree fall; b) probability of impacting a target based on area use; and c) size of the affected part (Saavedra-Romero *et al*., 2019a). In addition, associated structural damage was identified to obtain a final risk rating.

Data analysis

A data matrix was created using Excel and InfoStat software (version 2020) for statistical analysis. Descriptive and parametric statistics were used. Tukey's test (α = 0.05) was used to determine differences. The horizontal analysis for the soil condition indicator was performed with the average of the three sampling depths (0–5, 5–10, and 10–15 cm).

RESULTS AND DISCUSSION

Tree structure and diversity

From the inventory, a record of 2210 trees was obtained. The results for DBH and total height (m) show that, although there are specimens of considerable size, most of the trees are small, with an average diameter of 23 cm and an average height of 11 m (Figure 2). According to Richards (1983), urban green areas with a balanced and acceptable population distribution should have the following DBH categories: a) 40 % of the population with diameters < 20 cm; b) 30 % of the trees with diameters between 20 and 40 cm; d) 20 % from 40 to 60 cm; and d) 10 % greater than 60 cm. Based on this criterion, most of the trees in the INAOE are young, with diameters less than 20 cm (58.5 %), and will eventually replace mature, ill, and dead trees; 30.6 % had diameters

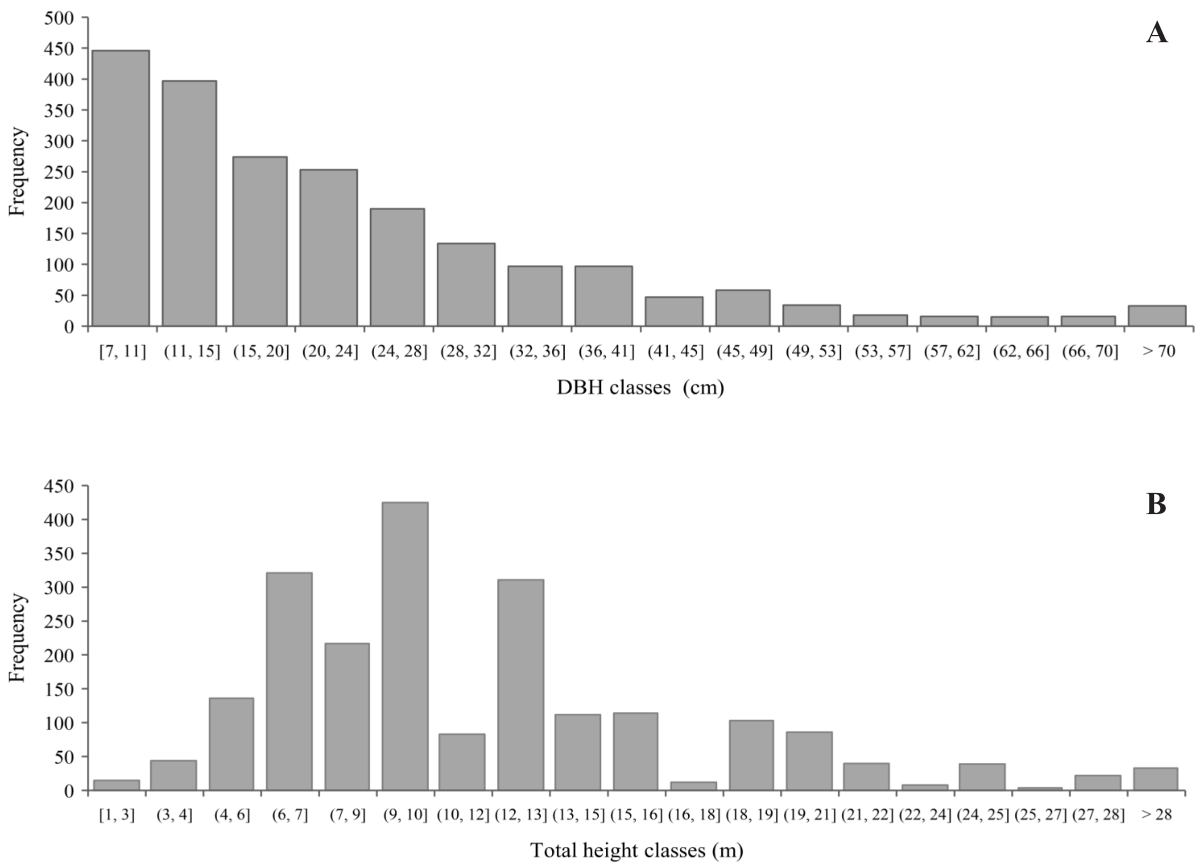

Figure 2. Frequency histograms for the 2210 trees evaluated at the INAOE in Santa Maria Tonantzintla, Puebla, Mexico. A: frequencies by diameter at breast height (DBH); B: frequencies by total height (m).

between 20 and 40 cm; 7.7 % between 40 and 60 cm; and finally, 3.1 % had values greater than 60 cm in diameter. It is advised not to plant any additional trees and to prioritize care for the young ones.

In terms of diversity, 20 botanical families of trees and two families of monocotyledons (Arecaceae and Asparagaceae) were identified. The most frequent families were Cupressaceae, Myrtaceae, Bignoniaceae, Oleaceae, and Casuarinaceae, among others, whose values were less than 7 %. Species richness was 32, with White cedar (*Hesperocyparis lusitanica* (Mill.) Bartel, synonym of *Cupressus lusitanica*), Red gum (*Eucalyptus camaldulensis* Dehnh.), Australian oak (*Casuarina equisetifolia* L.), Blue jacaranda (*Jacaranda mimosifolia* D. Don), and Evergreen ash (*Fraxinus uhdei* (Wenz.) Lingelsh) the most frequently occurring species (Figure 3). Two palm species were also recorded, Canary Island palm (*Phoenix canariensis* H. Wildpret) and Mexican fan palm (*Washingtonia robusta* H. Wendl).

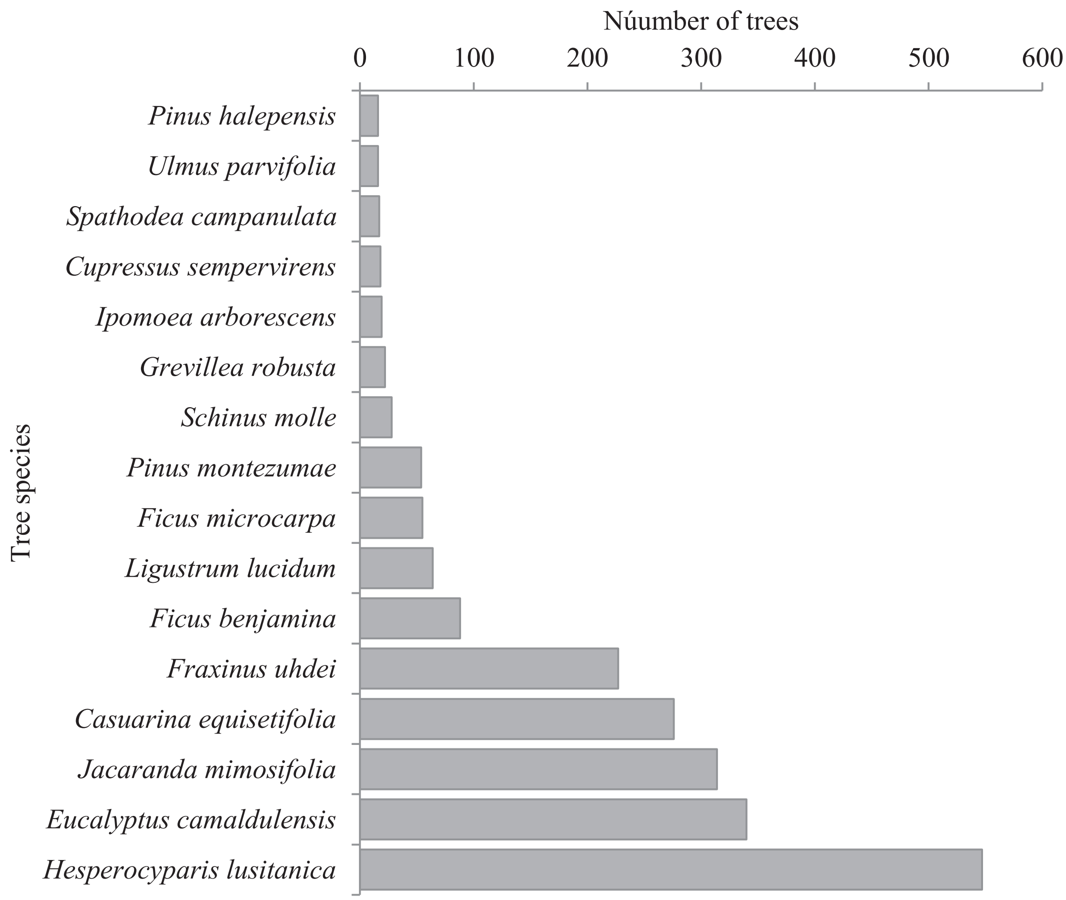

Figure 3. Main tree species identified in the green areas of INAOE in Santa María Tonantzintla, Puebla, Mexico (only 16 species are included).

For the diversity and stability of the tree community, maximum allowable percentages were proposed by species, genus, and family, which should not exceed 10, 20, and 30 %, respectively. The objective of this rule is to maximize the protection and conservation of urban forests against potential outbreaks of exotic and/or native pests and diseases (Calaza, 2021; Kendal *et al*., 2014; Saavedra-Romero *et al*., 2019a, 2019b). At INAOE, five species that do not meet the aforementioned standard (*Hesperocyparis lusitanica, Eucalyptus camaldulensis, Jacaranda mimosifolia, Casuarina equisetifolia*, and *Fraxinus uhdei)* present frequencies higher than 10 %. By genus, *Cupressus* exceeded 25 % of the tree population, and by family, none reached the established 30 % limit, so it is suggested not to increase the number of species mentioned and focus management activities on the existing ones.

Crown condition

In recent decades, comprehensive methods have been developed to assess, monitor, and detect early stress problems that impact the health of natural and urban forests (Alvarado-Rosales and Saavedra-Romero, 2021). The visual evaluation of the tree crown condition is one of the research lines of greatest interest because, through it, it is possible to distinguish symptoms of early and advanced stress, manifested by the amount of foliage present on the tree and by the way it is distributed along the trunk (Pontius and Hallet, 2014). At INAOE, during the dry season months (January to April), measurements of live crown ratio (Lcr), crown density (CDen), foliage transparency (FTra), and crown dieback (CDie) were recorded for tree species showing full leaf expansion only (for *Fraxinus uhdei* and *Jacaranda mimosifolia*, we waited until the rainy season). The percentages of Lcr were higher in *Cupressus sempervirens* and lower in *Eucalyptus camaldulensis* (Figure 4).

However, according to Saavedra-Romero *et al*. (2016), values above 30 % represent an adequate health condition. High foliage transparency (> 40 %) and low dieback rates were observed in some species. At least eight species had a moderate live crown ratio (31 to 50 %), and six had a poor to moderate crown density (< 40 %). According to different studies, the crown condition indicator displays a number of benefits, including its ability to detect symptoms of early stress and symptoms of imminent death. Therefore, all of its variables can be used to assess tree health.

Symptoms of early stress

Decreased photosynthetic efficiency is an initial symptom of loss of health (depending on species and season). However, this precedes, in many cases, the loss of foliage (increased transparency) (Pontius and Hallet, 2014). In the INAOE, species such as *Hesperocyparis lusitanica, Ligustrum lucidum, Eucalyptus camaldulensis,* and *Pinus montezumae* showed moderate transparencies, with values between 21 and 40 % (Figure 4), while *Pinus halepensis, Jacaranda mimosifolia,* and *Fraxinus uhdei* showed severe transparencies (> 40 %). While foliage loss may be caused by tree phenology, physiology, or both, it may also be caused by chronic stress; the latter is of particular importance.

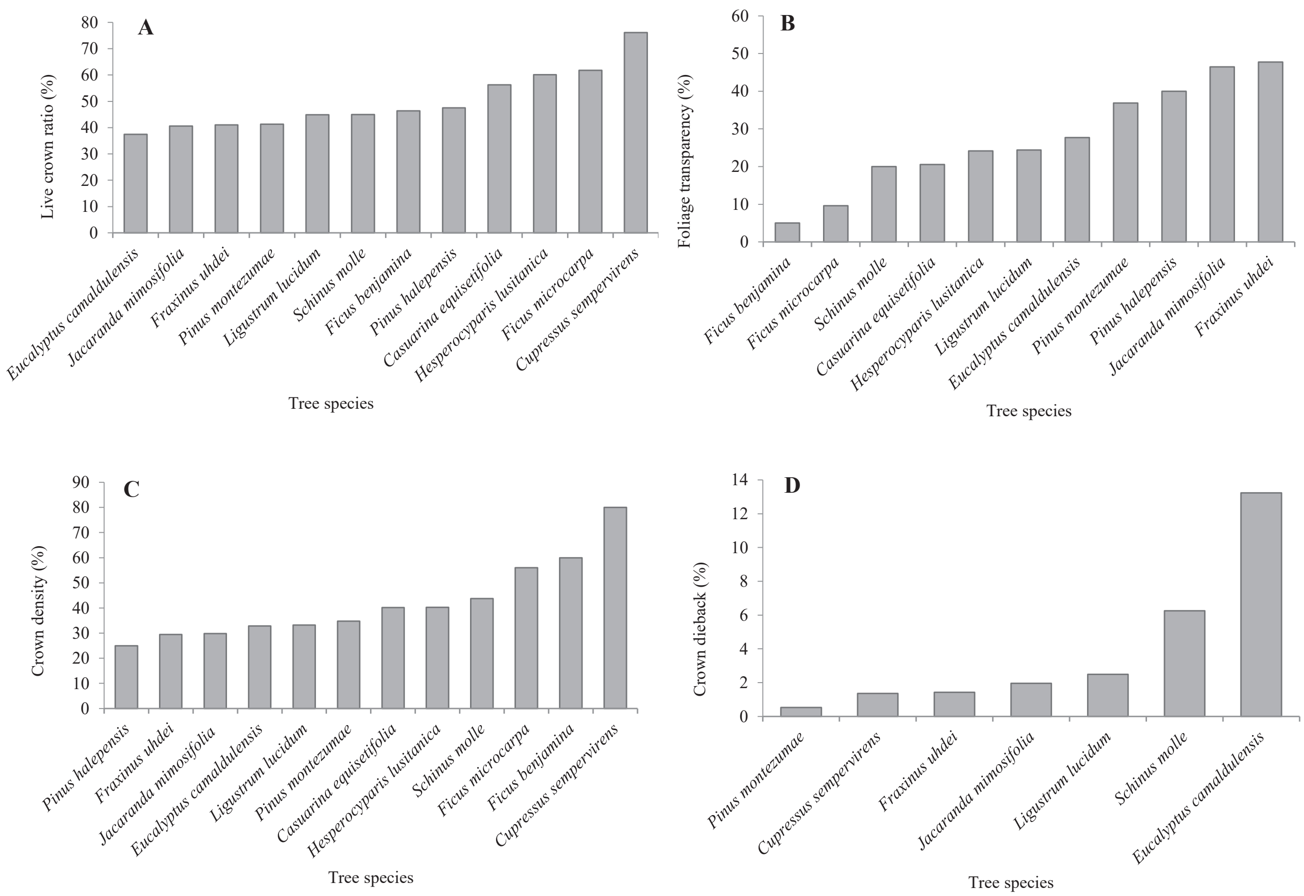

Figure 4. Average percentages of crown variables by tree species registered in the INAOE in Santa María Tonantzintla, Puebla, Mexico. A: live crown ratio; B: crown density; C: foliage transparency; D: crown dieback.

Symptoms of moderate stress

When predicting survival, crown dieback has been shown to be one of the most important variables (Morin *et al*., 2015). In response to moderate stress, dieback is evidenced by the appearance of clusters of bare branches and twigs (without foliage), starting at the terminal part of a branch and progressing towards the trunk (Randolph, 2023). The death of these fine twigs can be categorized as a measure of recent health impact (that the death of these tissues has occurred in recent years). In this regard, in the INAOE, dieback showed low averages; only *Schinus molle* and *Eucalyptus camaldulensis* showed percentages in the light category (6 to 20 %) (Alvarado-Rosales *et al*., 2021). However, other species such as *Fraxinus uhdei* and *Jacaranda mimosifolia*, whose twig dieback is increased by ball moss (*Tillandsia recurvata*) infestation, should not be overlooked.

Symptoms of decline

Among the final and obvious symptoms of tree health loss is the progressive crown reduction (crown shrinkage). In general, lower branches are first lost in several species due to shading, competition, or other damaging agents, until tufts of live foliage remain only in the upper part of the crown. In the green areas of the INAOE, at least eight species showed Lcr values in the moderate category (between 31 and 50 %). Four species were found in the adequate category (> 50 %) (Figure 4).

Healthy trees

Typically, trees with dense foliage (i.e., closed canopies) are associated with high growth rates, while small canopies and sparse foliage are related to a declining state (Randolph, 2018). The crown density variable, which is interpreted as the amount of foliage, branches, twigs, flowers, and fruits present in the crown, ranged from poor to moderate (0 to 40 %) in six species. The rest presented values above 50 % (adequate category); however, it was not possible to identify any individual in the optimum category. In summary, within a species, high values of crown density and low values of transparency and dieback are associated with healthy trees (Randolph, 2015). For INAOE trees, attention should be paid to trees showing the symptoms of decline described above at the time of maximum leaf expansion, depending on the species.

Damage agents

In the green areas of the INAOE, 44 damaging agents were identified in 956 trees (43.3% of the inventoried trees). Based on incidence, the ball moss or paxtle (*Tillandsia recurvata*) stood out with 37.23 %, followed by the felt fungus of evergreen ash (*Septobasidium* sp.) (6.17 %), bark beetle of evergreen ash (*Hylesinus aztecus*) (5.12 %), psyllid of red gum (*Glycaspis brimblecombei*) (5.12 %), black fungus of white cedar (*Septobasidium* sp.) (2.09 %), and the bark beetle of white cedar (*Phloesinus* sp.) (1.98 %) (Figure 5). By tree species, *Hesperocyparis lusitanica, Fraxinus uhdei*, and *Jacaranda mimosifolia* showed the highest populations of *T. recurvata*, with average severity levels of 2.6, 3.09, and 3.14 (on a Hawksworth rating system of 1 to 6), respectively, which could be an indicator that these species and the prevailing climatic conditions favor its development.

In white cedar, trunk cracks were prominent, making evident the prolonged periods of drought that have encouraged this damage. Finally, although bromeliads are reported as indicators of good growing conditions by providing enormous ecosystem benefits (Ladino *et al*., 2019), their high populations cause branches, particularly those of *Jacaranda mimosifolia*, to bear excessive weight, turning these individuals into risk trees. By green area (Figure 1), the trees in the Enrique Chavira Building had the highest populations of ball moss, with an average severity of 3.77, followed by El Solar with 3.11 and to a lesser degree, the Optics Building, with a value of 1.

Regarding the presence of insects, two bark beetles were identified: *Phloesinus* sp., classified as secondary and affecting 19 white cedars, and *Hylesinus aztecus* on 35 ash trees. The presence of these insects is of concern, as attacks have been reported only

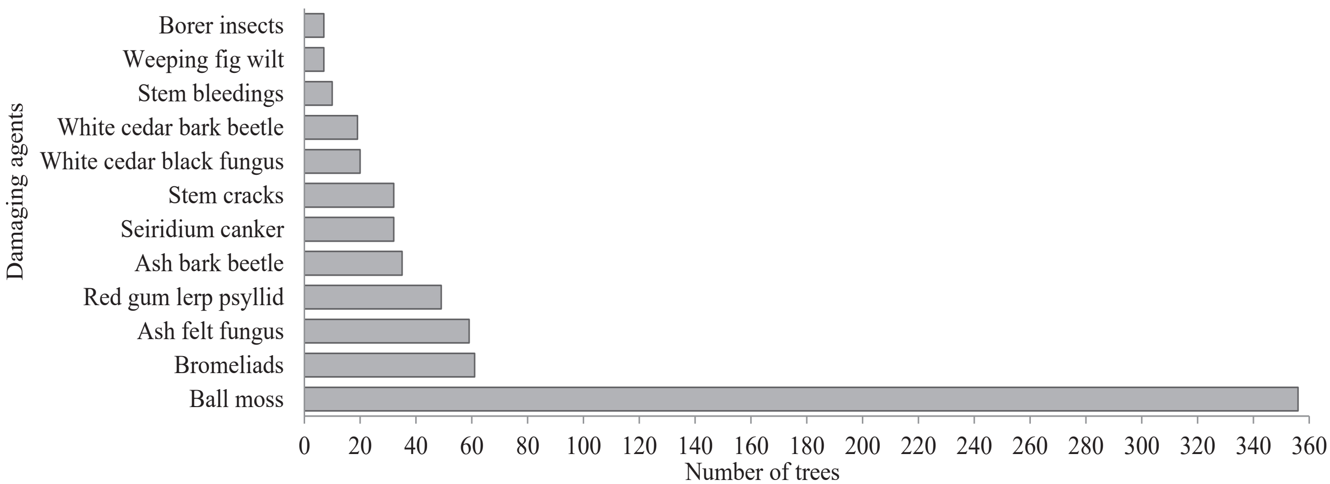

Figure 5. Damaging agents with greater representation in the green areas of the INAOE in in Santa María Tonantzintla, Puebla, Mexico. Twelve damaging agents affecting n ≥ 7 trees are shown.

on mature trees with large diameters. Unfortunately, in the INAOE, both insects are killing young trees that are perceived to be stressed, mainly due to high temperatures and a lack of soil moisture, factors that coexist with outbreaks of these type of insects, which have modified their growth patterns and larval development, causing the death of different woody species in different regions (Allen *et al*., 2010; Bentz *et al*., 2010).

Other agents that are causing damage are the felt fungus of ash and the black fungus of white cedar, both belonging to the genus *Septobasidium*. The first causes large tumors and the death of branches above the point of infection. Similar symptoms were reported by Galindo (1968) in the State of Mexico, Querétaro, Michoacán and Mexico City, who identified it as *Septobasidium curtisii* (Berk & Desm) Boed. & Stein, associated with two scales, *Melanaspis nigropunctata* and *Situlaspis* sp. A similar relationship is reported in Korea between *Septobasidum* spp., *Schisandra chinensis* (Turcz) Baill, and the scale *Pseudaulacaspis cockerelli* Cooley (Choi *et al*., 2016).

Regarding the black fungus of white cedar, it was observed that its growth is restricted to the lower branches of the crown, where shade and moisture conditions are higher. Once its development begins, the hymenium is beige in color, and when infections are old, it dehydrates and detaches in small black lamellae. Affected twigs have a brown coloration and die towards the tip. This fungus is also associated with a scale insect; however, there are few studies on its identity. Worldwide, *S. cupressi* Couch, *S. crustaceum* Couch, and *S. mexicanum* Sydow are reported on cedar (Gómez and Henk, 2004), but they are not reported associated with any scale. For INAOE, although the same fungal genus was identified in both hosts, the identity of the fungal and scale species is still unknown.

Based on this information, it is recommended that management activities be implemented to reduce ball moss populations by hand and by spraying sodium bicarbonate solutions. Removing and burning trees attacked by bark beetles. Finally, pruning of infected branches, with tumors and those killed by the evergreen ash felt fungus and white cedar black fungus.

Mortality

Tree mortality is a natural and essential process in all healthy forest ecosystems; however, changes in mortality rates require careful examination to identify possible causes. A high percentage of tree mortality may indicate that forest stands are over-mature (Ambrose *et al*., 2022), that there are problems with pests and diseases, or the effect of climate change. It is vital to identify the factors that influence tree death, their frequency, and the volume of timber they are affecting. This can help managers target resources needed for remediation activities and improve the condition of remnant trees, a practice that should certainly be contemplated in periodic management plans (Hilbert *et al*., 2019).

In the INAOE, the number of dead trees in its green areas was 3.3 %; that is, 75 trees were found in this condition. The genus *Cupressus* presented the highest number of dead individuals, followed by *Eucalyptus* and, to a lesser degree, *Fraxinus*. Regarding cedars, the main cause of death was bark stripping and prolonged periods of drought. As for the eucalyptus trees, most of them were large and old. It is suggested to remove and burn dead trees, particularly those attacked by bark beetles, in order to avoid dispersion to adjacent areas and to avoid the risk of falling due to weak structure.

Tree risk identification

All wooded areas, including institutional areas, require a program to detect trees at risk. A tree at risk is defined as those trees with an unstable structure and located at a short distance from impacting human lives and material assets, such as cars, and infrastructure, such as buildings, telephone, electricity, and drinking water lines. Twenty-one trees were identified with the aforementioned defects. Among them are *Pinus montezumae* (8), *E. camaldulensis* (5), *Erythrina coralloides* (3), *Fraxinus udhei* (1), *Schinus molle* (3), and *Buddleja cordata* (1).

The areas that require priority attention due to the presence of these trees are the internal parking lot (in front of the central garden), the garden next to the guardhouse, the Enrique Chavira Building, as well as the general parking lot, where white cedar and eucalyptus trees are of considerable size. In this sense, it is essential to implement management actions for the removal of these specimens, or part of them, in order to reduce the risk to students, teachers, and administrative personnel, as well as to the infrastructure.

Soil condition

Soil, as a substrate, is the most important component influencing plant survival and vitality. Trees require a constant, sufficient, and adequate supply of non-compacted soil, with excellent oxygen diffusion, good moisture retention, and drainage, among other properties. For most vegetated areas, such properties determine which plants and animals (macro- and microfauna) can live on or in the soil (Francini *et al*., 2018). Based on the properties evaluated in the INAOE soils, the average values for each one and the confidence intervals at 95 % are shown. The average pH was 6.54, with a confidence interval of 6.02 to 6.85 (Table 1).

Table 1. Descriptive statistics and confidence intervals (95 %) for the properties evaluated in the INAOE soils.

Variable	Depth (cm)	Mean	S.E.	L.L.	U.L.
pH	5	6.42	0.22	5.95	6.89
	10	6.41	0.29	6.00	6.83
	15	6.45	0.25	5.92	6.98
Electrical conductivity (EC) ($dS\ m^{-1}$)	5	3.35	0.41	2.47	4.22
	10	2.25	0.41	1.38	3.12
	15	1.80	0.28	1.19	2.40
Bulk density (BA) ($g\ cm^{-3}$)	5	1.15	0.07	0.99	1.31
	10	1.39	0.06	1.27	1.51
	15	1.38	0.05	1.26	1.49
Porous space (PS) (%)	5	56.70	2.32	51.83	61.57
	10	47.77	1.69	44.21	51.32
	15	47.79	1.64	44.13	51.46

S.E: standard error; L.I: lower limit; U.L: upper limit of the confidence interval.

Indirectly, soil reaction influences plant growth through its effect on ionic solubility and microbial activity. A satisfactory pH range for the growth of many plants ranges from 5.5 to 8.3. Other "acid soil loving" species do well at pH between 4.0 and 6.5. For the tree species identified in the study area, adequate development at the pH obtained is reported, but they can tolerate even alkaline soils (7.5 to 8.2) (Samson *et al*., 2017). Regarding electrical conductivity, the average was 2.46 $dS\ m^{-1}$ (Table 1). However, eight areas presented conductivities > 2.0, which could restrict the growth of sensitive species (Pallardy, 2008). Bulk density averaged 1.3 $g\ cm^{-3}$ (Table 1), and at least six sections of the INAOE had even higher densities. According to Hillel *et al*. (2004), bulk density values that can restrict root development vary according to soil texture, from 1.4 $g\ cm^{-3}$ in clay soils to 1.7 $g\ cm^{-3}$ in sandy soils. The pore space was greater than 50 %, which favors root penetration and a greater diversity of micro and macrofauna, fungi, bacteria, and ascomycetes (Goswami *et al*., 2020).

Finally, regarding soil-associated mycoflora, based on morphological characters (Barnett and Hunter, 1998; Leslie and Summerell, 2006), the filamentous fungi *Aspergillus* spp., *Fusarium* spp., *Penicillium* spp., *Alternaria* sp., *Cladosporium* sp., *Paecilomyces* sp., *Trichoderma* sp., and *Mucor* sp. were identified, the first three with more than one morphotype (variable colony color and shape). During the dry season, populations ranged from 2000 to 9 642 000 cfu g^{-1} (colony forming units per gram of soil), while in the rainy season, populations ranged from 2000 to 7 210 000 cfu g^{-1} soil. It is worth mentioning that, despite the expectation of finding higher populations during the rainfall season, this did not occur, possibly due to the xerophytic character of some genera such as *Aspergillus* (Piontelli, 2014). Finally, although fungal populations were high for some genera, low numbers of beneficial fungal propagules, such as *Trichoderma* and *Paecilomyces*, were evident.

The characterization of INAOE soils will help us to plan and execute activities aimed at improving their condition, including decompaction in areas such as the Propulsion Laboratory, El Solar, SUTINAOE, Casuarinas 1, the Computer Building, and GTM (Figure 1). For this purpose, the incorporation of compost, mulch, and beneficial microorganisms is strongly recommended. It is worth mentioning that the Institute continuously obtains organic waste from grass and tree pruning, which could be used to produce its own compost.

Within cities, tree species composition is variable among different land uses (Knapp *et al.*, 2009), but perhaps institutional green areas should have the highest quality in terms of health. They should also have greater biological diversity and excellent soil quality, but this is far from reality, so the authorities must strive to preserve and manage their green infrastructure with the few resources that are annually allocated to them. Exceptional cases include some private institutions that allocate resources to increase and preserve their forested areas. Finally, it is important to mention that there are protected natural places around the world that, due to their biological and usage qualities, are protected by the government and their inhabitants. The green areas of INAOE, a renowned institution in the field of astronomical sciences, deserve to be preserved and improved in order to contribute to the comfort and development of the activities of its staff, to reduce pollution and the impact of climate change on the environment.

CONCLUSIONS

Based on different health indicators, the following points can be highlighted about the tree stock at the National Institute of Astrophysics, Optics, and Electronics: (a) there are 32 tree species and 20 families; (b) most of the tree stock is young (40 %, with diameter at breast height < 20 cm) and at high planting densities; (c) there are early stress symptoms in *Pinus halepensis*, *Jacaranda mimosifolia*, and *Fraxinus uhdei* (higher transparencies), moderate in *Schinus molle* and *Eucalyptus camaldulensis* (low dieback percentages), and adequate health in seven species (high live crown ratio and crown density); (d) tree mortality was low (3.3 %); e) presence of two bark beetles, *Hylesinus aztecus* on evergreen ash (from which no previous reports exist on small diameter trees) and *Phloesinus* sp. on white cedar; f) there is presence of *Tillandsia recurvata* on jacaranda; g) there is presence of *Septobasidium* sp. on evergreen ash and white cedar; h) soils are compact and poor in beneficial mycoflora; and i) 21 trees are considered a risk to property and human lives. These aspects should be considered in any future management program in the study area.

ACKNOWLEDGMENTS

To the National Institute of Astrophysics, Optics, and Electronics (INAOE), for funding the study. In particular, to Miguel Ángel Barrera, Genaro Becerra M., and his team responsible for the management of the green areas, for their support and guidance during the development of the field phase.

REFERENCES

Abebe MT, Megento TL. 2017. Urban green space development using GIS-based multicriteria analysis in Addis Ababa metropolis. Applied Geomatics 94 (4): 247–261. https://doi.org/10.1007/s12518-017-0198-7

Allen CD, Macalady AK, Chenchouni H, Bachelet D, McDowell N, Vennetier M, Kitzberger T, Rigling A, Breshears DD, Hogg EH *et al*. 2010. A global overview of drought and heat-induced tree mortality reveals emerging climate change risks for forests. Forest Ecology and Management 259 (4): 660–684. https://doi.org/10.1016/j.foreco.2009.09.001

Alvarado-Rosales D, Saavedra-Romero L de L, Franco-Islas Y, Villa-Castillo J, Quiroz-Reygadas DA. 2021. Condición de copa de bosques y selvas de México: Análisis 2014. Madera y Bosques 27 (1): e2712114. https://doi.org/10.21829/myb.2021.2712114

Alvarado-Rosales D, Saavedra-Romero L de L. 2021. Tree damage and mistletoe impact on urban green areas. Revista Árvore 45: e4530. https://doi.org/10.1590/1806-908820210000030

Ambrose MJ, Hanavan R, Smith T. 2022. Tree mortality. *In* Potter KM, Conkling BL. (eds.), Forest Health Monitoring: National Status, Trends, and Analysis. General Technical Report SRS-266. U.S. Department of Agriculture Forest Service, Southern Research Station: Asheville, NC, USA, pp: 101–115. https://doi.org/10.2737/srs-gtr-266-chap5

Barnett HL, Hunter BB. 1998. Illustrated genera of imperfect fungi (Fourth edition). APS Press: St. Paul, MN, USA. 218 p.

Bentz BJ, Régniére J, Fettig CJ, Hansen EM, Hayes JL, Hicke JA, Kelsey RG, Negrón JF, Seybold SJ. 2010. Climate change and bark beetles of the Western United States and Canada: Direct and indirect effects. BioScience 60 (8): 602–613. https://doi.org/10.1525/bio.2010.60.8.6

Borelli S, Conigliaro M, Pineda F. 2018. Los bosques urbanos en el contexto global. Unasylva 69 (250): 3–10.

Calaza P. 2021. La infraestructura verde (urbana) como estrategia frente al cambio climático. Cuadernos de Ordenación del Territorio 6 (2): 31–60.

Choi IY, Lee WH, Lee JJ, Park MJ, Ko JA, Choi JR, Shin HD. 2016. Characterization of a *Septobasidium* sp. associated with felt disease of *Schisandra chinensis.* Mycobiology 44 (1): 58–62. https://doi.org/10.5941/myco.2016.44.1.58

Conway D, Li CQ, Wolch J, Khale C, Jerrett M. 2010. A spatial autocorrelation approach for examining the effects of urban greenspace on residential property values. Journal of Real Estate Finance and Economics 41 (2): 150–169. https://doi.org/10.1007/s11146-008-9159-6

Francini G, Hui N, Jumpponen A, Kotze DJ, Romantschuk M, Allen JA, Setälä H. 2018. Soil biota in boreal urban greenspace: responses to plant type and age. Soil Biology and Biochemistry 118: 145–155. https://doi.org/10.1016/j.soilbio.2017.11.019

Fuller RA, Gaston KJ. 2009. The scaling of green spaces coverage in European cities. Biology Letters 5 (3): 352–355. https://doi.org/10.1098/rsbl.2009.0010

Galindo AJ. 1968. El tumor del fresno causado por la asociación de cóccidos con *Septobasidium curtisii*. Agrociencia 3 (1): 97–100.

Gómez LD, Henk DA. 2004. Validation of the species of *Septobasidium* (Basidiomycetes) described by John N. Couch. Lankesteriana 4 (1): 75–96. https://doi.org/10.15517/lank.v4i1.22985

Goswami M, Malakar C, Deka S. 2020. Rhizosphere microbes for sustainable maintenance of plant health and soil fertility. *In* Sharma SK, Singh UB, Sahu PK, Singh HV, Sharma PK. (eds.), Rhizosphere microbes, soils and pant functions. Springer: Singapore, pp: 35–72. https://doi.org/10.1007/978-981-15-9154-9_2

Guerra-Hernández J, Díaz-Varela RA, Ávarez-González JG, Rodríguez-González PM. 2021. Assessing a novel modelling approach with high resolution UAV imagery for monitoring health status in priority riparian forests. Forest Ecosystems 8 (1). https://doi.org/10.1186/s40663-021-00342-8

Hawksworth FG. 1977. The 6-class dwarf mistletoe rating system. General Technical Report RM-48. U.S. Department of Agriculture, Forest Service, Rocky Mountain Forest and Range Experiment Station. Fort Collins, CO, USA.

Hilbert D, Roman L, Koeser AK, Vogt J, van Doorn NS. 2019. Urban tree mortality: A literature review. Arboriculture and Urban Forestry 45 (5): 167–200 https://doi.org/10.13140/RG.2.2.25953.15204

Hillel D, Rosenzweig C, Powlson D, Scow K, Singer M, Sparks D. 2004. Encyclopedia of soils in the environment. Academic Press: New York, NY, USA. 613 p.

Kendal D, Dobbs C, Lohr VI. 2014. Global patterns of diversity in the urban forest: Is there evidence to support the 10/20/30 rule? Urban Forestry and Urban Greening 13 (3): 411–417. https://doi.org/10.1016/j.ufug.2014.04.004

Knapp S, Kühn I, Bakker JP, Kleyer M, Klotz S. Ozing WA, Poschlod P, Thompson K, Thuiller W, Römermann C. 2009. How species traits and affinity to urban land use control large-scale species frequency. Diversity and Distributions 15 (3): 533–546. https://doi.org/10.1111/j.1472-4642.2009.00561.x

Ladino G, Ospina-Bautista F, Estévez-Varón J, Jerabkova L, Kratina, P. 2019. Ecosystem services provided by bromeliad plants: A systematic review. Ecology and Evolution 9 (12): 7360–7372. https://doi.org/10.1002/ece3.5296

Leslie JF, Summerell BA. 2006. The *Fusarium* laboratory manual. Blackwell Publishing Asia: Ames, IA, USA. 388 p.

Macías-Muro A, Martínez-Trinidad T, Valdez-Lazalde JR, Romero-Sánchez ME, Vaquera-Huerta H. 2022. Evaluación de la salud del arbolado urbano a través de imágenes satelitales en Guadalajara, México. Entreciencias: Diálogos en la Sociedad del Conocimiento 10 (24): 1–12. https://doi.org/10.22201/enesl.20078064e.2022.24.81200

McDonnell MJ, Kendal D. 2018. The ecology of urban forests. *In* Peh KSH, Corlett RT, Bergeron Y. (eds.), Handbook of forest ecology. Routledge: New York, NY, USA, pp: 623–633.

Morin RS, Randolph KC, Steinman J. 2015. Mortality rates associated with crown health for eastern forest tree species. Environmental Monitoring and Assessment 187 (3): 87. https://doi.org/10.1007/s10661-015-4332-x

Pallardy SG. 2008. Physiology of woody plants. Academic Press: New York, NY, USA. 454 p.

Peckham SC, Duinker PN, Ordóñez C. 2013. Urban forest values in Canada: views of citizens in Calgary and Halifax. Urban Forestry and Urban Greening 12 (2): 154–162. https://doi.org/10.1016/j.ufug.2013.01.001

Piontelli LE. 2014. Agentes comunes en las aspergilosis humanas: conceptos primarios en la diferenciación de sus complejos de especies. Boletín Micológico 29 (2): 63–100. https://doi.org/10.22370/bolmicol.2014.29.2.868

Pontius J, Hallet R. 2014. Comprehensive methods for earlier detection and monitoring of forest decline. Forest Science 60 (6): 1156–1163.

Randolph KC. 2015. Crown condition. *In* Potter KM, Conkling BL. (eds.), Forest health monitoring: national status, trends, and analysis 2013. General Technical Report SRS-207. U.S. Department of Agriculture Forest Service, Southern Research Station: Asheville, NC, USA, pp: 135–151.

Randolph KC. 2018. Crown condition. *In* Potter KM, Conkling BL. (eds.), Forest health monitoring: national status, trends, and analysis 2017. General Technical Report SRS-233. U.S. Department of Agriculture Forest Service, Southern Research Station: Asheville, NC, USA, pp: 115–132.

Randolph KC. 2023. Crown dieback and damages in the Eastern United States. *In* Potter KM, Conkling BL. (eds.), Forest Health Monitoring: national status, trends, and analysis. General Technical Report SRS-273. U.S. Department of Agriculture Forest Service, Southern Research Station: Asheville, NC, USA, pp: 105–126. https://doi.org/10.2737/SRS-GTR-273-Chap6

Richards NA. 1983. Diversity and stability in a street tree population. Urban Ecology 7 (2): 159–171. https://doi.org/10.1016/0304-4009(83)90034-7

Saavedra-Romero L de L, Alvarado-Rosales D, Hernández-de la Rosa, P, Martínez-Trinidad T, Mora-Aguilera G, Villa-Castillo J. 2016. Condición de copa, indicadores de salud en árboles urbanos del Bosque San Juan de Aragón, Ciudad de México. Madera y Bosques 22 (2): 15–27. https://doi.org/10.21829/myb.2016.2221321

Saavedra-Romero L de L, Alvarado-Rosales D, Martínez-Trinidad T, Hernández-de la Rosa P. 2019a. Identification of defects and risks in trees of San Juan de Aragon Forest, Mexico City. Revista Chapingo Serie Ciencias Forestales y del Ambiente 25 (1): 31–47. https://doi.org/10.5154/r.rchscfa.2018.06.049

Saavedra-Romero L de L, Alvarado-Rosales D, Martínez-Trinidad T, Hernández-de la Rosa P. 2020. Propiedades físicas y químicas del suelo urbano del Bosque San Juan Aragón, Ciudad de México. Terra Latinoamericana 38 (3): 529–540. https://doi.org/10.28940/terra.v38i3.644

Saavedra-Romero L de L, Hernández-de la Rosa P, Alvarado-Rosales D, Martínez-Trinidad T, Villa-Castillo J. 2019b. Diversidad, estructura arbórea e índice de valor de importancia en un bosque urbano de la Ciudad de México. Polibotánica 47: 25–37. https://doi.org/10.18387/polibotanica.47.3

Saavedra-Romero L de L, Martínez-Trinidad T, Alvarado-Rosales D, Hernández-de la Rosa P, Villa-Castillo J. 2021. Damaging agents and tree's health condition in an urban forest. Open Journal of Forestry 11 (3): 238–253. https://doi.org/10.4236/ojf.2021.113016

Samson R, Ningal TF, Tiwary A, Grote R, Fares S, Saaroni H, Hiemstra JA, Zhiyanski M, Vilhar U, Cariñanos P, Järvi L *et al*. 2017. Species-specific information for enhancing ecosystem services. *In* Pearlmutter D, Calfapietra C, Samson R, O´Brien L, Osoic SK, Sanesi G, del Amo RA, (eds.). The urban forest. Cultivating Green infrastructure for people and the environment. Springer: Cham, Switzerland, pp: 111–144. https://doi.org/10.1007/978-3-319-50280-9_12

SEDEMA (Secretaría del Medio Ambiente). 2017. Inventario de áreas verdes. Secretaría del Medio Ambiente. Ciudad de México, México. https://sedema.cdmx.gob.mx/programas/programa/inventario-de-areas-verdes (Retrieved: June 2023).

Turner-Skoff JB, Cavender N. 2019. The benefits of trees for livable and sustainable communities. Plants, People, Planet 1 (4): 323–335. https://doi.org/10.1002/ppp3.39

Zaragoza-Hernández AY, Cetina-Alcalá VM, López-López MA, Chacalo-Hilú A, de la Isla de Bauer ML, Alvarado-Rosales D, González Rosas H. 2015. Identification of tree damages of three parks of Mexico City. Revista Mexicana de Ciencias Forestales 6 (32): 63–82.

Agrociencia

FORAGE CHARACTERIZATION OF BUFFEL-GRASS (*Cenchrus ciliare* L.) IN SEMI-DRY TO SEMI-WARM CLIMATES IN ZACATECAS, MEXICO

Ricardo Alonso **Sánchez-Gutiérrez**[1,2], Francisco Guadalupe **Echavarría-Cháirez**[1,2], Edith **Ramírez-Segura**[3], Alan **Álvarez-Holguín**[4], Jesús Manuel **Ochoa-Rivero**[5], Alberto **Muro-Reyes**[2], Héctor **Gutiérrez-Bañuelos**[2*]

[1]Instituto Nacional de Investigaciones Forestales, Agrícolas y Pecuarias, Campo Experimental Zacatecas. Carretera Zacatecas-Fresnillo km 24.5, Calera de Víctor Rosales, Zacatecas, Mexico. C. P. 98500.
[2]Universidad Autónoma de Zacatecas Francisco García Salinas. Unidad Académica de Medicina Veterinaria y Zootecnia. Carretera Zacatecas-Fresnillo km 31.5, El Cordovel, Enrique Estrada, Zacatecas, Mexico. C. P. 98500.
[3]Instituto Nacional de Investigaciones Forestales, Agrícolas y Pecuarias. Centro Nacional de Investigación Disciplinaria en Agricultura Familiar. Carretera Ojuelos-Lagos de Moreno, Ojuelos de Jalisco, Jalisco, Mexico. C. P. 47540.
[4]Universidad Autónoma de Chihuahua. Facultad de Zootecnia y Ecología. Periférico Francisco R. Almada km 1, Chihuahua, Chihuahua, Mexico. C. P. 31453.
[5]Instituto Nacional de Investigaciones Forestales, Agrícolas y Pecuarias, Campo Experimental La Campana. Carretera Chihuahua-Ojinaga km 33.3, Aldama, Chihuahua, Mexico. C. P. 32190.
* Author for correspondence: hgutierrez@uaz.edu.mx

Citation: Sánchez-Gutiérrez RA, Echavarría-Cháirez FG, Ramírez-Segura E, Álvarez-Holguín A, Ochoa-Rivero JM, Muro-Reyes A, Gutiérrez-Bañuelos H. 2024. Forage characterization of Buffel-grass (*Cenchrus ciliare* L.) in semi-dry to semi-warm climates in Zacatecas, Mexico. **Agrociencia** 58(3): 331-337. https://doi.org/ 10.47163/ agrociencia.v58i3.3063

Editor in Chief:
Dr. Fernando C. Gómez Merino

Received: September 04, 2023.
Approved: January 23, 2024.
Published in Agrociencia: May 02, 2024.

ABSTRACT

Buffel grass (*Cenchrus ciliare* L.) is a species used for the production of forage that is characterized by its adequate adaptation to diverse environments. The aim was to evaluate the characteristics of forage and seeds from four materials and a variety of Buffel grass under rainfed conditions in the semi-dry and semi-warm weather of Zacatecas. The experiment was held in Huanusco, Zacatecas, Mexico, in a totally randomized block design with three replications. The materials were: M-42, M-45, M-66, M-S245, and the Titán variety as a control. For forage, two cuts were performed, considering the variables of plant height (PH), production of dry matter (DM), crude protein (CP), and *in vitro* digestibility of dry matter (IVDDM). Seed characteristics were determined upon physiological maturity using the variables of seed yield (SY), number of spikes per plant (Sp/plt), caryopsides per spikelet (Car/sp), and area of caryopsides (Area/Car). The data were analyzed in SAS, and the means were compared using Lsmeans. For the variable PH, M-42 stood out with an average height of 97.3 cm. In the production of DM, M-42 and M-45 surpassed Titán ($p < 0.05$), with yields higher than 4.4 Mg ha^{-1}. M-42 had the greatest CP content at 7.29 %, whereas M-45 and M-S245 had the highest IVDDM concentrations at 74.5 and 74.8 %, respectively. Regarding seed characteristics, M-42 surpassed Titán, with a SY of 295 kg ha^{-1}. The study concluded that M-42 is the best option for grassland management in Zacatecas, Mexico, where the weather is semi-warm and semi-dry.

Keywords: digestibility, seed, caryopsis, protein.

INTRODUCTION

Rainfed prairies are a source of high-quality forage for animal production systems. In addition to serving as a source of food for cattle, grasslands also reduce production costs for livestock farmers. They act as carbon sinks that contribute to the mitigation of climate change and promote agricultural and cattle sustainability. Grasslands in Mexico are constantly deteriorating due to overgrazing. Unfortunately, the renewal rate is no higher than 5 % (Enríquez-Quiroz *et al*., 2021). In order to counteract this problem, planting species adapted to the region of interest is recommended. Buffel grass (*Cenchrus ciliare* L.) is recommended for the establishment and management in grasslands due to its broad adaptation to climates and diverse soils (Rajora *et al*., 2021). In arid and temperate climates in Mexico where the average rainfall is between 298 and 550 mm, Buffel grass surpassed native species such as Sideoats Grama (*Bouteloua curtipendula*) and Blue Grama (*Bouteloua gracilis*), and even other African grasses such as Saw-tooth Love grass (*Eragrostis superva*), Weeping Love grass (*Eragrostis curvula*), and Kleingrass (*Panicum coloratum*) in dry matter production (Terrazas and Chávez, 2012a; Álvarez-Vázquez *et al*., 2022). In recent years, the National Research Institute for Livestock, Agriculture, and Forestry (INIFAP) evaluated a collection of Buffel grass in Mexico composed of 17 materials and two varieties (Formidable and T-4464). Out of these materials, four stood out in the production of forage and seeds (Terrazas and Chávez, 2012a; Terrazas and Chávez, 2012b). In a study that evaluated a collection of 126 ecotypes in Africa, values ranging from 1302 to 7442 kg MS ha^{-1} were reported (Sánchez-Gutiérrez *et al*., 2017), which sustains the need to evaluate materials in the same species to give pertinent recommendations for their use.

In Zacatecas, Mexico, there is an optimal and suboptimal potential area for Buffel grass of 96 624 and 2 693 005 ha, respectively (Medina *et al*., 2001). However, to date, the forage characteristics of the outstanding INIFAP materials, which may be a better forage alternative for the semi-dry and semi-warm Zacatecas climate, are unknown. Therefore, the aim of this study was to evaluate the forage and seed characteristics of four materials and one variety of Buffel grass under rainfed conditions in the semi-dry and semi-warm climate of Huanusco, Zacatecas, Mexico, to provide a recommendation for planting material.

MATERIALS AND METHODS

Study area

The experiment was conducted at the National Research Institute for Livestock, Agricultural, and Forestry (INIFAP), Los Cañones Experimental Station, located in the municipal area of Huanusco, Zacatecas, Mexico (102° 58’ W and 21° 44’ N), at an altitude of 1508 m. The soil is loamy, with a pH of 8.2 and a depth of over 1.5 m. The climate is semi-dry and semi-warm, with an annual average temperature of 29 °C and an average annual rainfall of 582 mm, with rains concentrating between June and September (Medina and Ruíz, 2004) (Figure 1).

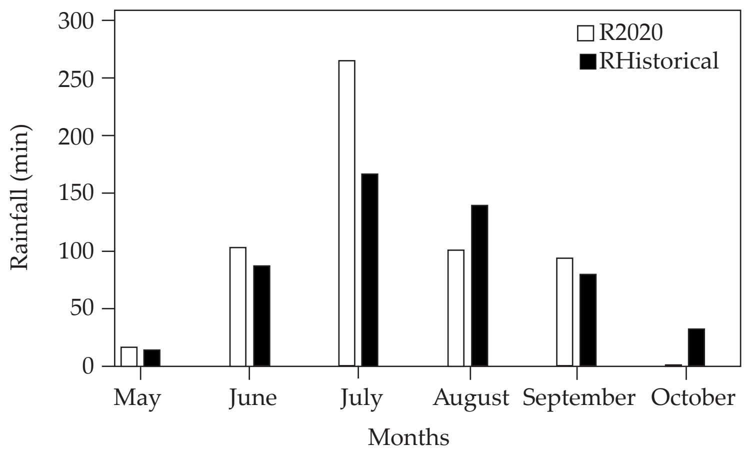

Figure 1. Monthly rainfall (mm) at Los Cañones Experimental Station in Huanusco, Zacatecas, Mexico, for 2020 (R2020) and the historical average (Rhistorical) (INIFAP Weather Station).

Design and experimental unit

The experiment was established in 2019 under a totally randomized experimental block design with three repetitions. Each block was established perpendicular to the slope, grafting plants manually. The materials evaluated were as follows: 1) M-42, 2) M-45, 3) M-66, 4) M-S245, and the Titán variety as a control. The experimental unit consisted of five rows, each 0.76 m wide and 15 m long. A distance of 0.75 m was set between plants. For the useful plot, 6 m were used in three central furrows, for a total of 18 plants.

Agronomical and bromatological analysis of the forage

The study began on May 12, 2020, with a standardization cut 5 cm above the ground level. To estimate the forage production, two cuts were made, one 45 days after the first rainfall (15 mm) and another 45 days later. The variables considered were: plant height (PH), dry matter production (DM), crude protein (CP), and *in vitro* digestibility of dry matter (IVDDM). For PH, a wooden ruler was used, and the measurement was taken from the base of the crown to the highest point of the forage or inflorescence. To estimate DM production, the useful plot was cut and the fresh forage was weighed. Later, a sample (500 g) was taken and placed in a forced air oven at 55 °C for 72 hours. The dry sample was then weighed, and the DM content was determined. The DM percentage was multiplied by the fresh weight of the plot, and the dry weight per hectare was extrapolated. Later, the samples were ground in a Willy mill with a 1 mm sieve.

The DUMAS method was used to determine the CP. The samples were processed with the LECO® FP-528 DSP equipment (Leco Instruments; Geleen, Netherlands). For the IVDDM, 0.5 g of sample were used in duplicate and stored in F57 bags. In addition to the blank (without forage), alfalfa and stubble samples were taken as references. The ruminal liquid was collected from calves with high-forage diets that were sacrificed in the municipal butchery. Finally, the procedures recommended by the manufacturer were followed using a Daisy incubator (ANKOM Technology; Macedon, NY, USA). All variables were determined in each cut. For DM production, the sum of the forage was recorded, and for the remaining variables, the means were considered.

Analysis of the seed

Seed characteristics were determined when they reached physiological maturity. The variables considered were: seed yield (SY), number of spikes per plant (Sp/plt), caryopsides per spikelet (Car/sp), and area of caryopsides (Area/Car). For SY, the seed was harvested by hand from the useful plot. In addition, four plants were chosen at random to count Sp/plt. Later, eight spikes were taken, and the caryopsides were extracted (Car/sp) by hand. To measure the Area/Car, 25 caryopsides were taken and observed in a Labomed CZM6 stereoscope (Labomed Inc.; Los Angeles, CA, USA).

Statistical analysis

Before the statistical analysis, the data underwent a normality test with Shapiro-Wilks and Bartlett tests for the homogeneity of variances. In both tests, normality and homogeneity were assumed, as long as they displayed a value of $p > 0.05$. Finally, the data were analyzed with "PROC GLM" of the SAS statistical package with a random block analysis. The means were compared using Lsmeans and were separated at a probability of less than 5 % (SAS, 2011).

RESULTS AND DISCUSSION

The total rainfall in this investigation during the crop cycle was 525 mm. The highest rainfall concentration was recorded between June and September (Figure 1). The materials presented differences ($p < 0.05$) in all the forage attributes evaluated. In PH, M-42 stood out, obtaining values higher than the control. The highest yields in the production of DM were obtained in M-42 and M-45, outperforming the control. For CP, the highest concentration ($p < 0.05$) was obtained in M-42, while the rest did not surpass 6 %. The highest IVDDM was found in M-45 and M-S245 with values of over 74 %, surpassing ($p < 0.05$) Titán (Table 1).

The weather conditions in this study were favorable for the materials since Titán presented a higher yield in comparison to other studies, in which DM production was 2370 kg ha^{-1} with 368 mm of rainfall (Beltrán-López *et al*., 2017). Additionally, the DM yields of all materials are within the ranges reported in the literature. Materials M-42 and M-45 are the best alternatives for the semi-dry and semi-warm climate of Zacatecas, resulting in a DM increase from 650 to 960 kg ha^{-1} more than Titán. This would represent over 62 thousand Mg of annual forage for the high-potential region of Zacatecas.

Table 1. Forage characteristics of five Buffel grass (*Cenchrus ciliare* L.) materials evaluated in Los Cañones Experimental Station, Huanusco, Zacatecas, Mexico, under rainfed conditions.

Material	PH (cm)	DM (kg ha^{-1})	CP (%)	IVDDM (%)
M-42	97.3 a	4771.1 a	7.29 a	73.19 b
M-45	80.3 b	4461.5 a	5.89 b	74.48 a
M-66	88.87 ab	3382.8 c	5.81 b	72.66 b
M-S245	80.61 ab	4411.96 ab	5.33 b	74.79 a
Titán (control)	84.89 ab	3811.2 bc	5.88 b	72.84 b
R^2	0.66	0.82	0.73	0.82
C.V.	10.7	10.2	9.26	9.2

PH: plant height; DM: dry matter; CP: crude protein; IVDDM: *in vitro* digestibility of dry matter; R^2: coefficient of determination; C.V.: coefficient of variation. Different letters between columns indicate significant differences ($p < 0.05$).

On the other hand, the mean value of CP in Titán (5.88 %) is similar to the 6.1 % reported in the flowering stage by Beltrán-López *et al*. (2017). M-42 represents an alternative to lower feed costs for CP supplementation since it outperformed Titán by 1.4 %. According to studies in forage genetic breeding, every unit increase in IVDDM results in a 3.2 % increase in daily yield per head (Casler and Vogel, 1999). M-45 could improve animal performance by increasing IVDDM by 2.25 % as compared to the control.

All seed characteristics varied across materials. M-42 had the largest seed production (75 % higher than Titán), although it was statistically similar ($p < 0.05$) to M-45 and M-66 yields. For spikelets per plant, M-42 presented a value 113 % higher than the control variety, but equal to the value for M-45. M-42 outperformed the control in Car/sp and Area/Car by 146 and 62 %, respectively (Table 2).

Table 2. Characteristics of seeds in five Buffel grass (*Cenchrus ciliare* L.) materials evaluated in Los Cañones Experimenal Station, Huanusco, Zacatecas, Mexico, under rainfed conditions.

Material	SY (kg ha^{-1})	Sp/plt	Car/sp	Area/Car (mm^{-2})
M-42	295.19 a	77 a	64 a	3.13 a
M-45	179.7 ab	51 ab	17 b	2.07 b
M-66	184.1 ab	26 b	14 b	1.8 b
M-S245	170.8 b	32 b	15 b	2.38 b
Titán (control)	140.9 b	36 b	26 b	1.93 b
R^2	0.72	0.72	0.67	0.73
C.V.	33.7	36.8	65	17.6

SY: seed yield; Sp/plt: spikelets per plant; Car/sp: caryopsides per spikelet; Area/Car: area of caryopsides; R^2: coefficient of determination; C.V.: coefficient of variation. Different letters within columns indicate significant differences ($p < 0.05$).

Seed production is similar to that of the outstanding genotypes in a collection of Buffel grass evaluated in Colombia, where the rainfall is over 1500 mm, finding a value of over 210 kg ha^{-1} (Erazo *et al*., 2022). In addition, the means presented for both Sp/plt and Car/sp are within the range reported in the 157 materials evaluated in Ethiopia (Sánchez-Gutiérrez *et al*., 2020). The results with M-42 are higher than those reported in the varieties Común, Nueces, and Formidable, since Conde-Lozano *et al*. (2011) mention that the value of Sp/plt did not surpass 33, and for Car/sp, it was lower than 39. Hernández-Guzmán *et al*. (2021) concluded that the larger the caryopsides, the greater the increase in biomass production in Buffel and Rhodes grasses. Due to the above, M-42 is proposed as an option in arid climates like the one used in this study to restore regions where forage is in decline. Since M-42's caryopsides are larger, it is also anticipated that the establishment's success will increase.

CONCLUSIONS

When compared to the control (Titán), material M-42 had the highest protein concentration, the highest production of dry matter, and better seed characteristics. These attributes make it a viable and nutritious choice, particularly when forage area recovery is required since the expected establishment of this grass would be more significant. On the other hand, M-45 produces more dry fodder and has higher digestibility rates than Titán, making it suitable for use in the research area's meteorological conditions. As a result, materials M42 and M-45 are viable options for grassland rehabilitation and management programs in the Zacatecas' semi-warm and semi-dry climates.

REFERENCES

Álvarez-Vásquez P, Rojas-García AR, Joaquín-Cancino S, Velázquez-Martínez M, Rodríguez-Ortega LT, Hernández-Guzmán FJ. 2022. Producción de forraje y semilla de ocho pastos al establecimiento en Tulancingo, Hidalgo. Revista Mexicana de Ciencias Agrícolas 13 (6): 1041–1053. https://doi.org/10.29312/remexca.v13i6.3027

Beltrán-López S, García-Díaz CA, Loredo-Osti C, Urrutia-Morales J, Hernández-Alatorre JA, Gámez-Vázquez HG. 2017. "Titán" y "Regio", variedades de pasto Buffel (*Penisetum ciliare*) (L.). Link para zonas áridas y semiáridas. Revista Mexicana de Ciencias Pecuarias 8 (3): 291–295. https://doi.org/10.22319/rmcp.v8i3.4159

Casler MD, Vogel KP. 1999. Accomplishments and impact from breeding for increased forage nutritional value. Crop Science 39 (1): 12–20. https://doi.org/10.2135/cropsci1999.0011183x003900010003x

Conde-Lozano E, Martínez-González JC, Briones-Encinia F, Saldivar-Fitzmaurice AJ. 2011. Producción de semilla de pasto Buffel (*Cenchrus ciliaris* L.) bajo diferentes ambientes agroecológicos en Tamaulipas, México. Revista de la Facultad de Agronomía de la Universidad del Zulia 28 (3): 360–375.

Erazo EB, Mojica-Rodríguez JE, Brochero-Aldana GA, Mejía-Salazar JR, Mejía-Kerguelen L, Burghi VH. 2022. Variation in floral morphology and seed production of Buffel and Rhodes grass. Journal of Agricultural Science and Technology 24 (2): 155–168.

Enríquez-Quiroz JF, Esqueda-Esquivel VA, Martínez-Méndez D. 2021. Rehabilitación de praderas degradadas en el trópico de México. Revista Mexicana de Ciencias Pecuarias 12: 243–260. https://doi.org/10.22319/rmcp.v12s3.5876

Hernández-Guzmán FJ, Rodríguez-Ortega LT, Velázquez-Martínez M, Landa-Salgado P, Rodríguez-Ortega A, Castrellón-Montelongo JL. 2021. Influencia del tamaño de cariópside y embrión en el desarrollo de plántulas de pastos. Interciencia 6 (7–8): 309–316.

Medina GG, Salinas GH, Rubio AF. 2001. Potencial productivo de especies forrajeras en el Estado de Zacatecas, libro técnico 1. Instituto Nacional de Investigaciones Forestales, Agrícolas y Pecuarias. Centro de Investigación Regional Norte Centro, Campo Experimental Zacatecas. Calera, México. 157 p.

Medina GG, Ruiz CA. 2004. Estadísticas climatológicas básicas del Estado de Zacatecas. Libro técnico 3. Instituto Nacional de Investigaciones Forestales, Agrícolas y Pecuarias. Centro de Investigación Regional Norte Centro, Campo Experimental Zacatecas. Calera, México, pp: 40–41.

Rajora MP, Jadon KS, Roy PK, Patidar M, Bhatt RK. 2021. Forage yield performance of five elite genotypes of Buffel grass in hot arid region of Rajasthan. Range Management and Agroforestry 42 (2): 198–204.

Sánchez-Gutiérrez RA, Morales-Nieto CR, Hanson J, Santellano-Estrada E, Jurado-Guerra P, Villanueva-Avalos JF, Melgoza-Castillo A. 2017. Caracterización forrajera de ecotipos de zacate Buffel en condiciones de temporal en Debre Zeit, Etiopía. Revista Mexicana de Ciencias Agrícolas 8 (1): 13–24. https://doi.org/10.29312/remexca.v8i1.68

Sánchez-Gutiérrez RA, Hanson J, Jones C, Jurado-Guerra P, Santellano-Estrada E, Melgoza-Castillo A, Morales-Nieto C. 2020. Caracterización morfológica de genotipos de pasto Buffel con potencial para la producción de forraje y semilla. Revista Fitotecnia Mexicana 43 (3): 343–347. https://doi.org/10.35196/rfm.2020.3.343

SAS Institute. 2011. SAS/STAT 9.3 User´s Guide. SAS Institute Inc. Cary, North Carolina, USA.

Terrazas PJG, Chávez MC. 2012a. Rendimiento y calidad de forraje de materiales sobresalientes de zacate Buffel *Cenchrus ciliaris* en cinco estadios de crecimiento. *In* Baez IF. (ed.), Resultados de Investigación sobre Zacate Buffel *Cenchrus ciliaris* de Temporal en la Región Centro de Chihuahua. Instituto Nacional de Investigaciones Forestales, Agrícolas y Pecuarias, Campo Experimental Delicias: Delicias, México, pp: 21–38.

Terrazas PJG, Chávez MC. 2012b. Rendimiento y calidad de semilla de materiales sobresalientes de zacate Buffel *Cenchrus ciliaris* en condiciones de temporal en la zona centro sur de Chihuahua. *In* Baez IF. (ed.), Resultados de Investigación sobre Zacate Buffel *Cenchrus ciliaris* de Temporal en la Región Centro de Chihuahua. Instituto Nacional de Investigaciones Forestales, Agrícolas y Pecuarias, Campo Experimental Delicias: Delicias, México, pp: 39–49.

Agrociencia

IMPACT OF THE 'KENT' MANGO (*Mangifera indica* L.) JAM FORMULATION WITH DIFFERENT GELLING AGENTS ON THE PHYSICOCHEMICAL AND SENSORY PROPERTIES

Eber Addí **Quintana-Obregón**[1], María Dolores **Muy-Rangel**[2], Manuel Alejandro **Vargas-Ortiz**[1], José Basilio **Heredia**[2], Verónica **Pérez-Rubio**[2], Rosa María **López-Romero**[3], Cesar **San-Martín-Hernández**[3*]

[1]CONAHCYT-Centro de Investigación en Alimentación y Desarrollo A. C. Carretera Gustavo Enrique Astiazarán Rosas 46, La Victoria, Hermosillo, Sonora, Mexico. C. P. 83304.
[2]Centro de Investigación en Alimentación y Desarrollo A.C. Coordinación Culiacán. Carretera a Eldorado km 5.5, Culiacán, Sinaloa, Mexico. C. P. 80110.
[3]Colegio de Postgraduados Campus Montecillo. Carretera México-Texcoco km 36.5, Montecillo, Texcoco, State of Mexico, Mexico. C. P. 56264.
* Author for correspondence: sanmartin.cesar@colpos.mx

Citation: Quintana-Obregón EA, Muy-Rangel MD, Vargas-Ortiz MA, Heredia JB, Pérez-Rubio V, López-Romero RM, San-Martín-Hernández C. 2024. Impact of the 'Kent' mango (*Mangifera indica* L.) jam formulation with different gelling agents on the physicochemical and sensory properties.
Agrociencia 58(3): 338-351. https://doi.org/ 10.47163/agrociencia.v58i3.2813

Editor in Chief:
Dr. Fernando C. Gómez Merino

Received: February 24, 2023.
Approved: January 07, 2024.
Published in Agrociencia: April 11, 2024.

ABSTRACT

Pectin content decreases as mango (*Mangifera indica* L.) maturity progresses. When making jam, a hydrocolloid will be required, which can impact the physicochemical and sensory properties of the processed product. The objective of this work was to evaluate the effect of two mango maturity stages (60 and 100 %) and four different gelling agents (pectin, xanthan gum, guar gum, and corn starch) on the physicochemical and sensory properties of jams, using a commercial jam as a control. Eight treatments were obtained, and a completely randomized experimental design was applied. The experimental unit was a glass jar (250 g) of jam with three replicates for physicochemical and sensory analysis. Analysis of variance and comparisons of means with Tukey's test were carried out with SAS® software. The physicochemical properties of the jam were affected according to its formulation. Those with 100 % ripe mango plus pectin or corn starch showed maximum pH values of 3.7 and 3.8, respectively, but lower acidity (0.6 %). The jams with 60 % ripe mango and pectin or corn starch had higher levels of dietary fiber (1.42 and 1.47 %) and protein (0.97 and 0.79 %), with no differences from the control. In terms of texture, the formulation with 60 % ripe mango plus pectin was statistically superior to the other jams. The jam with 60 % ripe mango and corn starch had the highest sensory color and was comparable to the control, but in hue, it was instrumentally different from the other formulations. Changes in fruit maturity from 60 to 100 % and the type of gelling agent modified the physicochemical properties and sensory color of 'Kent' mango jam, confirming the effect of formulation on the attributes evaluated.

Keywords: mango ripening, microbiological analysis, texture profile, sensory analysis.

INTRODUCTION

In Mexico, mango (*Mangifera indica* L.) is largely consumed as a fresh fruit. One of the largest producing cultivars is 'Kent', with about 26 000 ha planted (SIAP, 2020). Mango production is mainly destined for export. To market 'Kent' mango, an acceptable level of maturity with a firmness of 121.6 N and 7.4 °Brix are required (NMX-FF-058-SCFI-2006). Mangoes that do not meet the minimum export criteria may be distributed domestically or may be used in the high value-added food industry.

The amount of pulp varies among different mango cultivars such as 'Criollo Mara', 'Irwin', 'Gleen', 'Zill', 'Haden', 'Carrusell', 'Manzana', 'Tommy', 'Valencia Pride', and 'Palmer', while others such as 'Sprinfels', 'Ford', and heavier 'Kent' have high pulp contents (75 %), requiring at least 65 % for the processing market (Ramírez-Méndez *et al*., 2010). When mangoes reach eating maturity, their acidity is reduced, their soluble ~~s~~ solid content increases by more than 15 %, and develop yellow and orange colors (Villamizar-Vargas *et al*., 2019), which are important attributes for the processing industry.

Jam is a product formulated from fruit and sugar, plus the addition of acidifiers and pectin to obtain a gel. Gelation is achieved when the mixture reaches 65 °Brix by adding acidifier and pectin from 0.5 to 1 % (Ávila-Cubillos, 2015). Acidity can be obtained by citric acid from lemon juice, while gelation can be achieved with different hydrocolloids such as modified starch, agar, carrageenan, high and low methoxyl pectin, gums, alginate, and methyl and hydroxymethyl cellulose, among others (Wüstenberg, 2015). Increasing concentrations of 0.8 to 1.2 % pectin plus 50 to 70 % sucrose in ripe mango jam have been reported to increase hardness, shear work, thickening, and adhesion work, while sensory acceptability improves only when sucrose in the processed product increases (Basu and Shivhare, 2010). In a similar study, the gelling agents high methoxyl pectin, carboxymethyl cellulose, and sago starch (*Metroxylon sagu*) used in the formulation of mango jam modified the sensory and textural characteristics (hardness, shear work, stickiness, and adhesion work) of the processed product (Javanmard *et al*., 2012).

In jams, the gelling ingredient commonly utilized is pectin, a substance found in mango fruit (San Martín-Hernández *et al*., 2020). However, as ripening continues, total soluble solids increase, acidity and firmness decrease, and pectin content decreases due to the effect of endogenous pectinases that degrade pectin polymeric chains (Jamsazzadeh Kermani, 2015; Villamizar-Vargas *et al*., 2019). Therefore, to achieve proper gelation in a jam, some specific substance is required for that purpose.

Based on research on jam development, this study hypothesized that the behavior of the physicochemical and sensory attributes of jam are modified by using 'Kent' mango pulp with different ripening degrees and different gelling agents in its formulation. The objective of this work was to evaluate the effect of the formulation of jam made with different gelling agents and mango with 60 and 100 % ripeness on the physical, chemical, and sensory attributes of the product.

MATERIALS AND METHODS

Plant material and fruit determinations

The jams and the evaluation of their physicochemical parameters were carried out at the nutrition laboratory of the Food and Development Research Center (CIAD) in Culiacán, Sinaloa, Mexico. The 'Kent' mango was obtained from the supply market *in* Culiacán. Corn starch, high methoxyl pectin, guar gum, and xanthan gum were purchased as food-grade gelling agents from Bioproceso® (Culiacán, Mexico). The fruits were washed with potable water, surface disinfected with NaClO (150 mg L^{-1}) for 10 minutes, and rinsed with water. Based on standard procedures and those reported in the literature, the physicochemical analysis of the fruit (total soluble solids, pH, titratable acidity, firmness, and color) was carried out. The mango pulp was obtained to make the jams according to its maturity. Based on firmness and total soluble solids reported by the National Mango Board in USA (NMB, 2019) for 'Kent' mango at the harvest site (Table 1), the fruits were classified as mangoes with 60 and 100 % maturity. Firmness (N) was determined at two opposite points of the equatorial zone of the fruit without pericarp using a penetrometer (Ametek® Chatillon CS225 Series, Agawam, USA) equipped with a flat cylindrical probe of 8 mm diameter (Ø).

Table 1. 'Kent' mango maturity at harvest in the country of production (NMB, 2019).

Maturity attribute	Maturity scale				
	1	2	3	4	5
Firmness (N)	213–98	129–62	93–49	49–22	27–4
Total soluble solids (°Brix)	6–8	7–12	11–15	12–17	16–20
Proportional maturity (%)	1–20	21–40	41–60	61–80	81–100

Color was measured at two opposite points in the equatorial zone of the interior of each sliced lateral "cheek" section of the fruit using a colorimeter (Minolta® CR-3000, Tokyo, Japan) that recorded L^* (lightness), a^*, and b^* values in CIE L^* a^* b^* space. The hue angle (°) and color saturation (chroma) were calculated with the formulas: hue (°) = $\tan^{-1}$ (b/a); chroma= $(a^2+b^2)^{1/2}$.

Titratable acidity (TA), pH, and total soluble solids (TSS) were evaluated, respectively, by methods 942.15, 981.12, and 932.12 of the AOAC (2000). The determination of TSS in °Brix was made with 10 g of sample using a refractometer (Mettler Toledo® RE40D, Barcelona, Spain); pH and TA in the same processed sample were measured with a titrator (Mettler Toledo® DL-21, Schwerzenbach, Switzerland) using NaOH (0.1 N) until the equivalence point at pH 8.2.

Jam making

Jam was made according to methodologies reported by Basu and Shivhare (2010) and CODEX STAN (CXS 296-2009) (Codex Alimentarius, 2020), with some modifications for the addition of lemon juice and gelling agents. Mango pulp (200 g) was mixed with sucrose (40 %), Mexican lemon juice (0.2 %), water (50 mL), and a gelling additive (1.2 %). Subsequently, by boiling, the mixture was evaporated at 90 °C until obtaining a TSS of 65 °Brix. The jam was placed in sterilized glass jars (250 mL), pasteurized (NOM-130-SSA1-1995) for 20 min at 85 °C, cooled, and stored at room temperature for 20 d until physical, chemical, and sensory characterization.

Variables evaluated

Color (brightness, chroma, and hue)

Color was analyzed in two jam subsamples of 20 g per repetition and treatment on a Petri dish (90 mm Ø). With the colorimeter (Minolta® CR-3000, Tokyo, Japan), the values of L^* (brightness), a^*, and b^* in the jams were obtained, with which the hue angle (°) and chroma were determined with the formulas: hue (°)= $\tan^{-1}(b/a)$; chroma= $(a^2+b^2)^{1/2}$.

TA (% citric acid) and pH

Similar to the fruit, pH and TA were measured in 10 g of each jam with an automatic titrator (Mettler Toledo® DL-21, Schwerzenbach, Switzerland) using NaOH (0.1 N) up to the equivalence point pH 8.2.

Proximal analysis

In jams, ash, fat, protein, total dietary fiber, and moisture contents were quantified by AOAC (2000) methods 942.05, 920.39, 988.05, 985.29, and 925.10, respectively.

Texture profile analysis (TPA)

The texture profile was evaluated in the jams, where the parameters measured in N mm^{-1} were adhesiveness, consistency, viscosity, shear work, and firmness in Newtons. The texturometer used (AMETEK® Test & Calibration Instrument LS1, Largo, USA) was operated with the Neygen Plus 3 software. The determinations were made using a cylindrical probe with a 50 mm Ø sample holder and a 40 mm Ø flat strut. The jam was placed in the sample holder up to a height of 8 cm. Then, using the flat strut with a 50 Newtons load cell, consecutively without waiting time, two compression cycles were performed at a rate of 0.25 mm s^{-1} until a deformation of 25 % in height of the specimen was achieved (Farahnaky *et al*., 2014).

Microbiological analysis

Microbiological analysis was performed on each jam formulation, according to the Official Mexican Standard (NOM-130-SSA1-1995) for foods packaged in hermetically sealed containers and subjected to heat treatment, for aerobic mesophiles (NOM-092-SSA1-1994), molds and yeasts (NOM-111-SSA1-1994), and total coliforms (NOM-113-SSA1-1994). In addition, to evaluate the possibility of microbial growth, water activity was measured in each jam with an AquaLab® 3TE (METER Group, Pullman, USA).

Sensory analysis

Sensory evaluation was performed with an untrained panel (72 people) at CIAD, Culiacán, Mexico. To perform this analysis, the jams were timed for one hour at room temperature, and 3 to 5 g were served in 15 mL beakers labeled with three random digits. For each sample, panelists were provided with white bread and water to neutralize the palate. Sensory properties: color, odor, taste, texture, and overall acceptability were evaluated on a 9-point hedonic scale (9 = like extremely, 8 = like very much, 7 = like moderately, 6 = like slightly, 5 = neither like nor dislike, 4 = dislike slightly, 3 = dislike moderately, 2 = dislike very much, and 1 = dislike extremely) (Basu and Shivhare, 2010). Data were evaluated with an analysis of variance followed by a mean comparison test with the Tukey test ($p \leq 0.05$) (Lawless and Heymann, 2010).

Experimental design and statistical analysis

The experimental design was completely randomized. The one-way classification factor was the mango jam formulation with eight levels, plus a commercial jam as a control. The treatments were obtained by combining two stages of mango maturity (60 and 100 % ripe) with four gelling additives (high methoxyl pectin, xanthan gum, guar gum, and corn starch). The experimental unit was a jar with 250 g of jam and three replicates. Data for physical, chemical, and sensory attributes were subjected to analysis of variance, and averages were compared with the Tukey test ($p \leq 0.05$) using SAS v9.4 2012 (SAS®, Cary, USA).

RESULTS AND DISCUSSION

The 100 % ripe mango had lower titratable acidity, firmness, and color (hue and brightness), but higher TSS (Table 2). As the fruit ripens, the content of organic acids decreases (Quintero *et al*., 2013) and the amount of TSS increases (Cárdenas-Coronel *et al*., 2012).

Firmness and TSS recorded in mango fruit (Table 2) may be suitable for jam processing. The higher the TSS content of the fruit, the higher the sugar content (Cárdenas-Coronel *et al*., 2012), favoring the lower incorporation of this ingredient in jam. In the processing industry of mango products, pulps are expected to reach TSS equivalent to 13 °Brix (Cañizares-Chacín *et al*., 2009) and low firmness to facilitate industrial processing.

Color, TA, and pH

The color was affected according to the jam formulation. In the three-color attributes, the control jam showed the lowest values and was statistically different from formulation two. The jam with 60 % ripe mango and corn starch had the highest hue

Table 2. Physical and chemical attributes in 'Kent' mango fruit at 60 and 100 % maturity.

Attribute	Fruit maturity	
	60 %	100 %
Total soluble solids (°Brix)	14.07 ± 1.21†	18.05 ± 0.47
TA (% citric acid)	0.98 ± 0.13	0.57 ± 0.03
pH	3.83 ± 0.05	4.30 ± 0.04
Firmness (N)	74.24 ± 1.11	7.13 ± 0.56
Brightness	66.50 ± 2.79	64.03 ± 0.29
Chroma	40.17 ± 3.06	52.69 ± 0.89
Hue (°)	97.12 ± 2.96	74.23 ± 0.59

†Average values (n = 4) ± standard deviation.

(74°) and was reduced by 12.5 % when 100 % ripe mango was used in formulation six. Similarly, when fruit of higher maturity was used in the jams, lightness declined. The highest lightness (39.2) of formulation two declined when 100 % ripe mango was used, and the reduction was accentuated by 17.5 and 16.7 % in jams with xanthan and guar gums, respectively. The jams with corn starch, 60 % ripe mango, and 100 % ripe mango had the highest chroma with values of 22 and 21, respectively, although statistically similar results can be obtained when using guar or xanthan gums, but without important changes due to fruit maturity (Table 3).

Table 3. Effect of mango jam formulation and control on brightness (L*), chroma, hue, titratable acidity (TA), and pH.

Formulation			*L**	Chroma	Hue	TA	pH
No.	Fruit maturity	Gelling agent			(°)	(% citric acid)	
1	60 %	Pectin	34.25 ab	13.30 c	69.23 ab	1.08 ab	3.47 cd
2		Corn starch	39.20 a	21.93 a	74.07 a	0.94 bc	3.57 bcd
3		Xanthan gum	35.33 ab	16.00 abc	64.67 bc	1.05 ab	3.56 bcd
4		Guar gum	35.00 ab	16.90 abc	63.77 bcd	1.16 a	3.40 d
5	100 %	Pectin	33.26 ab	14.60 bc	56.37 d	0.62 e	3.72 ab
6		Corn starch	37.10 ab	20.57 ab	64.80 bc	0.61 e	3.83 a
7		Xanthan gum	32.35 b	14.57 bc	58.72 cd	0.91 cd	3.62 bc
8		Guar gum	32.65 b	16.13 abc	57.40 cd	0.79 d	3.60 bcd
Control			32.10 b	14.65 bc	57.75 cd	0.78 d	3.5 cd
		HSD†	6.18	6.65	8.13	0.14	0.21
		p-value	0.0108	0.0021	< 0.0001	< 0.0001	< 0.0001
		Coefficient of variation (%)	6.40	12.90	4.70	5.22	2.23

†HSD: honest significant difference; a, b, c, d: averages with different letters in columns indicate statistical differences (Tukey, $p \leq 0.05$).

In ‘Kent’ mango pulp, the most abundant carotenoids are β-carotene (responsible for the orange color) and violaxanthin (yellow color) (Rodríguez-Velázquez and Zamora-Peredo, 2018). As mango ripens, the hue changes from pale yellow to yellow-orange (Venkateswarlu and Reddy, 2014), reducing both hue from 91 to 79 °, as well as brightness at consumption maturity (Nolasco-González and Osuna-García, 2017), a condition that influenced the hue and brightness of the jam. Invariably, at fruit maturity, corn starch gave the jam greater luminosity, hue, and chroma. The gelling agents used were yellowish, except for white corn starch, an aspect that could influence the color of the jams. When corn starch was used to coat dehydrated pumpkin slices, their brightness, chroma, and hue increased ($p \leq 0.05$) (Song *et al*., 2018).

Formulation affected the pH and TA of the jams (Table 3). The highest TA and pH values were recorded for formulations four and six, respectively, which were 49 and 9 % higher than the control jam. Formulations with 100 % ripe mango plus pectin or corn starch showed the highest pH with 3.7 and 3.8, respectively, but lower acidity (0.6 %). A pH value ≤ 4.6 is adequate for a jam (NOM-130-SSA1-1995). In this case, all jams presented pH values within the standard. As the fruit ripens, organic acids degrade and pH increases (Quintero *et al*., 2013).

In climacteric, starch is degraded by α-amylase, β-amylase, and other hydrolases, generating sugars and residues (hydroxyls) (Ubonbal *et al*., 2017) that can raise pH, and consequently, acidity is reduced. Pectin, consisting of a mixture of pectinic acids, can increase acidity, while corn starch, composed of starch with amylose and amylopectin chains (Bertoft, 2017), tends to reduce acidity. However, the effect of these gelling agents on the acidity of the jam is irrelevant because of the low concentration (1.2 %) used. Therefore, the effect of fruit maturity was determinant in the acidity and pH of the jams. In food, pathogenic bacteria inhibit their growth at pH levels below 3.8 (Hamad, 2012), which favored the microbiological quality of the formulations and was confirmed by microbiological analysis.

Proximal analysis

Jam formulation affected dietary fiber, protein, and ash content (Table 4). Statistical differences were found between ‘Kent’ mango jams and the control, which had 50 % less ash. In mango jam with lemon pectin, levels of 0.7 % protein, 46 % moisture, and 0.62 % ash have been recorded (Emelike and Akusu, 2019), equivalent to this work. In mango, ash content varies from 0.17 to 0.5 g 100 g^{-1} of fresh pulp (Ara *et al*., 2014), values that can impact formulations, as observed in this study.

The formulation affected the fiber values, which were twice as high in the 60 % ripe mango and corn starch jam compared to the 100 % ripe mango and xanthan gum jam, but showing no differences with the control. In protein, differences were observed between the pectin-based formulation with 60 % ripe mango (1.2 times more protein) and the jam with corn starch and 100 % ripe mango. In dietary fiber and protein, the lowest values were obtained in the 100 % ripe mango formulations. The reduction in fiber and protein is due to changes in mango ripening (Lobo and Sidhu, 2017). In

Table 4. Effect of mango jam formulation and control on proximate properties (% wet basis).

No.	Formulation: Fruit maturity	Formulation: Gelling agent	Dietary fiber (%)	Protein (%)	Ash (%)	Moisture (%)
1	60 %	Pectin	1.42 ab	0.97 a	0.40 a	37.33 a
2		Corn starch	1.47 a	0.79 ab	0.34 a	46.46 a
3		Xanthan gum	1.18 ab	0.73 ab	0.35 a	45.04 a
4		Guar gum	1.36 ab	0.73 ab	0.39 a	43.72 a
5	100 %	Pectin	0.87 abc	0.53 ab	0.31 a	44.01 a
6		Corn starch	0.71 bc	0.45 b	0.33 a	45.94 a
7		Xanthan gum	0.49 c	0.69 ab	0.30 a	46.00 a
8		Guar gum	0.82 abc	0.68 ab	0.30 a	46.53 a
Control			1.36 ab	0.64 ab	0.16 b	38.22 a
		HSD[†]	0.71	0.47	0.14	11.13
		p-value	0.0033	0.0498	0.0027	0.0894
		Coefficient of variation (%)	12.60	13.30	11.00	4.80

[†]HSD: honest significant difference; a, b, c: averages with different letters in columns indicate statistical differences (Tukey, $p \leq 0.05$).

'Kent' mango, the solubilization and enzymatic depolymerization of pectic substances and starches associated with dietary fiber change as maturity advances (Cárdenas-Coronel *et al*., 2012), where protein content also tends to decrease.

Texture profile analysis (TPA)

The formulation type affected the attributes of the TPA. Three trends were distinguished in the formulations: 1) when fruit maturity changed from 60 to 100 %, TPA values decreased; 2) the corn starch-based jam showed the lowest value in each TPA attribute, with this trend accentuated when 100 % ripe mango was used; 3) among the formulations, the jam with 60 % ripe mango and pectin had the highest records in the attributes of adhesiveness, consistency, shear work, viscosity, and firmness, which were 91, 106, 100, 82, and 235 % superior to the control, respectively, and this superiority was even greater with 9, 7, 8, 8, and 16 times in the same attributes evaluated in comparison with the corn starch and 100 % ripe mango jam (Table 5).

The primary cell wall consists mostly (85 %) of cellulose, hemicellulose, and pectins, but during fruit ripening, these compounds are degraded by expansins, glucanases, transglycosylases, xylosidases, polygalacturonases, pectinases, pectin methyl esterases, and other hydrolases, generating a softening of the tissue (Cosgrove, 2015). As 'Kent' mango ripens, firmness abates on average from 235 to 15 N (Nolasco-González and Osuna-García, 2017), reducing further in 100 % ripe fruit to 7 N (Table 2).

In this study, we observed that TPA parameters were significantly increased in the formulation based on 60 % ripe fruit and pectin compared to the control. Pectin, in

Table 5. Effect of mango jam formulation and control on adhesiveness, consistency, shear work, viscosity, and firmness.

No.	Formulation: Fruit maturity	Formulation: Gelling agent	Adhesiveness (N mm^{-1})	Consistency (N mm^{-1})	Shear work (N mm^{-1})	Viscosity (N mm^{-1})	Firmness (N)
1	60 %	Pectin	49.75 a	73.47 a	123.41 a	47.36 a	11.63 a
2		Corn starch	14.88 c	18.56 ef	33.45 d	14.88 d	2.01 ef
3		Xanthan gum	20.62 bc	30.90 cd	51.52 c	20.00 cd	4.43 bc
4		Guar gum	25.08 b	45.46 b	65.77 b	29.43 b	5.55 b
5	100 %	Pectin	16.08 c	22.63 de	38.71 d	17.12 d	3.32 cde
6		Corn starch	5.14 d	8.86 f	13.90 e	5.40 e	0.68 f
7		Xanthan gum	14.37 c	25.04 cde	39.42 d	14.37 d	2.54 de
8		Guar gum	15.38 c	23.93 de	39.32 d	15.38 d	3.94 bcd
Control			26.00 b	35.68 bc	61.68 bc	26.00 bc	3.47cde
		HSD[†]	7.88	11.59	11.09	8.27	1.68
		p-value	< 0.0001	< 0.0001	< 0.0001	< 0.0001	< 0.0001
		Coefficient of variation (%)	14.61	15.11	8.65	15.56	15.55

[†]HSD: honest significant difference; a, b, c: averages with different letters in columns indicate statistical differences (Tukey, $p \leq 0.05$).

its chemical structure, forms gels with water, favoring the stability of the matrix in food (Thakur *et al*., 2019), and therefore, the texture is maintained longer, justifying its preference in the preparation of jams, besides being a low-cost ingredient.

In the formulation of jam with corn starch, the lowest TPA values were obtained under the two conditions of fruit maturity. This is explained by the poor stability of the gel formed by the swelling of starch in mixtures with high sugar content. On the one hand, sugars interacting with water restrict the swelling of starch with water, decreasing the size of the granules formed, and consequently, viscosity diminishes. On the other hand, decreasing the granule size may favor the rearrangement of starch components, mainly amylose and amylopectin, which are aligned in parallel, precipitating and fracturing the gel formed, thus generating retrogradation (Fu *et al*., 2015), and together with storage at room temperature, may favor syneresis in the jam.

Microbiological analysis

Microbiological analysis showed the absence of aerobic mesophiles, molds, yeasts, and total coliforms in the processed jams and the control (data not shown). In water activity, which ranged from 0.82 to 0.845, no differences were found among the jams evaluated. Water activities close to 0.8 can be obtained in products with high sugar content. Foods with water activities greater than or equal to 0.86 are perishable due to their susceptibility to spoilage and the growth of pathogenic microorganisms, since these need water to survive (Hamad, 2012). The safety of the processed product was confirmed prior to sensory evaluation.

Sensory analysis

No differences were found in odor, taste, texture, and acceptability between formulations, except for sensory color. The corn starch jam with 60 % ripe mango recorded a color (7.46) similar to the control and was 23 % statistically superior to the formulation with xanthan gum and 100 % ripe mango (Figure 1). In a similar study, a sensory color of 7.35 evaluated on the same 9-point hedonic scale was reported in mango jam formulated with citrus pectin (Emelike and Akusu, 2019). This value is similar to the color results obtained in this study. Color is the first criterion consumers use in their purchase decisions (Wu and Sun, 2013). As mango ripens, the hue angle reduces (Nolasco-González and Osuna-García, 2017), a phenomenon that was corroborated in the instrumental analysis of both the raw material and the jams (Tables 2 and 3).

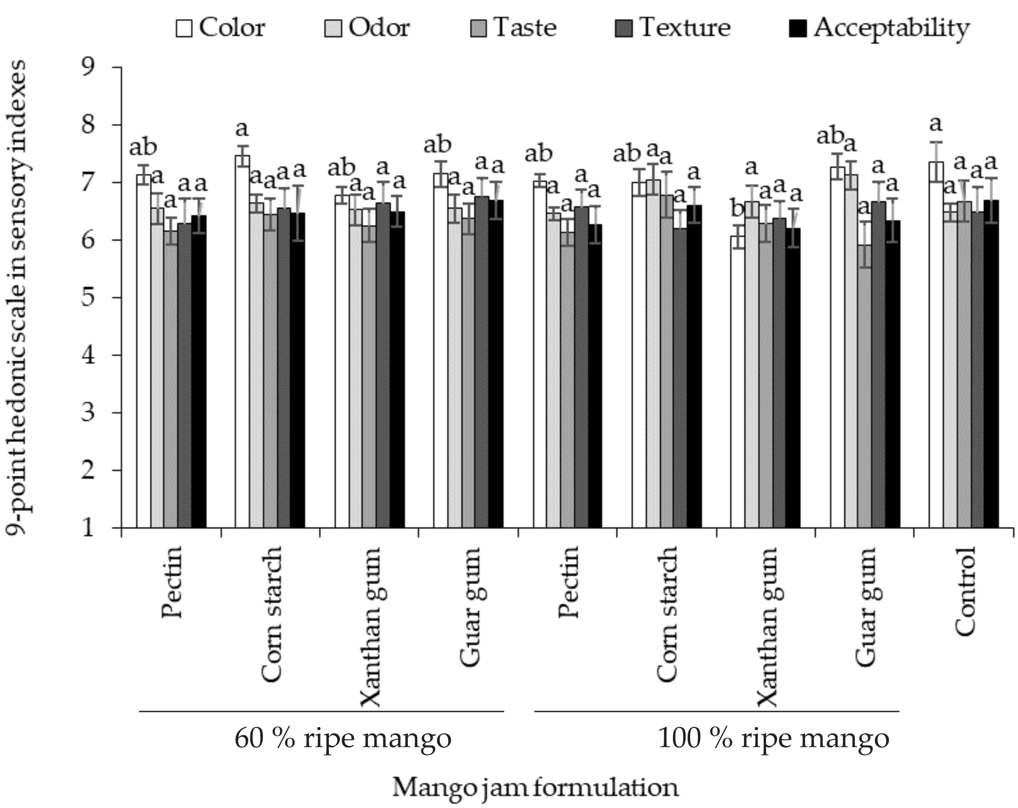

Figure 1. Color, odor, taste, texture, and sensory acceptability measured on a 9-point hedonic scale (9 = like extremely, 8 = like very much, 7 = like moderately, 6 = like slightly, 5 = neither like nor dislike, 4 = dislike slightly, 3 = dislike moderately, 2 = dislike very much, and 1 = dislike extremely) in mango jam formulations with two maturity levels and four gelling agents, plus a commercial jam as a control. Bars ± standard deviation with different letters in each sensory index indicate statistical differences (Tukey, $p \leq 0.05$).

The results recorded for odor, taste, texture, and acceptability showed no effect of formulation, so based on these sensory attributes, the use of the four gelling agents and two stages of fruit maturity can be recommended. It is often difficult to distinguish sensory differences with untrained panels (Curtis, 2013), as observed in this study.

In general, 'Kent' mango at 60 % maturity and the gelling agents corn starch, xanthan gum, and guar gum can be used in the preparation of mango jams in the absence of pectin. This ease of changing gelling agents in the formulation of jam allows the use of mangoes that do not meet the quality criteria to be marketed fresh. Likewise, the production of these products is not limited to mango-producing areas, where their geographical location constitutes a barrier to obtaining raw materials such as gelling agents.

CONCLUSIONS

The physicochemical attributes of jam are modified according to the formulation of the processed product. Contrary to 100 % ripe fruit pulp, 60 % ripe pulp favors instrumental color (hue and brightness), sensory color, adhesiveness, consistency, firmness, viscosity, shear work, titratable acidity, dietary fiber, protein, and a lower pH value. On the other hand, the type of gelling agent induces differential responses among the formulations: a) when pectin is used, the texture profile attributes are superior to the other formulations; b) corn starch improves the values of dietary fiber, brightness, chroma, hue, and pH in relation to the control; and c) guar gum achieves a higher percentage of acidity than commercial jam. Combinations of 60 % ripe mango plus pectin or corn starch are suitable for the formulation of jams since they provide the best benefits in terms of physicochemical and sensory properties. A jam made with 60 % ripe mango and pectin reaches the highest level of texture profile, but when the gelling agent is replaced by corn starch, the highest levels of fiber, instrumental, and sensory color are achieved, with a sensory acceptability comparable to a commercial formulation.

ACKNOWLEDGEMENTS

We thank the financial support received from FORDECYT Project #292474, "Multidisciplinary strategies to increase the added value of the productive chains of coffee, beans, mango, agave mezcal, and aquaculture products (Tilapia) in the South Pacific region through science, technology, and innovation." Thanks are also due for the technical support during proximate determinations given by M.C. Eduardo Sánchez Valdéz of the Food Nutrition Laboratory of the Centro de Investigación en Alimentación y Desarrollo, A.C., Coordinación Regional Culiacán, and Dr. Manuel Vargas-Ortiz of the Investigadores por México program, project number 372 "Frutos tropicales como fuente de fenoles y fibra, interacciones moleculares en digestión simulada," supported by CONAHCYT.

REFERENCES

AOAC (Association of Official Analytical Chemists). 2000. Official methods of analysis of AOAC International (17th edition). AOAC International: Gaithersburg, MD, USA. 2200 p.

Ara R, Motalab M, Uddin MN, Fakhruddin ANM, Saha BK. 2014. Nutritional evaluation of different mango varieties available in Bangladesh. International Food Research Journal 21 (6): 2169–2174.

Ávila-Cubillos EP. 2015. Manual mermelada. Cámara de Comercio de Bogotá: Bogotá, Colombia. 29 p.

Basu S, Shivhare US. 2010. Rheological, textural, micro-structural and sensory properties of mango jam. Journal of Food Engineering 100 (2): 357–365. https://doi.org/10.1016/j.jfoodeng.2010.04.022

Bertoft E. 2017. Understanding starch structure: recent progress. Agronomy 7 (3): 56. https://doi.org/10.3390/agronomy7030056

Cañizares-Chacín AE, Bonafine O, Laverde D, Rodríguez R, Méndez-Natera JR. 2009. Caracterización química y organoléptica de néctares a base de frutas de lechosa, mango, parchita y lima. Revista UDO Agrícola 9 (1): 74–79.

Cárdenas-Coronel WG, Vélez-de la Rocha R, Siller-Cepeda JH, Osuna-Enciso T, Muy-Rangel MD, Sañudo-Barajas JA. 2012. Cambios en la composición de almidón, pectinas y hemicelulosas durante la maduración de mango (*Mangifera indica* cv. Kent). Revista Chapingo Serie Horticultura 18 (1): 5–19.

Codex Alimentarius. 2020. Standard for jams, jellies and marmalades CXS 296-2009. Food and Agriculture Organization of the United Nations, World Health Organization. Rome, Italy. 12 p.

Cosgrove DJ. 2015. Cell walls: structure, formation, and expansion. *In* Taiz L, Zeiger E, Moller IM, Murphy A. (eds.), Plant Physiology and Development (Sixth edition). Sinauer Associates Inc. Publishers: Sunder Land, MA, USA, pp: 379–405.

Curtis PC. 2013. Untrained sensory panels. *In* Kerth CR. (ed.), The Science of Meat Quality. John Wiley and Sons: Ames, IA, USA, pp: 215–231.

Emelike NJT, Akusu OM. 2019. Quality attributes of jams and marmalades produced from some selected tropical fruits. Journal of Food Processing and Technology 10 (5): 790.

Farahnaky A, Alishahi A, Majzoobi M, Al-Hakkak J. 2014. Effect of mixing speed and time on some textural and physicochemical properties of wheat starch gels. Journal of Food Engineering 142: 138–145. https://doi.org/10.1016/j.jfoodeng.2014.06.009

Fu Z, Chen J, Luo SJ, Liu CM, Liu W. 2015. Effect of food additives on starch retrogradation: a review. Starch 67 (1–2): 69–78. https://doi.org/10.1002/star.201300278

Hamad SH. 2012. Factors affecting the growth of microorganisms in food. *In* Bhat R, Alias AK, Paliyath G. (eds.), Progress in Food Preservation. John Wiley and Sons: Chichester, UK, pp: 405–427. https://doi.org/10.1002/9781119962045.ch20

Jamsazzadeh Kermani Z, Shpigelman A, Houben K, ten Geuzendam B, van Loey AM, Hendrickx ME. 2015. Study of mango endogenous pectinases as a tool to engineer mango purée consistency. Food Chemistry 172: 272–282. https://doi.org/10.1016/j.foodchem.2014.09.077

Javanmard M, Chin NL, Yusof YA, Endan J. 2012. Application of sago starch as a gelling agent in jam. CyTA-Journal of Food 10 (4): 275–286. https://doi.org/10.1080/19476337.2011.653693

Lawless HT, Heymann H. 2010. Acceptance Testing. *In* Lawless HT, Heymann H. (eds.), Sensory Evaluation of Food. Food Science Text Series (Second edition). Springer: New York, NY, USA, pp: 325–347. https://doi.org/10.1007/978-1-4419-6488-5_14

Lobo MG, Sidhu JS. 2017. Biology, postharvest physiology, and biochemistry of mango. In Siddiq M, Brecht JK, Sidhu JS. (eds.), Handbook of Mango Fruit: Production, Postharvest Science, Processing Technology and Nutrition. John Wiley and Sons: Oxford, UK, pp. 37–60. https://doi.org/10.1002/9781119014362.ch3

NMB (National Mango Board). 2019. Guía de madurez y maduración del mango. Orlando, FL, USA. https://www.mango.org/wp-content/uploads/2017/10/Maturity-poster_SP_hi.pdf (Retrieved: January 2021).

Nolasco-González Y, Osuna-García JA. 2017. Calidad postcosecha en mango 'Kent' con fertilización normal y alta. Revista Mexicana de Ciencias Agrícolas 19: 4009–4022. https://doi.org/10.29312/remexca.v0i19.669

Quintero CV, Giraldo GG, Lucas AJ, Vasco LJ. 2013. Caracterización fisicoquímica del mango común (*Mangifera indica* L.) durante su proceso de maduración. Biotecnología en el Sector Agropecuario y Agroindustrial 11 (1): 10–18.

Ramírez-Méndez R, Quijada O, Castellano G, Burgos ME, Camacho R, Marin RC. 2010. Características físicas y químicas de frutos de trece cultivares de mango (*Mangifera indica* L.) en el municipio Mara en la planicie de Maracaibo. Revista Iberoamericana de Tecnología Postcosecha 10 (2): 65–72.

Rodríguez-Velázquez J, Zamora-Peredo L. 2018. ¿Un mango se madura desde el hueso hacia la cáscara? Materia, Ciencia y Nanociencia 1 (1): 38–47.

San Martín-Hernández C, Pérez-Rubio V, Muy-Rangel MD, Vargas-Ortiz MA, Quintana-Obregón EA. 2020. Caracterización del polvo y pectina del pericarpio del mango (*Mangifera indica* L.) 'Ataulfo' maduro y análisis FODA para su procesamiento. TIP Revista Especializada en Ciencias Químico-Biológicas 23: 1–10. https://doi.org/10.22201/fesz.23958723e.2020.0.274

SAS (Statistical Analysis System). 2012. SAS/STAT User's Guide. Software versión 9.4. SAS Institute Inc. Cary, NC, USA.

SIAP (Servicio de Información Agroalimentaria y Pesquera). 2020. Anuario estadístico de la producción agrícola. Servicio de Información Agroalimentaria y Pesquera. Ciudad de México, México. https://nube.siap.gob.mx/cierreagricola/ (Retrieved: April 2020).

Song J, Wang X, Li D, Liu C, Yang Q, Zhang M. 2018. Effect of starch osmo-coating on carotenoids, colour and microstructure of dehydrated pumpkin slices. Journal of Food Science and Technology 55 (8): 3249–3256. https://doi.org/10.1007/s13197-018-3258-z

Thakur S, Chaudhary J, Kumar V, Thakur VK. 2019. Progress in pectin-based hydrogels for water purification: trends and challenges. Journal of Environmental Management 238: 210–223. https://doi.org/10.1016/j.jenvman.2019.03.002

Ubonbal R, Porsoongnoen S, Duduang J, Klaynongsruang S, Duduang S. 2017. Purification and characterization of two isoforms of native α amylase from Ok-Rong mango (*Mangifera indica* Linn. Cv Ok-Rong). Turkish Journal of Biochemistry 42 (6): 624–632. https://doi.org/10.1515/tjb-2016-0218

Venkateswarlu K, Reddy PSK. 2014. Mango: carotenoids. International Journal of Pharmamedix India 2 (2): 741–744.

Villamizar-Vargas R, Quiceno-Gómez C, Giraldo-Giraldo G. 2019. Comportamiento de características fisicoquímicas durante la maduración del mango Tommy Atkins luego de cosechado. Revista U.D.C.A Actualidad y Divulgación Científica 22 (1): e1159. https://doi.org/10.31910/rudca.v22.n1.2019.1159

Wu D, Sun DW. 2013. Colour measurements by computer vision for food quality control – A review. Trends in Food Science and Technology 29 (1): 5–20. https://doi.org/10.1016/j.tifs.2012.08.004

Wüstenberg T. 2015. Cellulose and cellulose derivates in the food industry, fundamentals and applications. John Wiley and Sons: Weinheim, Germany. 525 p. https://doi.org/10.1002/9783527682935

Agrociencia

PHYSICOCHEMICAL CHARACTERISTICS OF RED WINES (CABERNET SAUVIGNON AND TEMPRANILLO) FROM ENSENADA, BAJA CALIFORNIA

Liliana del Rocío **Castro-López**[1], Lizzette **Velasco-Aulcy**[2], Alejandra **Chávez-Márquez**[1], Cynthia d**e Lira-García**[1], Carolina **Mata-Miranda**[1], Guillermo **Castillo**[1]*

[1]Universidad Autónoma de Baja California. Facultad de Enología y Gastronomía. Carretera Transpeninsular Ensenada-Tijuana 3917, Colonia Playitas, Ensenada, Baja California, Mexico. C. P. 22860.

[2]Universidad Autónoma de Baja California. Facultad de Ciencias Facultad de Ciencias Administrativas y Sociales. Boulevard Zertuche y Boulevard de Los Lagos S/N, Fracc. Valle Dorado, Ensenada, Baja California, Mexico. C.P. 22890.

*Author for correspondence: castillo.guillermo@uabc.edu.mx

ABSTRACT

Ensenada wine country, in the State of Baja California, Mexico, accounts for approximately 70–80 % of Mexico's wine production. Despite its significance, detailed knowledge of the physical and chemical properties of wines remains limited. In this study, we examined nine physicochemical properties of 69 commercial red wines produced from the Tempranillo and Cabernet Sauvignon varietals in the San Vicente, Santo Tomás, and Guadalupe valleys. The pH, total acidity, acetic acid, lactic acid, malic acid, total polyphenols, glucose/fructose ratio, alcohol content, and red color intensity were all analyzed. Tempranillo wines showed significantly higher levels of acetic acid, lactic acid, and total acidity, but lower levels of total polyphenols and malic acid than Cabernet Sauvignon wines. Furthermore, wines from the Santo Tomás region have significantly higher alcohol content, glucose/fructose ratio, total polyphenols, red color intensity, and total acidity, distinguishing them from the wines of San Vicente and Guadalupe. Our results highlight the influence of the grape variety on wine chemistry, emphasizing the possibility for further optimization of the winemaking processes for the benefit of vine growers, enologists, and wine production in the region.

Keywords: *Vitis vinifera* L., viticulture, San Vicente Valley, Santo Tomás Valley, Guadalupe Valley.

Citation: Castro-López LR, Velasco-Aulcy L, Chávez-Márquez A, de Lira-García C, Mata-Miranda C, Castillo G. 2024. Physicochemical characteristics of red wines (Cabernet Sauvignon and Tempranillo) from Ensenada, Baja California. **Agrociencia** 58(3): 352-360. https://doi.org/ 10.47163/ agrociencia.v58i3.3103

Editor in Chief:
Dr. Fernando C. Gómez Merino

Received: November 06, 2023.
Approved: April 16, 2024.
Published in Agrociencia: April 23, 2024.

INTRODUCTION

Wine terroir refers to the combination of environmental factors and cultural practices that give wine its unique characteristics. These are shaped by several factors, including the variety of fermented grapes, the vineyard's geographical setting (including mesoclimate, topoclimate, and microclimate), soil geology and composition, as well as agronomic management practices (Alexandre, 2020). Climate, particularly temperature, is a crucial determinant of vine physiology and wine quality (Cabello-

Pasini *et al*., 2017), making climatic variation a key factor in the establishment of successful vineyards and the characteristics of grapes and wines produced in a region (Anderson *et al*., 2012). As such, climate is considered one of the most important factors influencing wine terroir.

About 70–80 % of wine production in Mexico occurs in the municipality of Ensenada, in the State of Baja California (Buendía-Muñoz and del Valle-Sánchez, 2017). There are more than 60 wineries in the region, ranging from very small businesses producing approximately 500 cases per year to considerably larger companies generating more than 15 million cases per year (Covarrubias and Thach, 2015; González-Andrade, 2015). According to state data, there are 3 359.75 ha of vines for winemaking in Ensenada. Approximately 87 % of state production is concentrated in three major wine-producing regions: Guadalupe (46 %), San Vicente (34 %), and Santo Tomás (7 %) (OEIDRUS, 2011).

Due to its Mediterranean climate (rainfall in winter and hot, dry summers), Baja California is regarded as the premier region for high-quality wine production in Mexico (Davis *et al*., 1996). This is primarily attributed to an average temperature of 19.8 °C from April to October, which corresponds to the growth cycle of *Vitis vinifera* L., and an average temperature of 20.4 °C in September, when the fruit ripens (Meraz-Ruiz and Ruiz-Vega, 2016). Although viticulture is practiced in several wine valleys in Baja California, Guadalupe, Santo Tomás, and San Vicente stand out as three of the most important due to their distinct climatic characteristics.

Valenzuela-Solano and Tonietto (2012) studied the viticultural climate of the main wine production areas in Baja California and found climatic diversity between regions, resulting in different viticultural potentials (Table 1). According to Macías-Carranza and Cabello-Pasini (2021), San Vicente and San Antonio de las Minas are classified as Region IV (temperate-warm) and Santo Tomás and Guadalupe as Region V (warm and very warm zones). Additionally, evapotranspiration in San Vicente and San Antonio de las Minas was 15 % lower than in Santo Tomás and Guadalupe. Nonetheless, climate forecasts for Baja California are predicted to change over the next 30 years, posing a threat to the region's ability to produce high-quality wines (Valenzuela-Solano *et al*., 2018).

Table 1. Average yearly total precipitation, minimum temperature, maximum temperature, mean temperature, and evaporation of the studied winemaking regions in Baja California, Mexico (SMN, 2019).

Region	Total precipitation (mm)	Min. Temp. (°C)	Max. Temp. (°C)	Mean Temp. (°C)	Evaporation (mm)
San Vicente	18.0	9.1	25.9	17.6	131.8
Santo Tomás	21.4	8.6	27.3	18.0	151.5
Guadalupe	25.2	8.3	24.8	16.6	130.8

Despite their importance, little is known about the physical and chemical properties of Baja California wines (Covarrubias and Thach, 2015; Castillo-Sánchez *et al.*, 2018). Espitia-López *et al*. (2015) found differences in the content of wood phenolic compounds in a Mexican red Merlot wine from the Guadalupe Valley matured in barrels compared to wood chips. Likewise, Cabello-Pasini *et al*. (2013) evaluated the concentration of Ca, Mg, K, and Na in wines produced in Baja California. In a recent study, Espinoza-Cruz *et al*. (2020) determined major and minor trace elements (K, Na, Mg, Ca, Rb, Sr, Mn, Fe, Al, Cu, and Cr) in Mexican red wines, including five wines from Guadalupe Valley. Chávez-Márquez *et al*. (2022) described the validation of an untargeted metabolomics method for the characterization of Cabernet Sauvignon wines from two vineyards and two vintages in Mexico. Similarly, information on the physicochemical characteristics of grapes and wines, as well as their relationship to the climate factors that prevail in Baja California's grape-growing valleys, is still scarce. To our knowledge, only one study has investigated the relationship between mesoclimatic variability within the Guadalupe Valley and the concentration of total soluble solids, titratable acidity, and pH of Nebbiolo grapes (Cabello-Pasini *et al*., 2017).

In this context, the objective of this study was to contribute to the decision-making process for winemaking in Baja California through the description of nine physicochemical characteristics (pH, total acidity, acetic acid, lactic acid, malic acid, alcohol content, total polyphenols, glucose/fructose ratio, and red color intensity) of commercial monovarietal red wines of Cabernet Sauvignon and Tempranillo varietals produced in three of the most important wine-producing areas of Baja California (Santo Tomás, San Vicente, and Guadalupe valleys). We also explored whether there are differences in red wines produced from the Cabernet Sauvignon and Tempranillo varietals, as well as in the wine regions of Santo Tomás, Guadalupe, and San Vicente, depending on the analyzed characteristics. Generating such information is one of the first steps in the search for the chemical identity of Baja California wines.

MATERIALS AND METHODS

We sampled 69 different commercial red wines of Tempranillo and Cabernet Sauvignon varietals produced in the San Vicente (SV), Santo Tomás (ST), and Guadalupe (GV) valleys from the 2012–2017 vintage. A sample size of 10 mL was obtained directly from each bottle. We followed an enzymatic approach, using a Y15 Biosystem enological analyzer (Biosystems, Barcelona, Spain) to measure the physicochemical characteristics (pH, total acidity, acetic acid, lactic acid, malic acid, total polyphenols, and glucose/fructose ratio). Alcohol content at 20 °C was measured using a Dujardin-Salleron 160000 ebulliometer (Dujardin-Salleron, France). All analyses were performed in duplicate, then averaged.

The Principal Component Analysis (PCA) is a multivariate technique used to reduce dimensionality in original data while retaining as much information as possible (Syms, 2008). This allows for a two-dimensional study of the wines and the determination of the directions in which the majority of the information is stored. Thus, using the main factors derived from the original data, it is possible to investigate the differences between different wines and determine which variables contribute the most to such variances (Câmara *et al*., 2006). As a result, we conducted a PCA using the physicochemical properties of the wines and retrieved the first four main component scores from the analysis.

We used ANOVA models to determine the main component differences between Cabernet Sauvignon and Tempranillo, as well as the wine-producing regions (ST, SV, and GV). The models PC1, PC2, PC3, and PC4 score as response factors, and the terms Varietal, Region, and Vintage (as covariates to compensate for storage time and environmental differences across years) serve as predictive factors. When the term Region showed significant results in an ANCOVA model, a Tukey-Kramer *post hoc* test was used to assess differences between variable levels ($\alpha = 0.05$). All statistical analyses were carried out using JMP version 14 (JMP Statistical Discovery; NC, USA).

RESULTS AND DISCUSSION

The sampled wines exhibited analytical values within the normal range observed in the global wine industry (Buendía-Muñoz and del Valle-Sánchez, 2017), indicating appropriate vinification techniques and standard quality measures (Table 2). Variations in the physicochemical parameters were found. PC1, PC2, PC3, and PC4 accounted for 75.96 % of the total multivariate variation from the original data (27.4 and 23.8 %, respectively). Variables with higher loading contributions to PC1 were acetic acid (0.883), lactic acid (0.8001), total acidity (0.721), total polyphenols (-0.481), and

Table 2. Summary statistics of nine physicochemical variables evaluated for Cabernet and Tempranillo red wines produced in the San Vicente, Santo Tomás, and Guadalupe valleys in Baja California, Mexico.

	Cabernet Sauvignon (mean ± SE)			Tempranillo (mean ± SE)		
	San Vicente	Santo Tomás	Guadalupe	San Vicente	Santo Tomás	Guadalupe
Glucose-fructose (g L^{-1})	2.85±1.37	2.39±0.43	2.38±0.50	4.26±1.79	2.45±0.75	1.90±0.34
Alcohol content (g L^{-1})	14.3±0.96	13.6±0.97	14.5±0.95	14.8±1.58	14.27±1.28	14.66±1.09
pH	3.83±0.12	3.93±0.05	3.82±0.18	3.85±0.14	3.89±0.20	3.86±0.17
Lactic acid (g L^{-1})	1.29±0.23	1.45±0.19	1.25±0.42	1.65±0.34	1.63±0.36	1.66±0.63
Malic acid (g L^{-1})	0.13±0.06	0.10±0.30	0.26±0.25	0.13±0.04	0.20±0.18	0.14±0.19
Acetic acid (g L^{-1})	0.87±0.23	0.99±0.19	0.76±0.21	0.97±0.16	1.14±0.12	0.95±0.34
Total acidity (g L^{-1})	5.28±0.62	4.82±0.31	5.06±0.61	5.36±0.62	5.22±0.21	5.19±0.14
Total polyphenols (mg L^{-1})	1985.00±327.49	1954.80±201.19	1057.81±199.86	1992.67±293.11	1975.50±278.60	1889.39±195.20
Red color intensity	9.82±2.37	8.05±1.19	9.57±1.89	12.32±4.51	9.03±2.06	8.78±1.14

SE: standard error.

malic acid (-0.559). On the other hand, variables that loaded higher into PC2 were red color intensity (0.882), total polyphenols (0.638), glucose/fructose ratio (0.619), ethanol content (0.554), and total acidity (0.347). Variables with higher loading contributions to PC3 were pH (0.928) and total acidity, while malic acid (0.635) and the glucose/fructose ratio (-0.406) contributed the most to PC4.

ANCOVA analysis for PC1 detected a significant effect of the term Varietal ($F = 7.29$, df (degrees of freedom) = 1, $p = 0.0089$). The mean PC1 scores were lower for Cabernet Sauvignon compared to Tempranillo wines (Figure 1). On the other hand, ANCOVA analysis for PC2 found a significant effect of the term Region ($F = 3.95$, $df = 2$, $p = 0.024$). Tukey-Kramer HSD *post hoc* analysis found that mean PC2 scores were significantly higher in ST compared to SV and VG, which did not differ between each other (Figure 1). ANCOVA analysis for PC3 detected a significant effect of the term Vintage ($F = 4.15$, $df = 1$, $p = 0.0044$), and a posterior regression analysis showed a positive relationship between Vintage values and PC3 scores ($y = -364.5 + 0.1805 \times$ Vintage, $R^2 = 0.1$, $p = 0.0074$).

ANCOVA of PC1 scores revealed that Tempranillo wines had significantly greater levels of acetic acid, lactic acid, and total acidity but lower levels of total polyphenols and malic acid than Cabernet Sauvignon wines (Figure 1). This indicates that grape variety is an important factor contributing to the differences in acidity profiles among the analyzed wines (Miao *et al*., 2022). Particularly, the Cabernet Sauvignon variety showed higher PC1 scores compared to Tempranillo, reflecting a more pronounced acidity profile (Figure 1). However, the acidity is not just determined by the type of grapes used but also by the winemaking process itself, including fermentation conditions and techniques (Jakabová *et al*., 2021).

Likewise, the lower levels of malic acid observed in Cabernet Sauvignon compared to Tempranillo wines might be the result of vinification decisions intended to achieve a “rounder and creamier mouthfeel” throughout an extensive malolactic fermentation (Virdis *et al*., 2021). On the other hand, polyphenol levels could be attributed to the thickness of the grape skins of each variety. Cabernet Sauvignon grapes are renowned for their thick skins, which may impede the extraction of phenolic compounds, resulting in lower polyphenol content (Apolinar-Valiente *et al*., 2016; Gombau *et al*., 2020). The obtained acidity profile and total phenol content may be the result of different factors such as canopy management, extraction techniques, winemaking practices, and grape thickness (Jakabová *et al*., 2021). Further research is warranted to elucidate the specific mechanisms underlying these differences and to explore the potential implications for wine production in the region.

On the other hand, ANCOVA of PC2 scores showed that wines produced in the Santo Tomás region had significantly higher alcohol content, glucose/fructose ratio values, total polyphenols, red color intensity, and total acidity than wines from San Vicente and Guadalupe, which did not differ between each other (Figure 1). This suggests that the geographic origin of the wines influenced the evaluated variables related to PC2. Elevated temperatures have been observed to increase alcohol content, glucose/

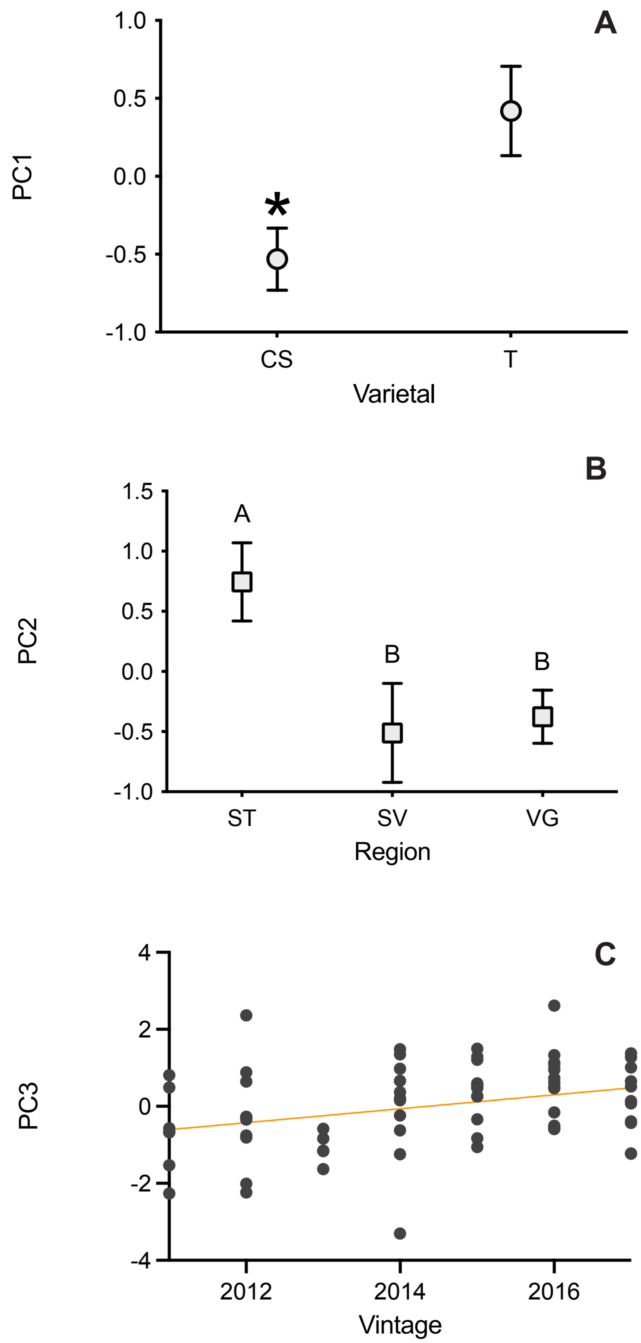

Figure 1. Principal component analysis score means (± SE). A: Principal Component 1 (PC1) of Cabernet Sauvignon and Tempranillo varietals; B: Principal Component 2 (CP2) of red wines produced on San Vicente, Santo Tomás, and Guadalupe valleys; C: relationship between Principal Component 3 (PC3) scores and Vintage values of studied wines. Means not sharing the same letter differ significantly after a Tukey-Kramer LSD *post hoc* test. *Significant differences between levels.

fructose levels, total polyphenols, and red color intensity while increasing total acidity (Delrot *et al*., 2020).

Finally, analyses revealed a significant relationship with Vintage, indicating that annual harvest variations have a significant influence on the chemical profiles of the studied wines. This suggests that interannual differences in climate conditions, cultivation practices, and grape maturity at the time of harvest can have considerable effects on the physicochemical characteristics of wines, specifically on parameters associated with PC3, such as pH and total acidity.

Temperatures in the various wine valleys of Baja California have risen significantly in recent years (Valenzuela-Solano *et al*., 2018). Given that Santo Tomás is already a warm valley, it can be expected that wines produced in this region will be among the first to experience the consequences of temperature surges. Winemakers in the region could benefit from the use of non-*Saccharomyces* yeasts, such as *Lachancea thermotolerans*, in co-culture with *Saccharomyces* strains as adaptation strategies to control pH, ethanol, and volatile acidity resulting from high temperatures (Benito, 2018; Pérez-Muñoz *et al*., 2023). They can also implement strategies such as irrigation and canopy management to reduce the effects of increasing temperatures (Delrot, 2020).

CONCLUSIONS

Based on their physicochemical characteristics, we were able to detect significant multivariate differences between varieties and regions. The analyzed wines exhibit standard values in all analytical measurements of the final product, suggesting proper winemaking practices were employed while highlighting the significant influence of grape variety on the chemical composition of wines in the region. However, in the face of the challenges derived from climate change, there is still room for monitoring, control, and improvement in the winemaking process.

ACKNOWLEDGEMENTS

Financial support was provided to *Cuerpo Académico* UABC-CA-292 by *Fortalecimiento de Cuerpos Académicos* 2018 Project 28890.

REFERENCES

Alexandre H. 2020. Wine yeast terroir: Separating the wheat from the chaff—for an open debate. Microorganisms 8 (5): 787. https://doi.org/10.3390/microorganisms8050787

Apolinar-Valiente R, Romero-Cascales I, Gómez-Plaza E, Ros-García JM. 2016. Degradation of Syrah and Cabernet Sauvignon grapes skin: Application of different enzymatic activities: A preliminary study. European Food Research and Technology 242 (12): 2041–2049. https://doi.org/10.1007/s00217-016-2702-4

Anderson JD, Jones GV, Tait A, Hall A, Trought MC. 2012. Analysis of viticulture region climate structure and suitability in New Zealand. Journal International des Sciences de la Vigne et du Vin 46 (3): 149–165. https://doi.org/10.20870/oeno-one.2012.46.3.1515

Benito S. 2018. The impacts of *Lachancea thermotolerans* yeast strains on winemaking. Applied Microbiology and Biotechnology 102 (16): 6775–6790. https://doi.org/10.1007/s00253-018-9117-z

Cabello-Pasini A, Macias-Carranza V, Mejía-Trejo A. 2017. Efecto del mesoclima en la maduración de uva Nebbiolo (*Vitis vinifera*) en el Valle de Guadalupe, Baja California, México. Agrociencia 51 (6): 617–633.

Cabello-Pasini A, Macías-Carranza V, Siqueiros-Valencia A, Huerta-Díaz MÁ. 2013. Concentration of calcium, magnesium, potassium, and sodium in wines from Mexico. American Society for Enology and Viticulture 64 (2): 280–284. https://doi.org/10.5344/ajev.2012.12080

Câmara JS, Alves MA, Marques JC. 2006. Multivariate analysis for the classification and differentiation of Madeira wines according to main grape varieties. Talanta 68 (5): 1512–1521. https://doi.org/10.1016/j.talanta.2005.08.012

Castillo-Sánchez G, Castro-López L, Méndez S. 2018. Contribution of Mexican scholars to viticultural and oenological research: where do we stand? OENO One 52 (4): 273–278. https://doi.org/10.20870/oeno-one.2018.52.4.2275

Chávez-Márquez A, Gardea AA, González-Ríos H, Vázquez-Moreno L. 2022. Characterization of Cabernet Sauvignon wines by untargeted HS-SPME GC-QTOF-MS. Molecules 27 (5): 1726. https://doi.org/10.3390/molecules27051726

Covarrubias J, Thach L. 2015. Wines of Baja Mexico: A qualitative study examining viticulture, enology, and marketing practices. Wine Economics and Policy 4 (2): 110–115. https://doi.org/10.1016/j.wep.2015.11.001

Espinoza-Cruz TL, Guerrero-Esperanza M, Wrobel K, Yanez-Barrientos E, Acevedo-Aguilar FJ, Wrobel K. 2020. Determination of major and minor elements in Mexican red wines by microwave-induced plasma optical emission spectrometry, evaluating different calibration methods and exploring potential of the obtained data in the assessment of wine provenance. Spectrochimica Acta Part B: Atomic Spectroscopy 164: 105754. https://doi.org/10.1016/j.sab.2019.105754

Davis GW, Richardson DM, Keeley JE, Hobbs RJ. 1996. Mediterranean-type ecosystems: the influence of biodiversity on their functioning. *In* Mooney HA, Cushman JH, Medina E, Sala OE, Schulze ED. (eds.), Functional Roles of Biodiversity: A Global Perspective. John Wiley and Sons Ltd: Hoboken, NJ, USA, pp: 151–183.

Delrot S, Grimplet J, Carbonell-Bejerano P, Schwandner A, Bert PF, Bavaresco L, Dalla L, Gaspero GD, Duchêne E, Hausmann L *et al*. 2020. Genetic and genomic approaches for adaptation of grapevine to climate change. *In* Kole C. (ed.), Genomic Designing of Climate-Smart Fruit Crops. Springer: Cham, Switzerland, pp: 157–270. https://doi.org/10.1007/978-3-319-97946-5_7

Espitia-López J, Escalona-Buendía H, Luna H, Verde-Calvo J. 2015. Multivariate study of the evolution of phenolic composition and sensory profile on mouth of Mexican red Merlot wine aged in barrels vs wood chips. CyTA-Journal of Food 13 (1): 26–31. https://doi.org/10.1080/19476337.2014.907826

Euromonitor International. 2019. Alcoholic drinks in Mexico. London, UK. http://www.portal.euromonitor.com (Retrieved: May 2022).

Gombau J, Pons-Mercadé P, Conde M, Asbiro L, Pascual O, Gómez-Alonso S, García-Morebi E, Canals JM, Hermosin-Gutiérrez I, Zamora F. 2020. Influence of grape seeds on wine composition and astringency of Tempranillo, Garnacha, Merlot and Cabernet Sauvignon wines. Food Science and Nutrition 8 (7): 3442–3455. https://doi.org/10.1002/fsn3.1627

González-Andrade S. 2015. Cadena de valor económico del vino de Baja California, México. Estudios fronterizos 16 (32): 163–193.

Macías-Carranza V, Cabello-Pasini A. 2021. Climatología y evapotranspiración en valles vitivinícolas de Baja California. Revista mexicana de ciencias agrícolas 12 (5): 849–863. https://doi.org/10.29312/remexca.v12i5.2816

Meraz-Ruiz L, Ruiz-Vega A. 2016. El enoturismo de Baja California, México: un análisis de su oferta y comparación con la región vitivinícola de La Rioja, España. Investigaciones Turísticas 12: 73–98. https://doi.org/10.14198/inturi2016.12.04

Miao Y, Wang H, Xu X, Ye P, Wu H, Zhao R, Shi X, Cai F. 2022. Chemical and sensory characteristics of different red grapes grown in Xinjiang, China: Insights into wines composition. Fermentation **8** (12): 689. https://doi.org/10.3390/fermentation8120689

Buendía-Muñoz AR, del Valle-Sánchez M. 2017. Productividad en la industria de la uva y la eficiencia de los recursos disponibles en el Valle de Guadalupe, Baja California. Semestre Económico 5 (2): 5–27. https://doi.org/10.26867/seconomico.v5i2.131

Pérez-Muñoz VA, Castro-López L del R, Martínez-Hernández LE, Cordero-Herrera D, Herrera-Martínez G, Castillo G. 2023. Evaluation of bio-acidifying yeast *Lachancea thermotolerans* as a strategy to reduce the effects of climate change in Tempranillo grape must vinification. BIO Web of Conferences 56: 02036. https://doi.org/10.1051/bioconf/20235602036

OEIDRUS (Oficina Estatal de Información para el Desarrollo Rural Sustentable). 2011. Estudio estadístico sobre producción de uva en Baja California. Gobierno del Estado de Baja California. Secretaría de Agricultura, Ganadería, Desarrollo Rural, Pesca y Alimentación. Oficina Estatal de Información para el Desarrollo Rural Sustentable. Mexicali, México. 31 p.

Jakabová S, Fikselová M, Mendelová A, Ševčík M, Jakab I, Aláčová Z, Kolačkovská J, Ivanova-Petropulos V. 2021. Chemical composition of white wines produced from different grape varieties and wine regions in Slovakia. Applied Sciences 11 (22): 11059. https://doi.org/10.3390/app112211059

SMN (Servicio Meteorológico Nacional). 2019. Información estadística climatológica. Gobierno de México. Secretaría de Medio Ambiente y Recursos Naturales. Comisión Nacional del Agua. Servicio Meteorológico Nacional. Ciudad de México, México. https://smn.conagua.gob.mx/es/climatologia/informacion-climatologica/informacion-estadistica-climatologica (Retrieved: May 2022).

Syms C. 2008. Principal components analysis. *In* Jørgensen E, Fath BD. (eds.), Encyclopedia of Ecology. Elsevier: Oxford, UK, pp: 2940–2949. https://doi.org/10.1016/B978-008045405-4.00538-3

Valenzuela-Solano C, Tonietto J. 2012. El clima vitícola de regiones productoras de uvas para vinos en Baja California, México. *In* Tonietto J, Sotés-Ruiz V, Gómez-Miguel VD. (eds.), Clima, Zonificación y Tipicidad del Vino en Regiones Vitivinícolas Iberoamericanas. CYTED: Madrid, España, pp: 287–295.

Valenzuela-Solano C, Ruiz-Corral JA, Ramírez-Ojeda G, Hernández-Martínez R. 2018. Efectos del cambio climático sobre el potencial vitícola de Baja California, México. Revista Mexicana de Ciencias Agrícolas 10: 2047–2059. https://doi.org/10.29312/remexca.v0i10.1043

Virdis C, Sumby K, Bartowsky E, Jiranek V. 2021. Lactic acid bacteria in wine: Technological advances and evaluation of their functional role. Frontiers in Microbiology 11: 612118. https://doi.org/10.3389/fmicb.2020.612118

Agrociencia

ANTIOXIDANT ACTIVITY AND PHENOLIC COMPOUNDS IN CACHICHÍN NUTS (*Oecopetalum mexicanum* Greenm. & C.H. Thomps.) EXPOSED TO DIFFERENT THERMAL TREATMENTS

Alejandro Esli **Hernández-Mora**[1], Fernando Carlos **Gómez-Merino**[1,2], Tania **Marín-Garza**[3], José Andrés **Herrera-Corredor**[1], Libia Iris **Trejo-Téllez**[2*]

[1]Colegio de Postgraduados Campus Córdoba. Carretera Córdoba-Veracruz km 348, Manuel León, Amatlán de los Reyes, Veracruz, Mexico. C. P. 94953.
[2]Colegio de Postgraduados Campus Montecillo. Carretera México-Texcoco km 36.5, Montecillo, Texcoco, State of Mexico, Mexico. C. P. 56264.
[3]Universidad Veracruzana. Facultad de Ciencias Químicas. Prolongación de Oriente 6 No. 1009, Orizaba, Veracruz, Mexico. C. P. 94340.
* Author for correspondence: tlibia@colpos.mx

ABSTRACT

The cachichín tree (*Oecopetalum mexicanum* Greenm. & C.H. Thomps.), present in the Sierra de Misantla, Veracruz, Mexico, produces fruits with bitter-tasting nuts, traditionally consumed as a healthy snack, boiled or toasted. These nuts have significant concentrations of lipids, proteins, fiber, and ash, although their antioxidant capacity and phenolic profile in response to different thermal treatments have not been explored. The objective of this study was to analyze the antioxidant activity and determine the concentrations of free and total phenolic compounds in the raw (T1) cachichín nuts and nuts subjected to different thermal treatments, including boiled (T2), commercial toast (T3), and controlled toast at laboratory level (T4). The nuts subjected to controlled toasting (T4) showed the highest mean in antioxidant activity (20.73 %), followed by commercial toasting (T3; 19.41 %) and raw nuts (T1; 15.38 %), while the boiled nuts (T2) showed the lowest values (9.68 %). Regarding free phenols, the highest concentration of catechin was found in raw nuts (T1), with 278.91 mg g^{-1} fresh biomass weight (FBW). Trans-ferulic acid was more abundant in the toasting treatments (7.09 ng g^{-1} FBW in T3 and 6.13 ng g^{-1} FBW in T4) compared to raw nuts (T1; 3.77 ng g^{-1} FBW). Trans-coumaric acid was higher with controlled toasting (T4; 2.67 ng g^{-1} FBW). In terms of total phenols, raw nuts (T1) showed the highest concentration of catechin (613.95 mg g^{-1} FBW), while chlorogenic acid was more abundant in commercial toasting (T3; 89.12 ng g^{-1} FBW). Total trans-ferulic acid was higher in boiled and toasted nuts (T2, T3, and T4), while trans-coumaric acid was highest in controlled toasting (T4) and lowest in boiled (T2). Cachichín nuts are concluded to contain phenolic compounds with beneficial functions, whose concentrations can be altered in response to the thermal treatments applied.

Keywords: Metteniusaceae, cacaté, nutraceutical value, antioxidants, phenols.

Citation: Hernández-Mora AE, Gómez-Merino FC, Marín-Garza T, Herrera-Corredor JA, Trejo-Téllez LI. 2024. Antioxidant activity and phenolic compounds in cachichín (*Oecopetalum mexicanum* Greenm. & C.H. Thomps.) exposed to different thermal treatments. **Agrociencia** 58(3): 361-374. https://doi.org/ 10.47163/ agrociencia.v58i3.3158

Editor in Chief: Dr. Fernando C. Gómez Merino

Received: August 01, 2023.
Approved: April 08, 2024.
Published in Agrociencia: May 13, 2024.

INTRODUCTION

The species *Oecopetalum mexicanum* Greenm. & C.H. Thomps., commonly known as cachichín or cacaté, is a tree that produces fruits with edible nuts. The species belongs to the Metteniusaceae family and is mainly distributed in southeastern Mexico and northern Central America. In the state of Veracruz, its growth and cultivation have deep roots with the indigenous peoples and local residents of the Sierra de Misantla. This plant species produces a globose fruit with a hard shell, greenish in color when immature, and brown when mature. Inside the fruit there is an ovoid nut, with a large endosperm, yellow in color, soft in texture, and a bitter taste (Lascurain *et al*., 2012; Hernández-Mora *et al*., 2024). Its cultivation and production happen in several municipalities that make up the Sierra de Misantla, and its marketing reaches the capital city of the state of Veracruz, Xalapa. The nut can be sold raw, boiled, or toasted (Lascurain *et al*., 2009).

Some research has been carried out on the nutritional properties of these nuts, and it has been found that, on average, they contain 10 % protein, 40 % lipids, 5 % fiber, 2 % ash, and less than 1 % sugars (Hernández-Mora *et al*., 2021). Additionally, the nuts contain saponins, sterols, and coumarins, which are antioxidant compounds important in nutrition and human health (Hernandez *et al*., 2013). In an exhaustive literature search, no detailed analyses were found that addressed the concentrations of phenolic compounds in cachichín nut, nor was information found about how various treatments could influence its antioxidant activity. Phenolic compounds can inhibit the development of human diseases, including hypertension, metabolic problems, incendiary infections, and neurodegenerative diseases.

Among the antioxidant compounds that plants can produce, phenols show various functions and, as part of the functional secondary metabolism, offer benefits to other organisms that consume them (Olivares-Vicente *et al*., 2018). In humans and other biological systems, phenols have shown effectiveness in the control of cholesterol and oxidized low-density lipoprotein (LDL) and important antioxidant and metal chelating activity at toxic concentrations (Kumar *et al*., 2013).

Although many food products can be consumed fresh, others must be subjected to thermal treatments for consumption. Such processing modifies their biochemical and nutritional properties. These modifications depend on the type of food and other factors such as storage time, pH, water activity, chemical compounds, and concentrations of the plant species, starches, and sugars involved. Furthermore, these factors influence the Maillard reaction, which may start at 115–120 °C, accelerate at 130 °C, and stop at 180 °C (Kumar *et al*., 2013). Consequently, this reaction produces a variety of early, intermediate, and advanced compounds and has both positive and negative effects on food quality (Chen *et al*., 2018). The beneficial contributions of the Maillard reaction are the generation of sensory attributes such as color, flavor, aroma, and texture, as well as improvements in antioxidant properties and inhibition of the proliferation of pathogenic microorganisms (Liu *et al*., 2020). The negative aspects are the appearance of unpleasant flavors, loss of flavor, discoloration, loss of nutritional value of proteins, and the formation of potentially carcinogenic compounds such as acrylamide (Kathuria *et al*., 2023).

The objective of this study was to determine the effect of different thermal treatments (i.e., raw nuts [T1], boiled [T2], commercially toasted [T3], and toasted under controlled laboratory conditions [T4]) on the antioxidant activity and the concentrations of free and total phenolic compounds in cachichín nuts.

MATERIALS AND METHODS

Obtention of nut samples

The cachichín nut samples were obtained from the "Café Dorantes" group, a collective of producers located in Misantla, Veracruz, Mexico. The evaluated treatments were: raw nuts (T1); boiled nuts (T2); nuts subjected to commercial toasting (T3); and nuts subjected to controlled toasting (T4). Boiling (T2) was done under empirical conditions in wood stoves, at a temperature of 100 °C for 15 min in a 20 L stainless steel container. Commercial toasting (T3) was carried out on clay or red clay comales from the Sierra de Misantla at temperatures that reached up to 180 °C. Cooking took 20 min over low heat in stoves fueled with firewood from trees in the same region. Controlled toasting at laboratory level was carried out in an aluminum saucepan and a heating grill (Thermo-Scientific SP131015Q; Waltham, MA, USA) at 134 °C for 25 min (Hernández-Mora *et al*., 2017). The external appearance of the nuts after thermal treatments is shown (Figure 1).

Figure 1. Cachichín (*Oecopetalum mexicanum* Greenm. & C.H. Thomps.) nuts subjected to different thermal treatments. A: raw nuts; B: boiled nuts; C: commercial toasted nuts; D: controlled toasted nuts.

Antioxidant activity

The antioxidant activity was determined using the 2,2-diphenyl-1-picrylhydrazyl (DPPH) technique, according to the methodology described by Kuskoski *et al*. (2005) (Figure 2).

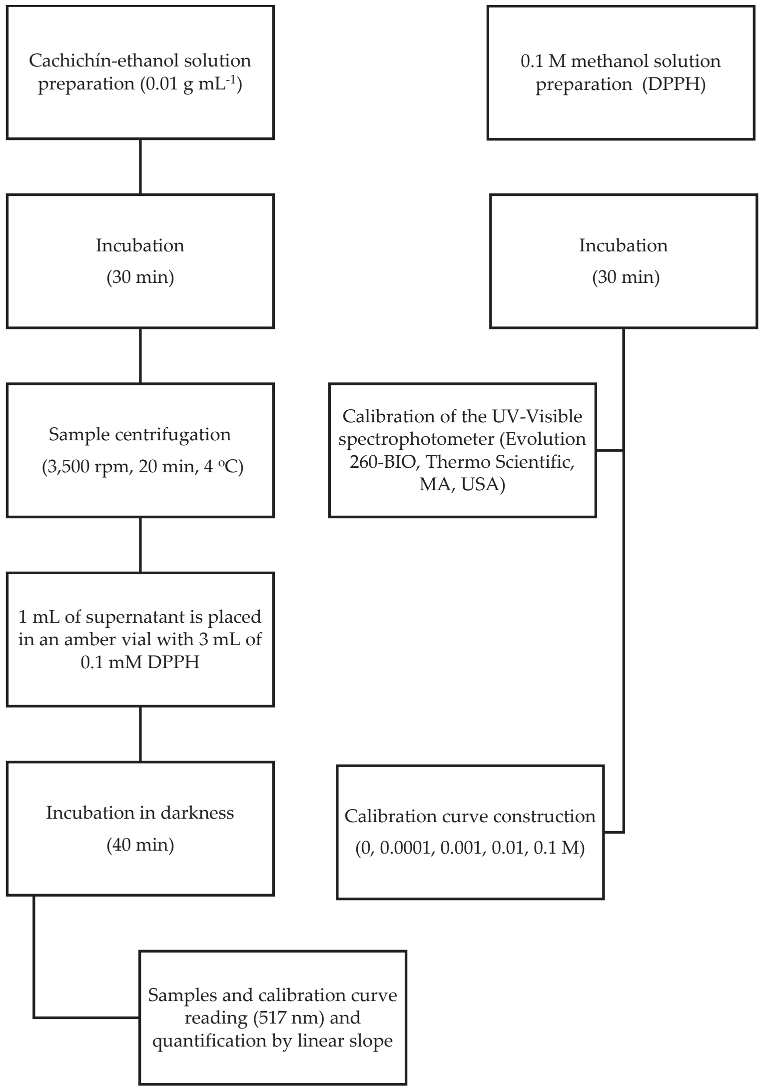

Figure 2. Methodology used to determine antioxidant activity in cachichín nuts (*Oecopetalum mexicanum* Greenm. & C.H. Thomps.) subjected to different thermal treatments.

Quantification of free phenols and total phenols

Sample conditioning

Free and total phenols were determined according to the methodology described by Leucuta *et al*. (2005), with some modifications. Ten previously ground and sifted nuts per treatment were used. A 0.1 g sample from each treatment was taken for total phenol and free phenol quantification. The samples were weighed using an analytical scale (OHAUS, AV213C; Parsippany, NY, USA) and placed in 1.5 mL microcentrifuge tubes. For free phenols, 200 μL of HPLC-grade water (J. T. Baker®) and 200 μL of methanol (J. T. Baker®) were added. For total phenols, 200 μL of HPLC-grade water and 200 μL of methanol were taken. The samples were incubated at 65 °C for 30 min in a water bath (Precision Fisher Scientific; Waltham, MA, USA) and then with 15 min of sonication in an ultrasonic bath (CS-UB32, Fisher Scientific). The reaction continued for another 20 min, and subsequently, 200 μL of methanol were added, and the solution was heated for an additional 10 min. The samples were centrifuged at 4000 rpm for 5 min in a centrifuge (Labnet Hermle, model Z 233 MK-2; Wehingen, Germany). The centrifugation process was repeated two more times, adding 1 mL of HPLC-grade water. The supernatant obtained was filtered through filter paper (Whatman™ Grade 1, 25 mm) in a 5 mL volumetric flask (Kimax, Kimble; Rockwood, TN, USA). Finally, the samples were filtered using 0.45 μm membrane syringe filters (0.45 μm Millex-HV, PVDF, 13 mm, Millipore; Carrigtwohill, Ireland) and stored at 4 °C until chromatographic analysis.

Chromatographic conditions for phenol quantification

The quantification of phenols was carried out in a high-performance liquid chromatography (HPLC) system (Gradient HPLC System, Agilent 1200 Series, Agilent Technologies; Waldbroon, Germany), with a DAD UV/VIS detector. For separation, a C18 150 x 4.6 mm 5 μm reversed phase column (Hypersil Gold model, ThermoFisher; Waltham, MA, USA) was used. A G1322A degasser and a G1311A quaternary gradient pump were used for gradient elution. The detection of the compounds was carried out at 330 nm. The chromatographic data were processed using Chemstation software (Agilent; Santa Clara, CA, USA).

The mobile phase was a binary gradient prepared from methanol (solvent A) and buffer (solvent B). The buffer solution was prepared by dissolving potassium dihydrogen phosphate (40 mM) in water. The pH of the solution was adjusted to 2.3 with 85 % orthophosphoric acid. The analysis was started with a linear gradient containing from 5 to 42 % solvent A for the first 35 min, followed by an isocratic elution with 42 % solvent A for the next 3 min. The flow rate was 1 mL min^{-1} and the injection volume was 10 μL. All the solvents were filtered through 0.5 μm filters (Sartorius) and degassed in an ultrasonic bath (Scientific, CS-UB32; Waltham, MA, USA).

Experimental design and statistical analysis

The treatments in the experiment were arranged in a completely random distribution. The data were processed using the statistical software RStudio version 1.2.5033. Once the assumptions of normality (Shapiro-Wilk test) and homogeneity (Levene test) of variances were proven, a one-way analysis of variance (ANOVA) was performed to determine significant differences with a confidence level of 95 % ($p \leq 0.05$) using Tukey's test.

RESULTS AND DISCUSSION

Phenolic compounds improve the antioxidant capacity of different edible grains and fruits. In the present study, we found that the different thermal treatments modified the antioxidant activity and the free and total phenolic compound profiles, including catechin, trans-ferulic acid, trans-coumaric acid, and chlorogenic acid.

Antioxidant activity

A significant increase in oxidant inhibition was observed in the commercial toasting (T3) and controlled toasting (T4) treatments, being 26.2 and 34.8 % higher, respectively, compared to raw nuts (T1). Conversely, the boiled treatment (T2) recorded a decrease of 37.1 %, compared to T1 (Table 1).

Table 1. Percentage of oxidant inhibition activity in raw cachichín (*Oecopetalum mexicanum* Greenm. & C.H. Thomps.) nuts under four applied thermal treatments.

	Treatment			
	Raw (T1)	Boiled (T2)	Commercial toasting (T3)	Controlled toasting (T4)
Inhibition percentage	15.38 ± 0.04 c	9.68 ± 0.04 d	19.41 ± 0.04 b	20.73 ± 0.10 a

Means ± SE with different letters in each column indicate significant statistical differences between treatments (Tukey, $p \leq 0.05$).

The increase in the percentage of inhibition found in treatments T3 and T4, compared to T1 (raw nuts), could be attributed to the possible solubilization of phenolic compounds exposed to temperatures of around 100–180 °C (Kim *et al*., 2011), as has been observed in the extraction of phenols from date (*Phoenix dactylifera*) nuts (Mrabet *et al*., 2022). In the case of controlled toasting at 134 °C, solubilization could also have occurred due to the prolonged exposure time to which the nut was subjected, increasing the internal temperature of the endosperm. The behavior of treatment T2 was inverse to T3 and T4, decreasing the percentage of inhibition by 37 % compared to T1. The reduction in the inhibition percentage during the boiling process could be the result of the leaching of phenolic compounds from the nut into the water, a phenomenon that has been found in previous studies with legumes and cowpea (*Vigna unguiculata* L.) nuts (Xu and Chang, 2008). This phenomenon occurs depending on the polarity of the phenolic compounds, a property inherent to phenols due to the hydroxyl functional groups present in their chemical structure (Yadav *et al*., 2018).

The highest percentage of inhibition observed in the cachichín nut with the T4 treatment was 55 % lower compared to the value found for black rice (*Oryza sativa*

L.) (Pedro *et al*., 2016), and 74 % lower than that reported in peanut (*Arachis hypogaea* L.) shells (Franco *et al*., 2018). It was also lower than those reported for chia (*Salvia hispanica* L.), grape (*Vitis vinifera* L.) nuts, and pistachio (*Pistacia vera* L.) (Munekata *et al*., 2020).

Concentration of free phenols

Regarding free phenols, the highest concentration of catechin (Table 2) was found in raw nuts (T1), while boiled (T2) and controlled toasting (T4) showed similar means. The lowest concentration of this phenolic compound was found in commercial toasted nuts (T3). The concentration of trans-ferulic acid was lower in raw nuts (T1) and in boiled nuts, whereas commercial (T3) and controlled (T4) toasted nuts showed higher means compared to raw nuts.

Table 2. Concentration of free phenolic compounds in cachichín (*Oecopetalum mexicanum* Greenm. & C.H. Thomps.) nuts subjected to four different treatments.

Treatment	Catechin	Trans-ferulic acid	Trans-coumaric acid
	mg g^{-1} FBW	ng g^{-1} FBW	
Raw (T1)	278.91 ± 69.03 a	3.77 ± 0.69 b	1.61 ± 0.15 b
Boiled (T2)	132.32 ± 3.71 b	5.49 ± 0.10 ab	1.30 ± 0.08 b
Commercial toast (T3)	69.57 ± 1.83 c	7.09 ± 0.57 a	1.48 ± 0.21 b
Controlled toast (T4)	124.98 ± 0.57 b	6.13 ± 0.49 a	2.67 ± 0.20 a

Means ± SE with different letters in each column indicate significant statistical differences between treatments (Tukey, $p \leq 0.05$). FBW: fresh biomass weight.

Boiled nuts showed means statistically similar to those observed in both raw nuts and toasted nuts (Table 2). Nuts with controlled toasting (T4) had the highest concentration of free trans-coumaric acid, compared to the rest of the treatments (T1, T2, and T3), which showed an average concentration of 1.46 ng g^{-1} FBW of trans-coumaric acid (Table 2).

Total concentration of phenols

Among the total phenols, catechin, chlorogenic acid, trans-ferulic acid, and trans-coumaric acid were identified in cachichín nuts (Table 3). Catechin showed its highest mean in raw nuts (T1), exceeding the concentrations recorded in the boiled (T2), commercial toasting (T3), and controlled toasting (T4) thermal treatments by 48.1, 37.8, and 44.2 %, respectively. The concentration of total chlorogenic acid (Table 3) was higher in nuts with commercial toasting (T3) by 43.5, 87.1, and 50.6 % compared to the concentrations recorded in raw nuts (T1), boiled nuts (T2), and nuts with controlled toasting (T4), respectively.

Table 3. Concentration of total phenolic compounds in cachichín (Oecopetalum mexicanum Greenm. & C.H. Thomps.) nuts subjected to four different thermal treatments.

Treatment	Catechin	Chlorogenic acid	Trans-ferulic acid	Trans-coumaric acid
	mg g^{-1} FBW		ng g^{-1} FBW	
Raw (T1)	613.95 ± 55.08 a	62.12 ± 6.15 b	2.81 ± 0.36 b	1.70 ± 0.16 ab
Boiled (T2)	318.40 ± 12.97 b	47.62 ± 0.92 b	5.04 ± 0.18 a	1.51 ± 0.04 b
Commercial toast (T3)	382.05 ± 25.90 b	89.12 ± 2.41 a	5.89 ± 0.23 a	1.96 ± 0.20 ab
Controlled toast (T4)	342.61 ± 43.62 b	59.16 ± 8.49 b	5.38 ± 0.42 a	2.35 ± 0.17 a

Means ± SE with different letters in each column indicate significant statistical differences between treatments (Tukey, $p \leq 0.05$). FBW: Fresh Biomass Weight.

Regarding total trans-ferulic acid, the highest means occurred in T2, T3, and T4, and were statistically higher than T1 by 93.5 % on average. On the other hand, the concentration of total trans-coumaric acid only showed differences between boiled nuts (T2) and nuts with controlled toasting (T4); T4 was 55.6 % greater than T2.

Phenolic compounds are secondary metabolites synthesized in plants that encompass molecules that contain hydroxybenzene, linked to aromatic or aliphatic structures (Rahman *et al*., 2021). Phenols are synthesized and genetically regulated in response to biotic and abiotic stress factors (Quideau *et al*., 2011). Phenolic compounds also contribute to the pigmentation of some plant tissues. For example, anthocyanins provide red, purple, or blue color in leaves, fruits, and flowers (Alappat and Alappat, 2020). Due to their high antioxidant capacity, phenolic compounds have gained great interest in nutrition and human health, and have shown effectiveness in the prevention of cancer, cardiovascular diseases, and neurological diseases such as Alzheimer's (Rahman *et al*., 2021).

The analysis of the total and free phenol profiles revealed that the thermal treatments applied to cachichín nuts decreased the concentration of free catechin. This reduction can be attributed to the instability of the epistructure of catechins at temperatures above 80 °C, because they tend to epimerize (Vuong *et al*., 2010). Despite the decrease in catechin concentration, cachichín nut still contained this compound after heat treatment, which shows antioxidant, anticancer, anti-inflammatory, antibacterial, antiviral, immune-regulating, and protective properties against neurodegenerative diseases (Yang *et al*., 2018).

Compared to raw nuts (T1), heat treatments increased free and total trans-ferulic acid concentrations, specifically in commercial (T3) and controlled (T4) toasts. However, the thermal treatments evaluated (boiling, commercial, and controlled toasting) did not affect the concentrations of total trans-coumaric acid, but they did affect those of free trans-coumaric acid, which increased in the controlled toasting treatment (T4) compared to raw nuts (T1). Chlorogenic acid, identified as total phenol, increased in T3 (commercially toasted) compared to T1 (raw nuts). Mung bean (*Vigna radiata* L.) nuts, dried in a microwave oven and in a conventional oven, had a higher concentration of phenolic compounds (Alkaltham *et al*., 2020).

Similar studies have found that heat treatments reduce the concentrations of phenolic compounds (Choi *et al*., 2012; Maghsoudlou *et al*., 2019). The increase in the concentration of these compounds in the present study can be explained by the rupture of the cellular matrix of the nut exposed to thermal treatments, which allows the release of soluble phenols from insoluble ester bonds (Chandrasekara and Shahidi, 2011; Zhang *et al*., 2022). In corn (*Zea mays* L.) kernels and corn bran, it was found that increasing the concentration of solubilized ferulic acid increases the total antioxidant activity (Dewanto *et al*., 2002). In soybean (*Glycine max* [L.] Merr.), the total antioxidant activity increased directly when increasing the concentration of chlorogenic acid. However, the solubilization of some phenolic acids occurs only at elevated temperatures (100–180 °C) (Kim *et al*., 2011; Choi *et al*., 2012). The latter is in accordance with the findings of the present study, in which we found significant increases in the concentrations of trans-ferulic acid, trans-coumaric acid, and chlorogenic acid in nuts exposed to the boiled (T2), commercial toasting (T3), and controlled toasting (T4) treatments.

The identification of phenolic compounds in cachichín nuts is of great relevance in nutraceutical terms. Trans-ferulic acid functions as an antioxidant and shows antidiabetic, anticancer, antimicrobial, antiviral, anti-inflammatory, neuro-protective, anti-apoptotic, anti-allergic, hepatoprotective, UV ray absorber (cosmetic use), lung protection, vasodilator, and antithrombotic compound action, in addition to helping increase sperm viability (Fong *et al*., 2016; Stompor-Gorący and Machaczka, 2021). In the food industry, this compound is a precursor to vanillin, useful as an aromatic compound and as an inhibitor of food discoloration (Rukkumani *et al*., 2004; Kumar and Pruthi, 2014).

Trans-coumaric acid shows antioxidant, antimicrobial, antiviral, anticancer, analgesic, antipyretic, hypopigmentant, antiulcer, antiarthritis, antiplatelet, and antiplatelet action, as well as being effective in the control of hyperglycemia (Pei *et al*., 2016). In the gastrointestinal tract, trans-coumaric acid has been observed to show better bioavailability than chlorogenic, caffeic, and trans-ferulic acids (Zhao and Moghadasian, 2010). Chlorogenic acid also presents antioxidant, antibacterial, hepatoprotective, cardioprotective, anti-inflammatory, antipyretic, neuroprotective, anticholesterolemic, antiviral, antimicrobial, antihypertensive, efficient free radical scavenger, and central nervous system stimulator activity (Santana-Gálvez *et al*., 2017). Furthermore, this phenolic compound can modulate lipid and glucose concentrations in patients with metabolic disorders (Naveed *et al*., 2018).

The exposure of cachichín nuts to high temperatures induced the Maillard reaction, during which a wide range of compounds known as Maillard reaction products (MRP) are produced. Given that in this work the effects of heat treatments on antioxidant activity and the concentration of phenolic compounds were determined, it is important to point out that the presence of phenols in foods can reduce or inhibit the production of MRP (Zhang *et al*., 2007a; Zhang *et al*., 2007b; Mildner-Szkudlarz *et al*., 2017). This effect can be attributed to the ability of phenolic compounds to eliminate free radicals. Furthermore, some polyphenols can inhibit acrylamide production through direct interaction with 3-oxo-propanamide, bypassing the reaction with a deamination of 3-aminopropionamide (3-APA) (Cheng *et al*., 2014; Xu *et al*., 2015).

During the Maillard reaction, heterocyclic amines (HAs) can also be produced, especially when foods have high protein concentrations. Within the HA, 2-amino-1-methyl-6-phenylimidazo[4,5-b]pyridine (PhIP), 2-amino-3,8-dimethylimidazo[4,5-f]quinoxaline (MeIQx), and 2-amino-3,4,8-trimethylimidazo[4,5-f]quinoxaline (4,8-DiMeIQx) are potentially carcinogenic compounds (Salazar *et al*., 2014; Sabally *et al*., 2016). Among the phenolic compounds, phloridzin shows inhibitory activity on the production of PhIP and chlorogenic acid in MeIQx. Such effects could be attributed to the capture of phenylacetaldehyde (the precursor of HA) through the formation of the polyphenol-phenylacetaldehyde linkage. These bonds formed by the capture of polyphenols by phenylacetaldehyde could have additional health benefits, such as anticancer capabilities (Cheng *et al*., 2007).

Regarding advanced glycation end products (AGEs) resulting from the Maillard reaction, these can cause inflammatory responses, oxidative stress, hyperglycemia, and hyperlipidemia, as well as endothelial dysfunction (Shen *et al*., 2020). The presence of phenolic compounds in foods could inhibit the synthesis and accumulation of AGEs through the elimination of free radicals formed during glycation or the capture of reactive carbonyl species (Yu *et al*., 2017). In the bark of the cinnamon (*Cinnamomum verum* J. Presl.) tree, proanthocyanidins were identified as causing the inhibition of specific AGEs (Peng *et al*., 2010). Thus, during the thermal processing of foods, phenolic compounds could have significant potential for reducing the formation of toxic MRPs and participating in the Maillard reaction to form beneficial compounds.

CONCLUSIONS

Cachichín nuts contain phenolic compounds and showed antioxidant activity, whose values may vary in response to the thermal treatments applied. Raw nuts (T1) showed the highest concentration of catechin, which decreased significantly in nuts subjected to heat treatments. Commercially toasted nuts (T3) showed the highest concentration of chlorogenic acid. Nuts subjected to heat treatments (T2, T3, and T4) presented higher concentrations of trans-ferulic acid compared to raw nuts (T1). Nuts subjected to controlled toasting (T4) showed the highest concentration of trans-coumaric acid. It is concluded that the thermal treatments tested affected the antioxidant capacity and the concentration of phenolic compounds measured, which demonstrates the importance of considering different processing methods for cachichín nut. In all cases, the results shown here reaffirm that cachichín nuts constitute an important source of antioxidant molecules with relevant functions in both nutrition and human health.

ACKNOWLEDGEMENTS

We thank the Consejo Nacional de Humanidades, Ciencias y Tecnologías (National Council of Humanities, Sciences, and Technologies; CONAHCYT) for the scholarship grant to A.E.H.-M., as well as the Plant Nutrition Laboratory of the Colegio de Postgraduados Campus Montecillo for having provided the necessary tools for the development of this study.

REFERENCES

Alappat B, Alappat J. 2020. Anthocyanin pigments: Beyond aesthetics. Molecules 25 (23): 5500. https://doi.org/10.3390/molecules25235500

Alkaltham M, Salamatullah A, Hayat K, Özcan M, Uslu N. 2020. The effects of germination and heating on bioactive properties, phenolic compounds and mineral contents of green gram nuts. LWT - Food Science and Technology 134: 110106. https://doi.org/10.1016/j.lwt.2020.110106

Chandrasekara N, Shahidi F. 2011. Antioxidative potential of cashew phenolics in food and biological model systems as affected by toasting. Food Chemistry 129 (4): 1388–1396. https://doi.org/10.1016/j.foodchem.2011.05.075

Chen X, Yu J, Cui H, Xia S, Zhang X, Yang B. 2018. Effect of temperature on flavor compounds and sensory characteristics of Maillard reaction products derived from mushroom hydrolysate. Molecules 23 (2): 247. https://doi.org/10.3390/molecules23020247

Cheng J, Chen X, Lu H, Chen Q, Zhang Y. 2014. Antioxidant-related and kinetic studies on the reduction effect of catechins and esterified catechins on acrylamide formation in a microwave heating model system. RSC Advances 4 (82): 43378–43386. https://doi.org/10.1039/c4ra04016c

Cheng KW, Wu Q, Zheng ZP, Peng X, Simon JE, Chen F, Wang M. 2007. Inhibitory effect of fruit extracts on the formation of heterocyclic amines. Journal of Agricultural and Food Chemistry 55 (25): 10359–10365. https://doi.org/10.1021/jf071820z

Choi JS, Kim HY, Seo WT, Lee JH, Cho KM. 2012. Toasting enhances antioxidant effect of bitter melon (*Momordica charantia* L.) increasing in flavan-3-ol and phenolic acid contents. Food Science and Biotechnology 21 (1): 19–26. https://doi.org/10.1007/s10068-012-0003-7

Dewanto V, Wu X, Liu RH. 2002. Processed sweet corn has higher antioxidant activity. Journal of Agricultural and Food Chemistry 50 (17): 4959–4964 https://doi.org/10.1021/jf0255937

Fong Y, Tang CC, Hu HT, Fang HY, Chen BH, Wu CY, Yuan SS, Wang HD, Chen YC, Teng YN, Chiu CC. 2016. Inhibitory effect of *trans*-ferulic acid on proliferation and migration of human lung cancer cells accompanied with increased endogenous reactive oxygen species and β-catenin instability. Chinese Medicine 11 (1): 45. https://doi.org/10.1186/s13020-016-0116-7

Franco D, Rodríguez-Amado I, Agregán R, Munekata PE, Vázquez JA, Barba FJ, Lorenzo JM. 2018. Optimization of antioxidants extraction from peanut skin to prevent oxidative processes during soybean oil storage. LWT-Food Science and Technology 88: 1–8. https://doi.org/10.1016/j.lwt.2017.09.027

Hernandez B, Luna G, Garcia O, Mendoza MR, Azuara E, Beristain CI, Jimenez, M. 2013. Extraction and characterization of *Oecopetalum mexicanum* nut oil. Industrial Crops and Products 43: 355–359. https://doi.org/10.1016/j.indcrop.2012.07.022

Hernández-Mora AE, Castillo-Morales M, García-Montalvo EA, Flores-Andrade E. 2017. Prueba de toxicidad aguda-oral del aceite de la semilla *Oecopetalum mexicanum* en ratones BALB/c. Journal CIM 5 (2): 1043–1050.

Hernández-Mora AE, Trejo-Téllez LI, Hernández-Cázares AS, Contreras-Oliva A, Gómez-Merino FC. 2021. Cachichín nut (*Oecopetalum mexicanum* Greenm. & CH Thomps.): Source of nutrients and bioactive compounds. Revista Chapingo Serie Agricultura Tropical 1 (2): 57–69. https://doi.org/10.5154/r.rchsat.2021.02.05

Hernández-Mora AE, Trejo-Téllez LI, Zavaleta-Mancera HA, Herrera-Corredor JA, Crosby-Galván MM, Gómez-Merino FC. 2024. Biochemical, anatomical, and histochemical characterization of cachichín (*Oecopetalum mexicanum* Greenm. & CH Thomps: Metteniusaceae) nuts exposed to different thermal treatments. PeerJ 12: e16663. https://doi.org/10.7717/peerj.16663

Kathuria D, Hamid, Gautam S, Thakur A. 2023. Maillard reaction in different food products: Effect on product quality, human health and mitigation strategies. Food Control 153: 109911. https://doi.org/10.1016/j.foodcont.2023.109911

Kim HG, Kim GW, Oh H, Yoo SY, Kim YO, Oh MS. 2011. Influence of toasting on the antioxidant activity of small black soybean (*Glycine max* L. Merrill). LWT-Food Science and Technology 44 (4): 992–998. https://doi.org/10.1016/j.lwt.2010.12.011

Kumar H, Choudhary N, Garg V, Swami NK, Kumar H, Seth R. 2013. Maillard browning: pros and cons in dairy and food industries. Journal of Dairy Science and Technology 2 (2): 9–18.

Kumar N, Pruthi V. 2014. Potential applications of ferulic acid from natural sources. Biotechnology Reports 4: 86–93. https://doi.org/10.1016/j.btre.2014.09.002

Kuskoski EM, Asuero AG, Troncoso AM, Mancini-Filho J, Fett R. 2005. Aplicación de diversos métodos químicos para determinar actividad antioxidante en pulpa de frutos. Ciência e Tecnologia de Alimentos 25 (4): 726–732. https://doi.org/10.1590/S0101-20612005000400016

Lascurain M, Avendaño S, López C, López JC, Covarrubias M. 2012. Ecological, productive and cultural values of cachichín (*Oecopetalum mexicanum*): An edible wild fruit from Veracruz, Mexico. BG Journal 9 (2): 13–16.

Lascurain M, López C, Zamora P. 2009. Production chain of *Oecopetalum mexicanum* ('cachichín'): a tropical fruit tree from Mexico. Acta Horticulturae 806: 519–524. https://doi.org/10.17660/actahortic.2009.806.65

Leucuta S, Vlase L, Gocan S, Radu L, Fodorea C. 2005. Determination of phenolic compounds from *Geranium sanguineum* by HPLC. Journal of Liquid Chromatography and Related Technologies 28 (19): 3109–3117. https://doi.org/10.1080/10826070500295211

Liu X, Xia B, Hu LT, Ni ZJ, Thakur K, Wei ZJ. 2020. Maillard conjugates and their potential in food and nutritional industries: A review. Food Frontiers 1 (4): 382–397. https://doi.org/10.1002/fft2.43

Maghsoudlou Y, Asghari-Ghajari M, Tavasoli S. 2019. Effects of heat treatment on the phenolic compounds and antioxidant capacity of quince fruit and its tisane's sensory properties. Journal of Food Science and Technology 56 (5): 2365–2372. https://doi.org/10.1007/s13197-019-03644-6

Mildner-Szkudlarz S, Siger A, Szwengiel A, Przygoński K, Wojtowicz E, Zawirska-Wojtasiak R. 2017. Phenolic compounds reduce formation of N(ε)-(carboxymethyl) lysine and pyrazines formed by Maillard reactions in a model bread system. Food Chemistry 231: 175–184. https://doi.org/10.1016/j.foodchem.2017.03.126

Mrabet A, Jiménez-Araujo A, Fernández-Prior Á, Bermúdez-Oria A, Fernández-Bolaños J, Sindic M, Rodríguez-Gutiérrez G. 2022. Date Nut: Rich source of antioxidant phenolics obtained by hydrothermal treatments. Antioxidants 11 (10): 1914. https://doi.org/10.3390/antiox11101914

Munekata PES, Gullón B, Pateiro M, Tomasevic I, Domínguez R, Lorenzo JM. 2020. Natural antioxidants from nuts and their application in meat products. Antioxidants 9 (9): 815. https://doi.org/10.3390/antiox9090815

Naveed M, Hejazi V, Abbas M, Kamboh AA, Khan GJ, Shumzaid M, Ahmad F, Babazadeh D, Fang FX, Modarresi-Ghazani F, Wen HL, Xiao HZ. 2018. Chlorogenic acid (CGA): A pharmacological review and call for further research. Biomedicine and Pharmacotherapy 97: 67–74. https://doi.org/10.1016/j.biopha.2017.10.064

Olivares-Vicente M, Barrajon-Catalan E, Herranz-Lopez M, Segura-Carretero A, Joven J, Encinar JA, Micol V. 2018. Plant-derived polyphenols in human health: Biological activity, metabolites and putative molecular targets. Current Drug Metabolism 19 (4): 351–369. https://doi.org/10.2174/1389200219666180220095236

Pedro AC, Granato D, Rosso ND. 2016. Extraction of anthocyanins and polyphenols from black rice *(Oryza sativa* L.) by modeling and assessing their reversibility and stability. Food Chemistry 191: 12–20. https://doi.org/10.1016/j.foodchem.2015.02.045

Pei K, Ou J, Huang J, Ou S. 2016. *p*-Coumaric acid and its conjugates: dietary sources, pharmacokinetic properties and biological activities. Journal of the Science of Food and Agriculture 96 (9): 2952–2962. https://doi.org/10.1002/jsfa.7578

Peng X, Ma J, Chao J, Sun Z, Chang RCC, Tse I, Li ETS, Chen F, Wang M. 2010. Beneficial effects of cinnamon proanthocyanidins on the formation of specific advanced glycation endproducts and methylglyoxal-induced impairment on glucose consumption. Journal of Agricultural and Food Chemistry 58 (11): 6692–6696. https://doi.org/10.1021/jf100538t

Quideau S, Deffieux D, Douat-Casassus C, Pouységu L. 2011. Plant polyphenols: chemical properties, biological activities, and synthesis. Angewandte Chemie International Edition 50 (3): 586–621. https://doi.org/10.1002/anie.201000044

Rahman MM, Rahaman MS, Islam MR, Rahman F, Mithi FM, Alqahtani T, Almikhlafi MA, Alghamdi SQ, Alruwaili AS, Hossain MS, Ahmed M, Das R, Emran TB, Uddin MS. 2021. Role of phenolic compounds in human disease: Current knowledge and future prospects. Molecules 27 (1): 233. https://doi.org/10.3390/molecules27010233

Rukkumani R, Aruna K, Suresh-Varma P, Padmanabhan-Menon V. 2004. Hepatoprotective role of ferulic acid: A dose-dependent study. Journal of Medicinal Food 7 (4): 456–461. https://doi.org/10.1089/jmf.2004.7.456

Sabally K, Sleno L, Jauffrit JA, Iskandar MM, Kubow S. 2016. Inhibitory effects of apple peel polyphenol extract on the formation of heterocyclic amines in pan fried beef patties. Meat Science 117: 57–62. https://doi.org/10.1016/j.meatsci.2016.02.040

Salazar R, Arámbula-Villa G, Hidalgo FJ, Zamora R. 2014. Structural characteristics that determine the inhibitory role of phenolic compounds on 2-amino-1-methyl-6-phenylimidazo[4,5-b]pyridine (PhIP) formation. Food Chemistry 151: 480–486. https://doi.org/10.1016/j.foodchem.2013.11.105

Santana-Gálvez J, Cisneros-Zevallos L, Jacobo-Velázquez DA. 2017. Chlorogenic acid: Recent advances on its dual role as a food additive and a nutraceutical against metabolic syndrome. Molecules 22 (3): 358. https://doi.org/10.3390/molecules22030358

Shen CY, Lu CH, Wu CH, Li KJ, Kuo YM, Hsieh SC, Yu CL. 2020. The development of Maillard reaction, and advanced glycation end product (AGE)-receptor for AGE (RAGE) signaling inhibitors as novel therapeutic strategies for patients with AGE-related diseases. Molecules 25 (23): 5591. https://doi.org/10.3390/molecules25235591

Stompor-Gorący M, Machaczka M. 2021- Recent advances in biological activity, new formulations and prodrugs of ferulic acid. International Journal of Molecular Science 22 (23): 12889. https://doi.org/10.3390/ijms222312889

Vuong QV, Golding JB, Nguyen M, Roach PD. 2010. Extraction and isolation of catechins from tea. Journal of Separation Science 33 (21): 3415–3428. https://doi.org/10.1002/jssc.201000438

Xu B, Chang SKC. 2008. Effect of soaking, boiling, and steaming on total phenolic content and antioxidant activities of cool season food legumes. Food Chemistry 110 (1): 1–13. https://doi.org/10.1016/j.foodchem.2008.01.045

Xu C, Yagiz Y, Marshall S, Li Z, Simonne A, Lu J, Marshall MR. 2015. Application of muscadine grape (*Vitis rotundifolia* Michx.) pomace extract to reduce carcinogenic acrylamide. Food Chemistry 182: 200–208. https://doi.org/10.1016/j.foodchem.2015.02.133

Yadav N, Kaur D, Malaviya R, Singh M, Fatima M, Singh L. 2018. Effect of thermal and non-thermal processing on antioxidant potential of cowpea nuts. International Journal of Food Properties 21 (1): 437–451. https://doi.org/10.1080/10942912.2018.1431659

Yang XJ, Dang B, Fan MT. 2018. Free and bound phenolic compound content and antioxidant activity of different cultivated blue highland barley varieties from the Qinghai-Tibet Plateau. Molecules 23 (4): 879. https://doi.org/10.3390/molecules23040879

Yu P, Xu XB, Yu SJ. 2017. Inhibitory effect of sugarcane molasses extract on the formation of N(ε)-(carboxymethyl)lysine and N(ε)-(carboxyethyl)lysine. Food Chemistry 221: 1145–1150. https://doi.org/10.1016/j.foodchem.2016.11.045

Zhang Y, Cai P, Cheng G, Zhang Y. 2022. A brief review of phenolic compounds identified from plants: Their extraction, analysis, and biological activity. Natural Product Communications 17 (1). https://doi.org/10.1177/1934578X211069721

Zhang Y, Chen J, Zhang X, Wu X, Zhang Y. 2007a. Addition of antioxidant of bamboo leaves (AOB) effectively reduces acrylamide formation in potato crisps and French fries. Journal of Agricultural and Food Chemistry 55 (2): 523–528. https://doi.org/10.1021/jf062568i

Zhang Y, Huang M, Wang Q, Cheng J. 2016. Structure-guided unravelling: phenolic hydroxyls contribute to reduction of acrylamide using multiplex quantitative structure-activity relationship modelling. Food Chemistry 199: 492–501. https://doi.org/10.1016/j.foodchem.2015.12.038

Zhang Y, Xu W, Wu X, Zhang X, Zhang Y. 2007b. Addition of antioxidant from bamboo leaves as an effective way to reduce the formation of acrylamide in fried chicken wings. Food Additives and Contaminants 24 (3): 242–251. https://doi.org/10.1080/02652030601064839

Zhao Z, Moghadasian MH. 2010. Bioavailability of hydroxycinnamates: a brief review of *in vivo* and *in vitro* studies. Phytochemistry Reviews 9 (1): 133–145. https://doi.org/10.1007/s11101-009-9145-5

Agrociencia

CHANGES IN PROLINE AND MINERAL CONCENTRATION IN CHILI (*Capsicum* spp.) GENOTYPES FROM CHIAPAS, MEXICO, IN RESPONSE TO NaCl

José de Jesús **Pérez-Gómez**[1], Nancy **Ruiz-Lau**[2*], Manuel **Martínez-Estévez**[3], Emanuel **Bojórquez-Quintal**[4], Blanca Olivia **Trejo-Paniagua**[1], Federico Antonio **Gutiérrez-Miceli**[1], Rosa Isela **Cruz-Rodríguez**[1], Esteban **Sánchez-Rodríguez**[5], María de Fátima **Medina-Lara**[3]

[1]Instituto Tecnológico de Tuxtla-Gutiérrez. Carretera Panamericana km 1080, Tuxtla Gutiérrez, Chiapas, Mexico. C. P. 29050.
[2]Instituto Tecnológico de Tuxtla-Gutiérrez. CONAHCYT-Tecnológico Nacional de México. Carretera Panamericana km 1080, Tuxtla Gutiérrez, Chiapas, Mexico. C. P. 29050.
[3]Centro de Investigación Científica de Yucatán. Unidad de Biología Integrativa. Calle 43 130, Chuburna de Hidalgo, Mérida, Yucatán, Mexico. C. P. 97200.
[4]El Colegio de Michoacán A.C. CONAHCYT-Laboratorio de Análisis y Diagnóstico del Patrimonio. Cerro de Nahuatzen 85, Jardines del Cerro Grande, La Piedad, Michoacán, Mexico. C. P. 59379.
[5]El Colegio de Michoacán A.C. Laboratorio de Análisis y Diagnóstico del Patrimonio. Cerro de Nahuatzen 85, Jardines del Cerro Grande, La Piedad, Michoacán, Mexico. C. P. 59379.
* Author for correspondence: nruizla@conacyt.mx; nancy.rl@tuxtla.tecnm.mx

Citation: Pérez-Gómez J de J, Ruiz-Lau N, Martínez-Estévez M, Bojórquez-Quintal E, Trejo-Paniagua BO, Gutiérrez-Miceli FA, Cruz-Rodríguez RI, Sánchez-Rodríguez E, Medina-Lara M de F. 2024. Changes in proline and mineral concentration in chili (*Capsicum* spp.) Genotypes from the state of Chiapas in response to NaCl. **Agrociencia** 58(3): 375-390. https://doi.org/ 10.47163/agrociencia.v58i3.2859

Editor in Chief:
Dr. Fernando C. Gómez Merino

Received: June 15, 2022.
Approved: January 22, 2024.
Published in Agrociencia: April 09, 2024.

ABSTRACT

Salt stress tolerance is an important quality in breeding cultivated plants to reduce crop loss. In this work, the tolerance to sodium chloride (NaCl) salinity of two *Capsicum* genotypes was evaluated: *C. annuum* (Blanco and Simojovel chili) and *C. frutescens* (Siete Caldos chili) from the state of Chiapas, Mexico. Seedlings were hydroponically maintained with Hoagland nutrient solution supplemented with 0, 60, and 120 mM NaCl for 8 days. Physiological response variables (SPAD units, dry and fresh weight of root and aerial part), percentage survival, proline concentration, and relative Na^+, K^+, and Cl^- concentration in the aerial part and roots were measured. The results showed that the Siete Caldos genotype was the most sensitive to NaCl stress, with a survival rate of 66.66 % at 120 mM. Stress affected chlorophyll by decreasing SPAD units and increasing proline concentrations at 60 mM and above. Furthermore, there was a high concentration of Na^+ in leaves and a low concentration in roots, indicating its translocation. On the other hand, the Simojovel genotype was the most tolerant, with 100 % survival and 86.66 % survival at 60 and 120 mM, low Na^+ accumulation in the aerial part, and a significant increase in proline concentration. Moderately salinity-tolerant genotypes could be an alternative for plant breeding. The results obtained here lay the basis for the selection of salt stress-tolerant chili genotypes in order to transfer this tolerance to other commercially important cultivars and to minimize the damage caused by excess salts in the soil through genetic improvement and the use of tolerant rootstocks.

Keywords: salinity, sodium, wild genotypes, tolerance.

INTRODUCTION

Plants, being sessile organisms, are exposed to constant environmental changes that are sometimes unfavorable to their growth and development. Adverse environmental conditions cause different types of stress in them, including biotic stress, caused by plant pathogens and herbivore attacks, and abiotic stress, caused by drought, heat, cold, nutrient deficiency and excess, metal toxicity, and excess salts or salinity in the soil (Yoshida *et al*., 2014). Drought, salinity, and temperature extremes are some of the major types of abiotic stresses that cause adverse effects on crop growth and productivity (Dutta *et al*., 2018). Salinity stress is one of the most limiting factors in agricultural production (Wang *et al*., 2022).

A saline soil has an electrical conductivity of more than 0.4 dS m^{-1} at 25 °C, an exchangeable sodium percentage of less than 15, and a pH of less than 8.5. The main cause of natural soil salinity is attributed to saltwater intrusion and salt deposition through wind; however, irrigation with high levels of salts in the water, inadequate irrigation, excessive fertilizer use, and poor soil drainage increase it (Chakdar *et al.*, 2019). The excess of soluble salts in the water reduces the leaching fraction in the soil, generating a saline over-accumulation of sodium sulfate (Na_2SO_4), sodium nitrate ($NaNO_3$), sodium chloride (NaCl), sodium bicarbonate ($NaHCO_3$), sodium carbonate (Na_2CO_3), potassium sulfate (K_2SO_4), calcium sulfate ($CaSO_4$), magnesium sulfate ($MgSO_4$), and magnesium chloride ($MgCl_2$). In general, these salts are necessary for plant development; however, their surplus is harmful when they accumulate in high concentrations in the cytosol (Mosa *et al*., 2017; Pandey *et al*., 2019).

Excess soluble salts in the soil, mainly NaCl, can cause osmotic, ionic, and oxidative stress in plants. These three factors reduce water and nutrient uptake and induce massive efflux of water and K^+ ions in plant cells, leading to water and nutrient imbalances. Sodium entry and accumulation in glycophytic species and the production of reactive oxygen species (ROS) reduce growth, yield, and production in economically important crops (Munns and Tester, 2008; Bojórquez-Quintal *et al*., 2012).

To counteract these negative effects of salt stress, plants possess different tolerance mechanisms, among which are the accumulation of compatible solutes such as proline, which participates in osmotic regulation; Na^+ homeostasis through the regulation of absorption; long-distance transport; compartmentalization in vacuoles and intracellular compartments; and flow or extrusion to the external environment. Another mechanism is the maintenance of K^+ homeostasis in plant cells through retention of this cation in the cytosol, remobilization, and uptake of K^+ (Deinlein *et al.*, 2014; Shabala and Pottosin, 2014).

In cultivated plants, wild relatives constitute an important reservoir of genes that can contribute to the solution of agricultural problems, such as resistance to pests and diseases and tolerance to abiotic factors. It has been reported that the development of *Capsicum chinense* grafts with wild *Capsicum annuum* Amashito and Muela chilis (*C. annuum* var. *glabriusculum*) as rootstocks shows better agronomic performance and crop productivity, as well as greater resistance to virosis (Navarrete-Mapen *et al*., 2020). In Mexico, there are wild or poorly domesticated populations of species that are closely related to cultivated plants of great economic and food importance, which have been little studied and are at risk of being lost. Hence the importance of working with backyard or semi-domesticated species of *Capsicum* from the state of Chiapas, Mexico, since these could have more efficient mechanisms of tolerance to salinity and be considered for the genetic improvement of plants of commercial interest.

In this work, *C. annuum* and *C. frutescens* were selected for study since they have limited information on salt stress tolerance and could possess characteristics that allow them to grow and develop in abiotic stress situations, in this case NaCl salinity. Therefore, the objective of our research was to characterize in a hydroponic system the response to salinity at the seedling level of *C. annuum* (Blanco and Simojovel chili) and *C. frutescens* (Siete Caldos chili) genotypes and to determine the most tolerant genotype to salt stress.

MATERIALS AND METHODS

Plant material and growing conditions

Chili seeds were obtained from the ripe fruits of Simojovel and Blanco chili peppers (*C. annuum*) and Siete Caldos (*C. frutescens*), which were collected in local markets in the city of Tuxtla Gutiérrez, Chiapas, Mexico. Seeds were hydrated for 72 h at 4 °C (Ruiz-Lau *et al*., 2016) and germinated in polystyrene seedbeds using peat (Peat Moss® peat) as substrate. The seedlings were irrigated at field capacity and kept in darkness at 25 °C. Emergence occurred approximately 10 days after sowing. Once the seedlings presented the first pair of true leaves, they were transplanted into polystyrene seedbeds using vermiculite as substrate. Irrigation was carried out with a 20 % Hoagland nutrient solution at pH 6.8 as the only source of nutrients. The photoperiod was 16 h light and 8 h dark, at a temperature of 28 ± 2 °C during 40 d. The Hoagland solution used (Hoagland and Arnon, 1950) contained 1.2 mM KNO_3, 0.8 mM $Ca(NO_3)_2$ $4H_2O$, 0.2 mM KH_2PO_4, 0.2 mM $MgSO_4$ $7H_2O$, 50 μM $CaCl_2$, 12.5 μM H_3BO_3, 1 μM $MnSO_4$ H_2O, 1 μM $ZnSO_4$ $7H_2O$, 0.5 μM $CuSO_4$, 0.1 μM $(NH_4)_6Mo_7O_{24}$ $2H_2O$, 0.1 $NiCl_2$ $6H_2O$, and 10 μM Fe-EDTA (Sigma Aldrich® A.C.S.) in distilled water.

Salt stress with NaCl

To determine the effects of NaCl on *Capsicum* spp., Siete Caldos (CSC) seedlings of the species *C. frutescens* and Blanco (CB) and Simojovel (CS) seedlings of the species *C. annuum* were utilized at 40 d after emergence (DAE). Each seedling represented an experimental unit. Seedlings were grown hydroponically in plastic containers (30 seedlings each) containing 500 mL of 20 % Hoagland nutrient solution for acclimatization for 10 d (Ruiz-Lau *et al*., 2016). Permanent oxygenation was applied by means of air pumps with a maximum capacity of 108 L h^{-1} (HiDOM® HD-8800). For each NaCl treatment, 30 seedlings were placed in a 500 mL capacity plastic container of nutrient supplemented with 0, 60, and 120 mM NaCl (Sigma Aldrich). To avoid osmotic shock, the NaCl concentration was gradually increased every 24 h by adding 30 mM until the desired concentration was reached, and from then on, the 8 days were counted for each treatment; the seedlings were maintained under saline conditions with a photoperiod of 16 h light and 8 h dark at an ambient temperature of 28 ± 2 °C. At the end of the stress treatment, the percentage survival and dry weight of the aerial part (leaf and stem) and roots were determined.

Electrical conductivity and measurement of SPAD units

To confirm that the seedlings were under salt stress, electrical conductivity (CE) was measured with a portable conductivity meter (CE/TDS/temperature HANNA DIST® 6; Italy) at each increase in NaCl concentration and at the end of the experiment. Chlorophyll estimation was determined by measuring leaf greenness with a SPAD-502 PLUS chlorophyllometer (Guzmán-Albores *et al*., 2020) and choosing three leaves at random from 10 seedlings per treatment for a total of 30 readings.

Relative concentration of Na^+, K^+, Cl^- by energy dispersive X-ray spectroscopy (EDS)

The relative elemental concentration was determined in the aerial part and roots previously dried in an oven at 60 °C for 5 days. These dried samples were ground, homogenized, and stored in polyethylene bags until further analysis by SEM-EDS. Determination of the relative concentration of Na^+, K^+, and Cl^- was performed with a scanning electron microscope (SEM) (JEOL model JSM6390LV, Japan; Software INCA Suite 4.08) equipped with an energy dispersive electron probe X-ray (EDS) system (LK-IE250 Oxford INCA Energy 250) for qualitative and quantitative elemental microanalysis. For the analysis, 10 and 2.5 mg of homogenized powder of the aerial part and roots, respectively, were weighed. Before SEM-EDS analysis, the sample was carefully placed on a metal support using double-sided carbon tape. The EDS scan time was set at 70 s in an area of 3.01 x 2.32 mm at 40X magnification and a scan energy of 20 kV (Procacci *et al*., 2021). The relative element concentration for each plant sample is shown as a percentage. Each sample (aerial part and roots) from each treatment was analyzed in triplicate.

Quantification of proline

Proline concentration was determined in leaves and roots following the method of Bates *et al*. (1973), with modifications reported by Bojórquez-Quintal *et al*. (2014). Acid ninhydrin was used for the extraction (Sigma Aldrich®, Germany; A. C. S.) and toluene (Meyer®, México; A. C. S.). Readings were taken with a spectrophotometer at 520 nm using toluene as a blank. Proline concentration was determined from an L-proline curve (Sigma Aldrich®, Germany; HPLC grade) and calculated based on fresh weight (usually expressed as μmol per gram of fresh weight, respectively). Calculations were performed with the following formula:

$$\mu\text{moles proline} * \text{g-1} = \left(\frac{\dfrac{(\mu\text{g proline} * \text{mL}^{-1})\ (\text{mL toluene})}{115.5\ \mu\text{g} + \mu\text{mol}^{-1}}}{\dfrac{\text{g sample}}{5}} \right)$$

Statistical analysis

A 3^2 factorial design was used, and the data were statistically analyzed with a two-way analysis of variance using chili genotypes (CSC, CB, and CS) and NaCl concentrations (0, 60, and 120 mM) as factors. Treatment means were compared with Tukey's multiple range test (STATGRAPHICS Centurion XVI, Inc., Madrid, Spain).

RESULTS AND DISCUSSION

Tolerance and physiological effects of NaCl salinity

To determine NaCl tolerance, *C. annuum* and *C. frutescens* seedlings of approximately 50 DAE were exposed to different concentrations of NaCl for 8 days. The CE in the solution increased at each concentration, reaching values of 10 and 12.13 dS m^{-1} at 60 and 120 mM NaCl, respectively, indicating that the plants were under stress. In general, the results showed that chili seedling survival and SPAD values for chlorophyll at different NaCl concentrations depended on genotype, according to which there were significant statistical differences. The lowest survival percentages were found in CSC (66.6 %) and CB (73.3 %) with the 120 mM NaCl dose. On the other hand, CS seedlings presented 100 and 86.6 % survival with 60 and 120 mM NaCl, being the least sensitive chili genotype under the evaluated salt stress conditions (Table 1).

Table 1. Effect of NaCl on survival percentage, chlorophyll content, and dry weight of *Capsicum* spp. genotypes.

Treatment	Survival (%)	Chlorophyll (SPAD)	Dry weight reduction (%)	
			Aerial part	Root
CSC0	100.00 ± 0.00 a	31.36 ± 1.68 b	0 ab	0 cd
CB0	100.00 ± 0.00 a	32.26 ± 2.41 ab	0 ab	0 cd
CS0	100.00 ± 0.00 a	36.5 ± 2.79 a	0 ab	0 cd
CSC60	80.00 ± 5.77 c	24.64 ± 0.62 cd	-12.38 ± 11.21 c	21.05 ± 9.51 a
CB60	86.66 ± 1.28 b	22.13 ± 0.56 d	22.97 ± 6.81 a	30.35 ± 6.72 a
CS60	100.00 ± 0.00 a	31.23 ± 1.25 b	1.46 ± 6.02 bc	-8.97 ± 5.91 d
CSC120	66.66 ± 1.28 e	26.50 ± 0.57 cd	17.90 ± 3.87 ab	1.70 ± 7.53 bcd
CB120	73.33 ± 1.28 d	22.63 ± 0.41 d	28.47 ± 1.91 a	19.60 ± 8.36 ab
CS120	86.66 ± 1.92 b	28.86 ± 0.92 bc	19.98 ± 13.77 ab	12.25 ± 8.04 abc
LSD	6.41	4.44	20.21	18.84

Means ± standard error with different letters in each column indicate significant statistical difference between treatments (Tukey, $p < 0.05$). LSD: least significant difference. Genotypes: CSC (Siete Caldos chili), CB (Blanco chili), CS (Simojovel chili); NaCl concentration at 0, 60, and 120 mM.

It was observed that seedlings exposed to salt stress showed symptoms of toxicity such as chlorosis, defoliation of old leaves, and loss of turgor, which were reflected in the SPAD readings (Table 1). SPAD values decreased with increasing NaCl concentration in all genotypes; however, statistical analysis showed no difference between 60 and 120 mM NaCl in each genotype, but at 120 mM NaCl, there is a difference between the two *C. annuum* genotypes (CB = 22.63 and CS = 28.86) (Table 1). These results show that there is a decrease in survival percentage and SPAD values as NaCl concentrations increased.

The chlorophyll content in the leaf is an indicator of the photosynthetic capacity of the plant. Chloroplasts are the first organelles to be damaged by ionic stress, and this manifests as chlorosis. Also, Na^+ mainly affects osmoregulation and is involved in turgor loss in plants (Isayenkov, 2012). During the experiment, leaf chlorosis was observed at 60 mM NaCl and a loss of turgor accompanied by defoliation at 120 mM NaCl. Because of this, plants suffered damage and even death, with the lowest survival rates for CSC and CB, as mentioned above (Table 1).

Salinity, drought, and temperature extremes are the main abiotic factors responsible for causing stress and severe damage to many crops worldwide. Stress can cause morphological, physiological, metabolic, and molecular changes that are detrimental to plant growth and survival. Abiotic stress, mainly salinity, leads to inhibition of plant growth (Dutta *et al.*, 2018). It has been reported that when NaCl concentration is above 40 mM, osmotic pressure above 0.2 MPa is generated. This increase in soil osmotic pressure negatively affects plant development, mainly the root, and can lead to a yield drop of 30 % (Chakdar *et al*., 2019). Of all the energy acquired by photosynthesis and fixed in carbon compounds, only a small portion (10–40 %) is used directly for biomass accumulation, even under optimal conditions (Munns and Gilliham, 2015).

On the other hand, the reduction of aerial part dry weight at different NaCl concentrations depends on the genotype, according to which there are significant statistical differences. Taking as 100 % the treatment without NaCl for each chili genotype, it could be observed that there is a decrease in the dry weight (DW) of the aerial part and in the root in the presence of NaCl in the genotypes evaluated. However, this reduction was not significant among all treatments. At 60 mM NaCl, the aerial part of CSC is not affected; however, root DW is significantly decreased by 21.05 % (Table 1).

One of the major consequences of NaCl stress is the loss of intracellular water, so many plant species accumulate compatible solutes in response to drought and salinity (Escalante-Magaña *et al*., 2020). The accumulation of proline is considered a mechanism of tolerance to salt stress and can even prevent the K + efflux from the roots (Bojórquez-Quintal *et al*., 2016). Hence the importance of determining the proline concentration in chili seedlings under salinity conditions and whether there are differences between genotypes and concentrations. In the aerial part, CB and CS showed a significant increase in proline concentration only with the 120 mM NaCl dose (Table 2). In the CSC genotype, only with the 60 mM NaCl dose was the proline concentration (20.24 mg proline g^{-1} dry weight) statistically higher (Table 2).

Table 2. Proline concentration in *Capsicum* spp. genotypes under NaCl stress conditions.

Treatment	Proline in aerial part (mg g^{-1} dry weight)	Proline in roots (mg g^{-1} dry weight)
CSC0	1.88 ± 0.35 c	0.73 ± 0.16 e
CB0	1.83 ± 0.43 c	0.57 ± 0.09 e
CS0	2.56 ± 0.34 c	0.52 ± 0.09 e
CSC60	20.24 ± 5.63 b	1.50 ± 0.37 de
CB60	8.00 ± 0.42 c	3.50 ± 0.90 cd
CS60	5.30 ± 0.52 c	1.90 ± 0.13 de
CSC120	2.38 ± 1.08 c	12.26 ± 2.29 a
CB120	28.02 ± 1.86 a	8.54 ± 0.41 b
CS120	28.76 ± 0.65 a	5.13 ± 0.99 c
LSD	6.21	2.40

Means ± standard error with different letters in each column indicate significant statistical difference between treatments. (Tukey, $p < 0.05$). LSD: least significant difference. Genotypes: CSC (Siete Caldos chili), CB (Blanco chili), CS (Simojovel chili); NaCl concentration at 0, 60, and 120 mM.

Salt stress limits plant development due to several adverse effects on biochemical and physiological processes such as photosynthesis, antioxidant metabolism, mineral homeostasis, and osmolyte accumulation, among others (Khan *et al*., 2012). The primary effects of salt stress are caused by the osmotic effect (increased solutes) and the presence of ions in the rhizosphere, limiting water uptake by the root system and causing an ionic imbalance, which reduces plant growth, while secondary effects are caused by enzyme inactivation, nutrient deficiency, ionic toxicity in tissues, and oxidative stress (ROS) (Nazar *et al*., 2011; Khan *et al*., 2012).

To reverse these adverse effects caused by salinity, plants have developed different tolerance strategies. One of them is the accumulation of compatible compounds, also called osmolytes (Nazar *et al*., 2011; Khan *et al*., 2012; Bojórquez-Quintal *et al*., 2014). These compounds are low molecular weight, water soluble, and non-toxic at millimolar concentrations, including proline, glycine betaine, trehalose, and others (Hayat *et al*., 2012). Osmolytes accumulate mainly in the cytoplasm without causing inhibition of enzyme activity and prevent dehydration of the cytosol by reducing water potential due to the accumulation of ions in vacuoles (Dutta *et al*., 2018). Furthermore, they are related to salinity tolerance due to their ability to counteract water and osmotic stress and maintain ion homeostasis as well as ion compartmentalization (Nazar *et al*., 2011; Khan *et al*., 2012).

Proline is one of the most studied osmolytes and accumulates in response to salt stress. This amino acid maintains osmotic balance by facilitating water uptake or reducing water loss, protecting cellular structures, and reducing oxidative damage (Alhasnawi, 2019; Escalante-Magaña *et al*., 2020; Palchetti *et al*., 2021). This explains the increased proline in plant tissue of chili genotypes exposed to NaCl. The concentration of proline present in the aerial part without salt treatment is low in all genotypes (Table 2) and is due to the naturally occurring proline synthesis of the plants.

The proline values obtained in the root were lower than those recorded in the aerial part; also, increasing values are observed in all genotypes with increasing NaCl levels (Table 2). The CSC genotype had the highest proline concentration in roots with 120 mM NaCl, indicating that when exposed to severe stress that diverts the main mechanisms such as biomass production and chlorophyll synthesis, this genotype allocates nutrients to increase proline synthesis and accumulation. This forces the plant to use the glutamate present in the cell as a precursor for proline production (Escalante-Magaña *et al*., 2020).

The survival of the CSC genotype is affected at 60 mM NaCl and above (80 % survival) (Table 1) because the main metabolic pathways that help it maintain normal growth and development are affected. This is mainly due to the high concentration of Na^+ in the plant tissue. Under these conditions, CSC activates mechanisms such as osmoregulation and protection of some enzymes so as not to suffer greater damage. This suggests that each genotype has different tolerance mechanisms according to the concentrations tested. Salinity tolerance is a trait controlled by many genes and involves several physiological, biochemical, and molecular mechanisms. Therefore, a combination of several of them is necessary to achieve a considerable increase in this (Adem *et al*., 2014).

Pareto analysis showed a main effect between NaCl concentration and genotype and an interaction between these two variables. NaCl concentration has a negative effect, and genotype has a positive effect on survival percentage and SPAD chlorophyll units. As for proline concentration, NaCl has a positive effect on proline concentration; however, genotype has a negative effect on root proline concentration (Figure 1).

Analysis of relative Na^+, K^+ and Cl^- concentrations

Salinity affects mineral nutrient uptake due to over-accumulation of Na^+ and Cl^-, which can lead to nutritional imbalance (Chakdar *et al*., 2019), affecting plant growth and development. To determine whether the effect of NaCl on dry weight and SPAD readings was related to the accumulation of Na^+ and Cl^- in the aerial part and roots, a relative concentration analysis of these elements was carried out by SEM-EDS. This semi-quantitative elemental analysis made it possible to determine the organ with the highest accumulation of Na^+, K^+, and Cl^-. The results show that the relative concentration of Na^+ and Cl^- in the aerial part and root increases significantly with increasing NaCl concentration (Table 3). However, in the CSC genotype, the Na^+ and Cl^- concentrations are lower in the aerial part than in the roots at 120 mM NaCl (Table 3) compared to CB and CS. This suggests that CSC seedlings exposed to high NaCl concentrations accumulate more Na^+ (3.15 %) and Cl^- (4.3 %) in the roots, preventing their translocation to the aerial part, which represents a tolerance mechanism.

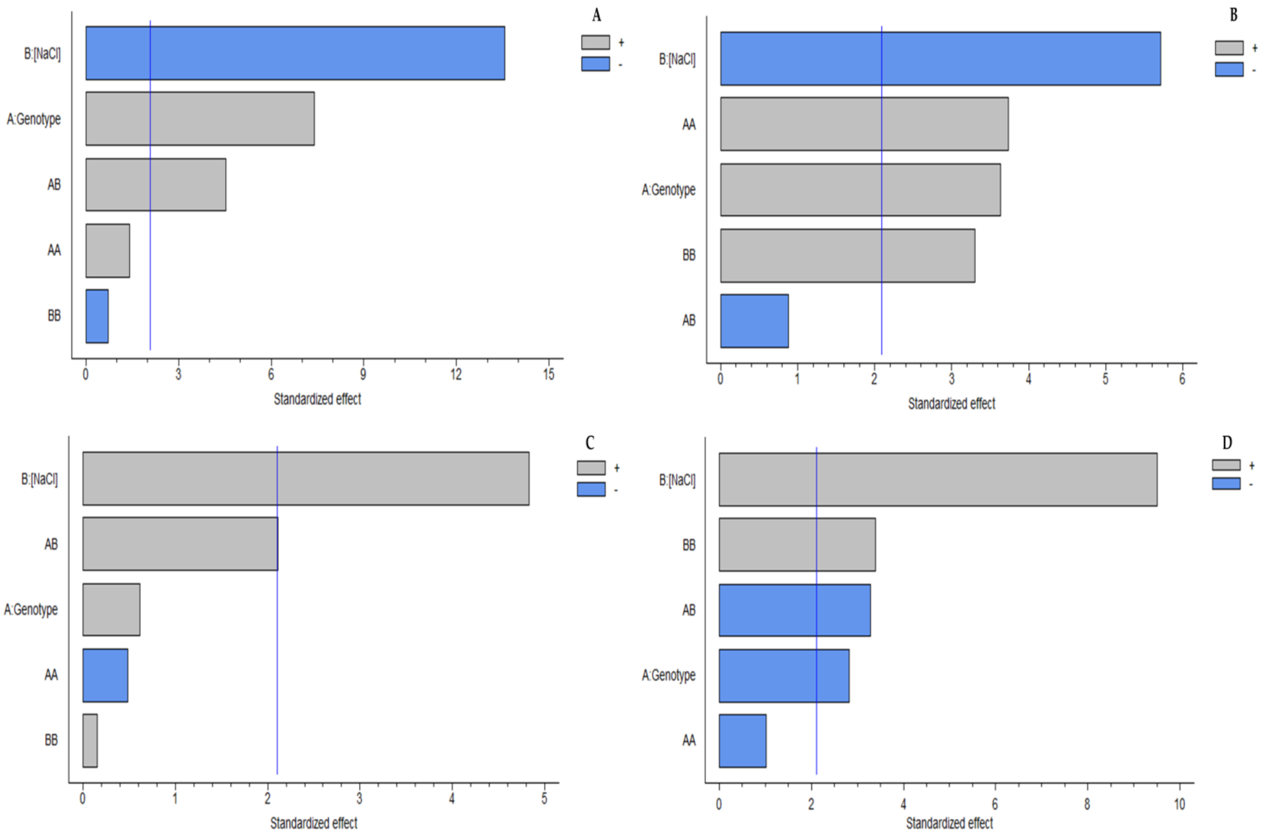

Figure 1. Analysis of the effect of NaCl concentration and genotype. A: survival percentage; B: SPAD units; C: leaf proline concentration; D: root proline concentration.

As for K^+, this is significantly reduced in the genotypes due to the presence of salt in both tissues, with the root being the organ that accumulates the least. Among the genotypes, CSC retains more K^+ in the aerial part at high salinity (120 mM NaCl) and in the root at 60 mM NaCl (Table 3). This ability to retain K^+ in root and leaf cells has been suggested as a mechanism of salt tolerance in chili plants (Bojórquez-Quintal *et al*., 2016). Potassium is a macronutrient for plants, constituting up to 10 % of their dry weight. Regulation of K^+ homeostasis is essential for plant adaptation to harsh environments (Anschütz *et al*., 2014; Shabala and Pottosin, 2014; Bojórquez-Quintal *et al*., 2016).

Statistical analysis showed that NaCl concentration has a positive effect on the relative Na^+ and Cl^- concentrations and a negative effect on K^+ in the aerial part and root (Figures 2 and 3). In the case of the genotype, this was not significant in the aerial part (Figure 2). Genotype had a positive effect on the relative Na^+ and Cl^- concentrations (Figure

Table 3. Relative concentration of sodium, chlorine, and potassium in *Capsicum* spp. genotypes under NaCl salinity conditions.

Treatment	Relative [Na^+] (%)	Relative [K^+] (%)	Relative [Cl^-] (%)
		Aerial part	
CSC0	0.18 ± 0.04 g	6.16 ± 0.22 a	0.76 ± 0.06 f
CB0	0.23 ± 0.03 g	5.83 ± 0.10 ab	0.85 ± 0.06 f
CS0	0.29 ± 0.04 g	5.81 ± 0.12 b	0.64 ± 0.07 f
CSC60	3.63 ± 0.12 c	3.15 ± 0.05 e	5.61 ± 0.08 b
CB60	3.17 ± 0.02 d	3.60 ± 0.08 d	4.74 ± 0.06 c
CS60	2.85 ± 0.06 e	3.65 ± 0.04 d	4.17 ± 0.05 d
CSC120	2.25 ± 0.09 f	4.12 ± 0.11 c	2.63 ± 0.07 e
CB120	3.89 ± 0.10 b	3.11 ± 0.03 e	5.69 ± 0.01 b
CS120	4.11 ± 0.03 a	2.90 ± 0.12 e	6.39 ± 0.13 a
LSD	0.20	0.33	0.21
		Root	
CSC0	0.21 ± 0.02 e	5.23 ± 0.11 a	0.65 ± 0.03 f
CB0	0.38 ± 0.03 e	4.29 ± 0.12 b	0.60 ± 0.03 f
CS0	0.35 ± 0.02 e	4.20 ± 0.09 b	0.60 ± 0.03 f
CSC60	1.35 ± 0.04 d	3.66 ± 0.07 c	2.75 ± 0.04 e
CB60	2.29 ± 0.01 c	2.90 ± 0.02 d	3.91 ± 0.04 c
CS60	2.54 ± 0.08 b	2.63 ± 0.01 e	3.69 ± 0.09 d
CSC120	3.15 ± 0.13 a	2.85 ± 0.01 d	4.37 ± 0.08 b
CB120	3.17 ± 0.02 a	2.76 ± 0.03 de	5.35 ± 0.05 a
CS120	3.02 ± 0.03 a	2.35 ± 0.04 f	4.05 ± 0.05 c
LSD	0.17	0.20	0.16

Means ± standard error with different letters in each column indicate significant statistical difference between treatments (Tukey, $p < 0.05$, n = 3). LSD: least significant difference. Genotypes: CSC (Siete Caldos chili), CB (Blanco chili), CS (Simojovel chili); NaCl concentration at 0, 60, and 120 mM.

3). Regulation of homeostasis is essential for plant adaptation to abiotic stresses, and genetic variability in plants allows them to respond to stress in different ways within the same species.

When analyzing the K^+/Na^+ ratio, it decreased drastically, both in the aerial part and in the roots, as NaCl levels increased. This ratio was higher in the roots of the CSC genotype (*C. frutescens*) at all NaCl concentrations compared to *C. annuum*. A smaller decrease in the K^+/Na^+ ratio could be observed with 60 mM NaCl in CS (aerial part) and in CSC at 120 mM NaCl (aerial part and roots) (Figure 4). The K^+/Na^+ ratio is considered an indicator of tolerance to salt stress; low values of this ion ratio are indicators of sensitivity (Bojórquez-Quintal *et al*., 2014; 2016).

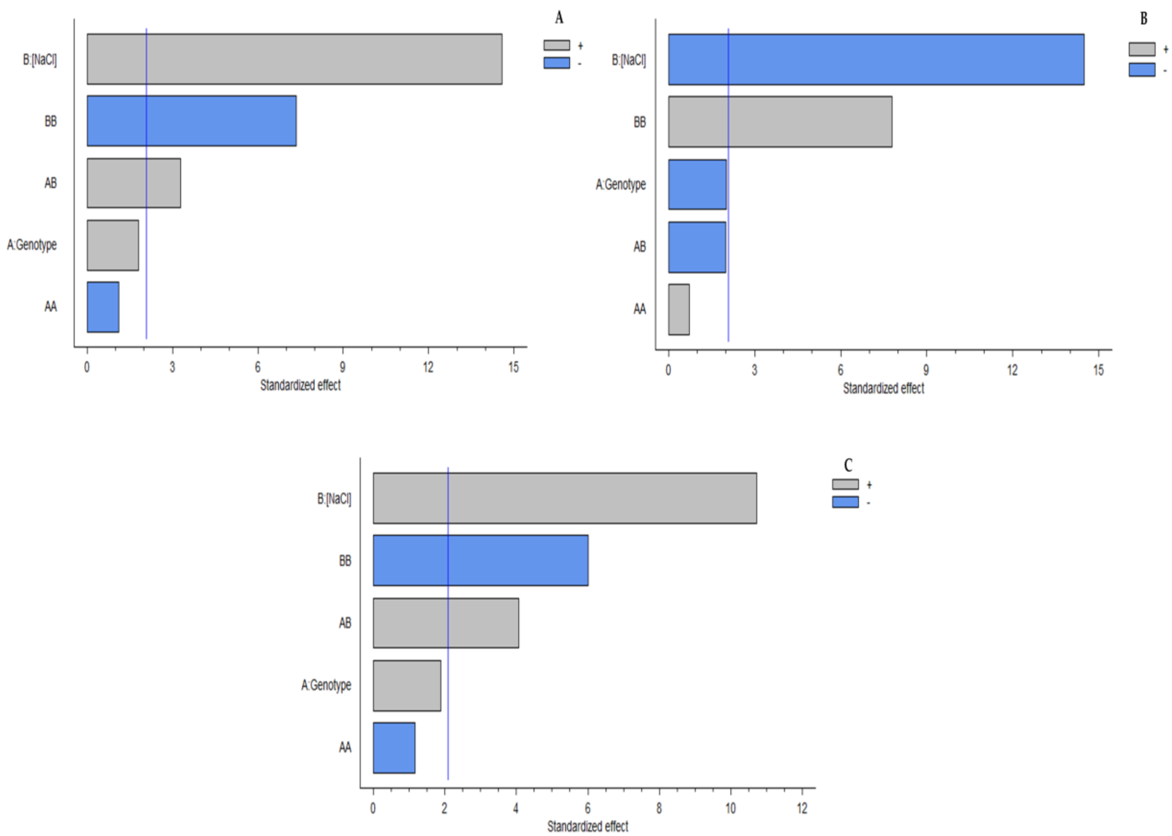

Figure 2. Analysis of the effect of NaCl concentration and genotype on the relative element concentration in leaves. A: Na^+ concentration; B: K^+ concentration; C: Cl^- concentration.

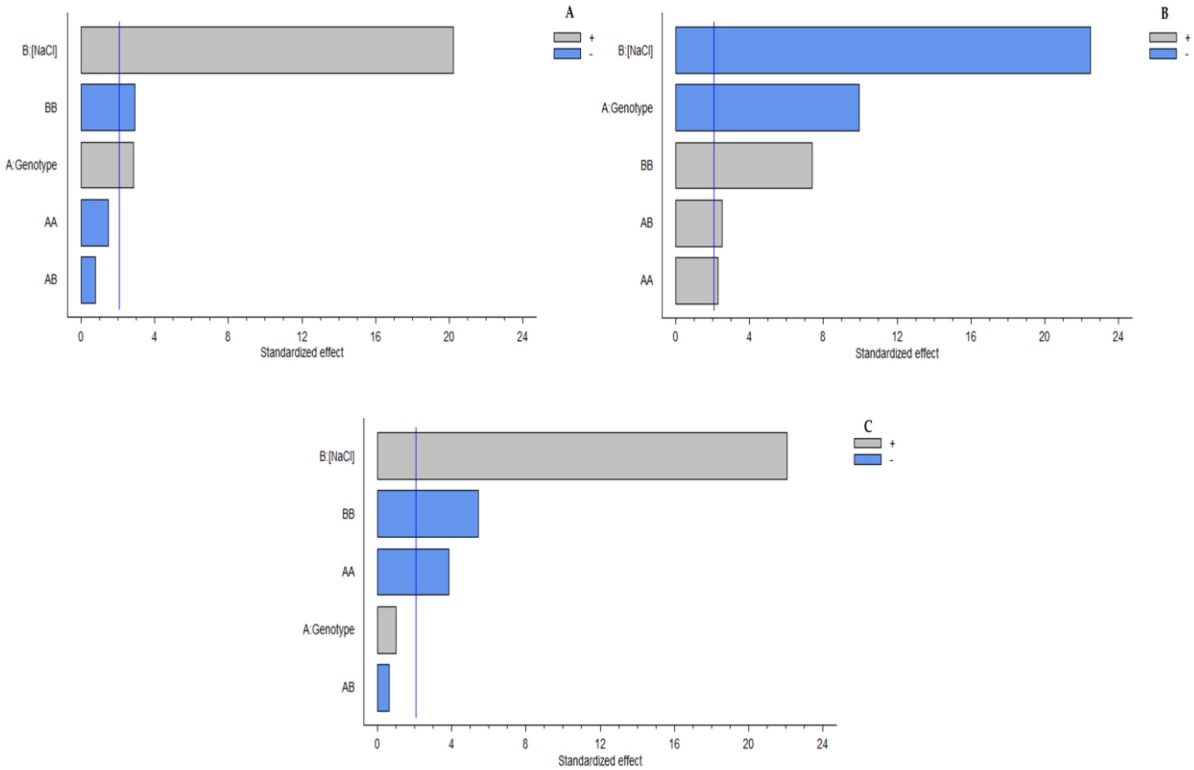

Figure 3. Analysis of the effect of NaCl concentration and genotype on the relative element concentration in the root. A: Na^+ concentration; B: K^+ concentration; C: Cl^- concentration.

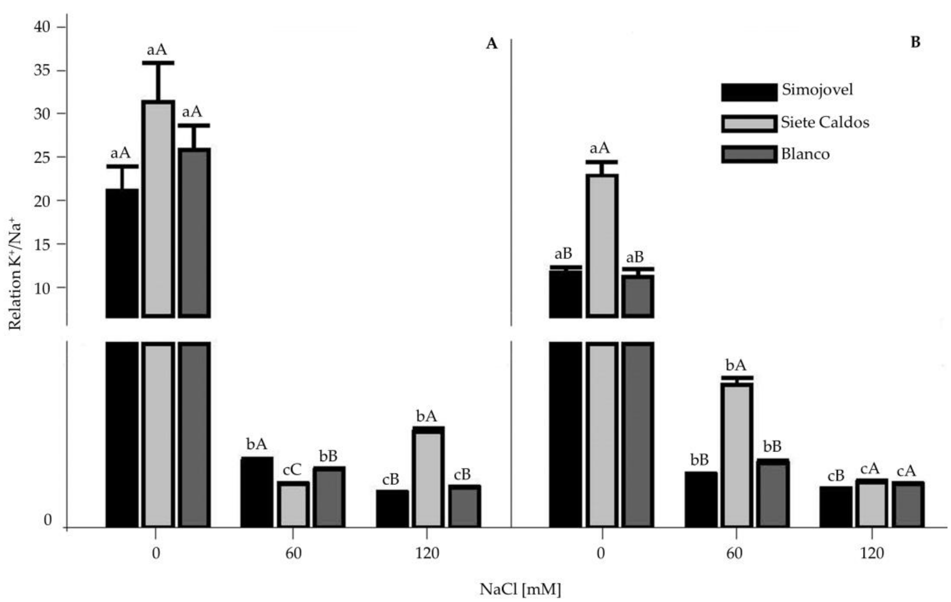

Figure 4. Potassium/sodium ratio in *Capsicum* spp. genotypes exposed to NaCl salinity. A: aerial part; B: roots. Capital letters indicate comparison between genotypes, and small letters between concentrations per genotype; different letters indicate significant statistical difference (Tukey, $p < 0.05$, n = 5).

The accumulation of salts in roots induces ionic stress by altering cellular ion homeostasis, as it causes an inhibition of ion uptake of essential elements such as K^+, Ca^{2+}, and NO_3^- and an accumulation of Na^+ and Cl^- (Machado and Serralheiro, 2017). Franco-Navarro *et al*. (2016) suggest that when Cl^- is supplied to glycophytic plants such as tobacco (*Nicotiana tabacum* L. var. Habana) at concentrations of 1 to 5 mol m^{-3}, it plays a role in regulating the osmotic and turgor potential of leaves, allowing plants to improve leaf water balance parameters. These concentrations are higher than necessary to meet requirements as a micronutrient but insufficient to cause toxicity.

CONCLUSIONS

With the results obtained, it is possible to suggest that Siete Caldos is a genotype sensitive to salinity starting at 60 mM NaCl, so that by 120 mM NaCl it has already entered a stage of deterioration, presenting a 66.66 % survival rate. Furthermore, it shows a decrease in chlorophyll, an increase in proline, and a high Na^+ concentration in leaves but low in roots, indicating a translocation of the ion. In response to stress, the Siete Caldos genotype retains more K^+ in its aerial part, with the retention or prevention of this ion leakage being an important point in the survival and tolerance of the plants.

On the other hand, the Simojovel genotype proved to be the most tolerant, with a 100 % survival rate at 60 mM NaCl. This may be caused by two situations: the Na^+ concentration in the aerial part and the root is lower, and proline accumulation increases considerably at 120 mM NaCl in the aerial part, suggesting that from this concentration onwards, this tolerance mechanism is activated. These results provide the basis for the selection of chili genotypes that are tolerant or moderately tolerant to salt stress, with the aim of transmitting this tolerance to other commercially important cultivars by means of different breeding techniques.

ACKNOWLEDGMENTS

To the *Consejo Nacional de Humanidades, Ciencia y Tecnología* (National Council of Humanities Science and Technology) for the master's scholarship of J.J.P.-G. and B.O.T.-P. To the *Unidad de Biología Integrativa del Centro de Investigación Científica de Yucatán* for its infrastructure and technical assistance during the stay of J.J.P.-G. for the proline determination and to the *Laboratorio de Análisis y Diagnóstico del Patrimonio, El Colegio de Michoacán, A. C. sede la Piedad* for its infrastructure for the mineral determination.

REFERENCES

Adem GD, Roy SJ, Zhou M, Shabala S. 2014. Evaluating contribution of ionic, osmotic and oxidative stress components towards salinity tolerance in barley. BMC Plant Biology 14 (1): 113. https://doi.org/10.1186/1471-2229-14-113

Alhasnawi AN. 2019. Role of proline in plant stress tolerance: A mini review. Research on Crops 20 (1): 223–229. https://doi.org/10.31830/2348-7542.2019.032

Machado RA, Serralheiro RP. 2017. Soil salinity: Effect on vegetable crop growth. management practices to prevent and mitigate soil salinization. Horticulturae 3 (2): 30. https://doi.org/10.3390/horticulturae3020030

Anschütz U, Becker D, Shabala S. 2014. Going beyond nutrition: Regulation of potassium homoeostasis as a common denominator of plant adaptive responses to environment. Journal of Plant Physiology 171 (8): 670–687. https://doi.org/10.1016/j.jplph.2014.01.009

Bates LS, Waldren RP, Teare ID. 1973. Rapid determination of free proline for water-stress studies. Plant and Soil 39 (1): 205–207. https://doi.org/10.1007/BF00018060

Bojórquez-Quintal JE, Echevarría-Machado I, Medina-Lara F, Martínez-Estévez M. 2012. Plants challenges in a salinized world: The case of *Capsicum*. African Journal of Biotechnology 11 (72): 13614–13626. https://doi.org/10.5897/ajb12.2145

Bojórquez-Quintal E, Ruiz-Lau N, Velarde-Buendía A, Echevarría-Machado I, Pottosin I, Martínez-Estévez M. 2016. Natural variation in primary root growth and K^+ retention in roots of habanero pepper (*Capsicum chinense*) under salt stress. Functional Plant Biology 43 (12): 1114–1125. https://doi.org/10.1071/FP15391

Bojórquez-Quintal E, Velarde-Buendía A, Ku-González A, Carrillo-Pech M, Ortega-Camacho D, Echevarría-Machado I, Pottosin I, Martínez-Estévez M. 2014. Mechanisms of salt tolerance in habanero pepper plants (*Capsicum chinense* Jacq.): proline accumulation, ions dynamics and sodium root-shoot partition and compartmentation. Frontiers in Plant Science 5: 605. https://doi.org/10.3389/fpls.2014.00605

Chakdar H, Borse DN Verma S, Choudhary P, Das S. 2019. Microbial management of crop salinity stress: Mechanisms, applications and prospects. *In* Akhtar MS. (ed.), Salt stress, microbes, and plant interactions: Mechanisms and molecular approaches. Springer: Singapore, pp: 1–25. https://doi.org/10.1007/978-981-13-8805-7

Deinlein U, Stephan AB, Horie T, Luo, Xu G, Schoeder I. 2014. Plant salt-tolerance mechanisms. Trends in Plant Science 19 (6): 371–379. https://doi.org/10.1016/j.tplants.2014.02.001

Dutta T, Neelapu NRR, Wani SH, Challa S. 2018. Compatible solute engineering of crop plants for improved tolerance toward abiotic stresses. *In* Wani SH. (ed.), Biochemical, physiological and molecular avenues for combating abiotic stress tolerance in plants. Academic Press: London, UK, pp: 221–254. https://doi.org/10.1016/B978-0-12-813066-7.00012-7

Escalante-Magaña CA, Echevarría-Machado I, Medina-Lara MF, Martínez-Estévez M. 2020. Capítulo 4: Salinidad en plantas: caso *Capsicum. In* Rodríguez Buenfil IM, Ramírez Sucre MO, Ramírez Rivera EJ. (eds.), Metabolómica y cultivo del chile habanero (*Capsicum chinense* Jacq.) de la península de Yucatán. Centro de Investigación y Asistencia en Tecnología y Diseño del Estado de Jalisco A. C.: Guadalajara, México, pp: 55–70.

Franco-Navarro JD, Brumós J, Rosales MA, Cubero-Font P, Talón M, Colmenero-Flores JM. 2016. Chloride regulates leaf cell size and water relations in tobacco plants. Journal of Experimental Botany 67 (3): 873–891. https://doi.org/10.1093/jxb/erv502

Guzmán-Albores JM, Montes-Molina JA, Castañón-Gonzáles M, Abud-Archila M, Gutiérrez-Miceli FA, Ruíz-Valdiviezo VM. 2020. Effect of different vermicompost doses and water stress conditions on plant growth and biochemical profile in medicinal plant, *Moringa oleifera* Lam. Journal of Environmental Biology 41 (2): 240–246. http://doi.org/10.22438/jeb/41/2/MRN-1164

Hayat S, Hayat Q, Alyemeni MN, Wani A, Pichtel S, Ahmad AJ. 2012. Role of proline under changing environments a review. Plant Signaling and Behavior 7 (11): 1446–1466. https://doi.org/10.4161/psb.21949

Hoagland DR, Arnon DI. 1950. The water-culture method for growing plants without soil. University of California, College of Agriculture, California Agricultural Experiment Station: Berkeley, CA, USA. 32 p.

Isayenkov SV. 2012. Physiological and molecular aspects of salt stress in plants. Cytology and Genetics 46 (5): 302–318. https://doi.org/10.3103/S0095452712050040

Khan MIR, Iqbal N, Masood A, Khan NA. 2012. Variation in salt tolerance of wheat cultivars: role of glycine betaine and ethylene. Pedosphere 22 (6): 746–754. https://doi.org/10.1016/S1002-0160(12)60060-5

Mosa KA, Ismail A, Helmy M. 2017. Introduction to plant stresses. *In* Mosa KA, Ismail A, Helmy M. (eds.), Plant Stress Tolerance: An Integrated Omics Approach. Springer: Cham, Switzerland, pp: 1–19. https://doi.org/10.1007/978-3-319-59379-1

Munns R, Gilliham M. 2015. Salinity tolerance of crops – what is the cost? New Phytologist 208 (3): 668–673. https://doi.org/10.1111/nph.13519

Munns R, Tester M. 2008. Mechanisms of salinity tolerance. Annual Review of Plant Biology 59 (1): 651–681. https://doi.org/10.1146/annurev.arplant.59.032607.092911

Navarrete-Mapen RZ, Cristóbal-Alejo J, Uc-Várguez A, Reyes-Ramírez A, Tun-Suárez JM, Alvarado-López CJ. 2020. Graft response of *Capsicum chinense-Capsicum annuum* var. *glabriusculum* to Begomovirus in field. Mexican Journal of Phytopathology 38 (2): 226–238. https://doi.org/10.18781/r.mex.fit.2001-2

Nazar R, Iqbal N, Syeed S, Khan NA. 2011. Salicylic acid alleviates decreases in photosynthesis under salt stress by enhancing nitrogen and sulfur assimilation and antioxidant metabolism differentially in two mung bean cultivars. Journal of Plant Physiology 168 (8): 807–815. https://doi.org/10.1016/j.jplph.2010.11.001

Palchetti MV, Reginato M, Llanes A, Hornbacher J, Papenbrock J, Barboza GE, Luna V, Cantero JJ. 2021. New insights into the salt tolerance of the extreme halophytic species *Lycium humile* (Lycieae, Solanaceae). Plant Physiology and Biochemistry 163: 166–177. https://doi.org/10.1016/j.plaphy.2021.03.054

Pandey AK, Ghosh A, Rai K, Fatima A, Agrawal M, Agrawal SB. 2019. Biotic stress in plants a general outline. *In* Hasanuzzaman M, Nahar K, Fujita M, Oku H, Islam MT. (eds.), Approaches for Enhancing Abiotic Stress Tolerance in Plants. CRC Press: Boca Raton, FL, USA. 530 p.

Procacci S, Bojórquez-Quintal E, Platamone G, Maccioni O, Vecchio VL, Morreale V, Alisi C, Balducchi R, Bacchetta L. 2021. *Opuntia ficus-indica* pruning waste recycling: Recovery and characterization of mucilage from cladodes. Natural Resources 12 (4): 91–107. https://doi.org/10.4236/nr.2021.124008

Ruiz-Lau N, Bojórquez-Quintal E, Benito B, Echevarría-Machado I, Sánchez-Cach LA, Medina-Lara MF, Martínez-Estévez M. 2016. Molecular cloning and functional analysis of a Na^+-insensitive K^+ transporter of *Capsicum chinense* Jacq. Frontiers in Plant Science 7:1980. https://doi.org/10.3389/fpls.2016.01980

Shabala S, Pottosin I. 2014. Regulation of potassium transport in plants under hostile conditions: implications for abiotic and biotic stress tolerance. Physiologia Plantarum 151 (3): 257–279. https://doi.org/10.1111/ppl.12165

Wang CF, Han GL, Yang ZR, Li YX, Wang BS. 2022. Plant salinity sensors: Current understanding and future directions. Frontiers in Plant Science 13: 1–13. https://doi.org/10.3389/fpls.2022.859224

Yoshida K, Miki N, Momonoi K, Kawachi M, Katou K, Okazaki Y, Uozumi N, Maeshima M, Kondo T. 2014 Synchrony between flower opening and petal-color change from red to blue in morning glory, *Ipomoea tricolor* cv. Heavenly Blue. Proceedings of the Japan Academy, Series B 85 (6): 187–197. https://doi.org/10.2183/pjab.85.187

Agrociencia

PINE BARK RATIO IN SUBSTRATE FOR CITRUS ROOTSTOCK NURSERY PRODUCTION

Andrea Guadalupe **Pacheco-Chacón**[1], Ángel **Villegas-Monter**[1*], Libia Iris **Trejo-Téllez**[1], Hilda Araceli **Zavaleta-Mancera**[1], Guillermo **Calderón-Zavala**[1]

[1]Colegio de Postgraduados Campus Montecillo. Carretera México-Texcoco km 36.5, Montecillo, Texcoco, State of Mexico, Mexico. C. P. 56264.
* Author for correspondence: avillega@colpos.mx

ABSTRACT

Fruit tree cultivation requires rootstocks that are resistant to both biotic and abiotic stresses. The container size and substrate used are essential components in their development. Despite this, there are few studies on the impact of substrates on plant development in citrus trees under nursery conditions. This study aimed to assess the effects of three different ratios of pine bark in the substrate of three developing citrus rootstocks in a protected environment (greenhouse). The study conducted at the Cazones Nursery in Cazones de Herrera, Veracruz, Mexico, hypothesized that an increase in bark proportion would lead to a rise in the physical and chemical characteristics of the substrate and the development of the three rootstocks. The study utilized a completely randomized design with a factorial arrangement (A × B). Factor A (rootstock) had three levels: *Citrus aurantium* L. (Sour Orange), *C. volkameriana* Pasq. (Volkamer Lemon), and *C. sinensis* L. × *Poncirus trifoliata* L. (Citrage C-35). Factor B (substrate) had four levels (0, 10, 20, and 30 % pine bark), resulting in 12 treatments with 20 repetitions each. The physical and chemical characteristics of the substrates were determined, and the plant height and stem diameter were measured. Pine bark positively affected the apparent and real densities, total porosity, electrical conductivity, and cation exchange capacity. The growth dynamics of the three rootstocks were greater during the second and third months after grafting. When grown in substrates with a total porosity of 46–54 %, Volkamer Lemon, Citrage C-35, and Sour Orange rootstocks reached a plant height of 124.1, 110.5, and 84.5 cm, respectively; the stem diameter reached 6.9 mm. Porosity and cation exchange capacity increased when pine bark was added to the substrates. By evaluating the substrates and managing them proportionally, it is possible to obtain plants suitable for grafting (with 5 to 6 mm of stem) within four months after transplanting. This results in less time spent in the nursery and reduced costs.

Keywords: *Citrus*, growth dynamics, substrate characterization.

Citation: Pacheco-Chacón AG, Villegas-Monter A, Trejo-Téllez LI, Zavaleta-Mancera HA, Calderón-Zavala G. 2024. Pine bark ratio in substrate for citrus rootstock nursery production.
Agrociencia 58(3): 391-404.
https://doi.org/ 10.47163/agrociencia.v58i3.2959

Editor in Chief:
Dr. Fernando C. Gómez Merino

Received: February 02, 2023.
Approved: January 23, 2024.
Published in Agrociencia:
April 19, 2024.

INTRODUCTION

In Mexico, fruit tree production in nurseries has traditionally been carried out in open environments (Soto-Plancarte *et al*., 2015; Barra *et al*., 2016) without knowledge of the genetic origin of the rootstock and cultivar. This propagation method increases the risk of pest infestations and the spread of diseases. Production has been carried out in protected spaces (greenhouse) using substrates in containers to ensure phytosanitary quality and improve establishment and development in the field (Haase *et al.*, 2021).

The substrate can be of mineral origin (perlite, vermiculite, sand, tezontle, and tepetzil), organic origin (peat moss, compost, coconut fiber, rice, and coffee husks), or subproducts of industrial-forestry activities such as pine bark. To achieve the physical and chemical characteristics required for optimal plant development in containers, nurseries use three to four material mixtures. These are designed to provide the necessary porosity, electrical conductivity, moisture retention, particle size, pH, and cation exchange capacity (Ceccagno *et al.*, 2019).

In Mexico, due to its physical and chemical characteristics, peat is commonly used as the main component in forestry and ornamental nurseries, along with agrolite and vermiculite (Fascella, 2015). However, pine bark could replace peat, which is imported and extracted from natural sources (Urák *et al.*, 2017). Pine bark increases total porosity, water availability, and nutrient absorption when mixed with organic and mineral components. This favors root development and plant growth and reduces damage from pathogens by not providing ideal conditions for their development and proliferation (Altland *et al.*, 2014).

Rootstocks are utilized in fruit trees to hasten and enhance production, provide pest and disease tolerance, and improve fruit quality (Shafqat *et al.*, 2019). The agronomic and phytosanitary quality of the plant is critical for its subsequent behavior in the field. Similarly, the substrate and bag size components are crucial to plant development in the nursery (Correa-Moreno *et al.*, 2022). This study aimed to assess the impact of different proportions of pine bark in the substrate on the growth of three citrus rootstocks during the nursery stage under greenhouse conditions. The hypothesis is that increasing the proportion of pine bark will improve the physical and chemical characteristics of the substrate, leading to enhanced development of the rootstocks.

MATERIALS AND METHODS

Study area location

The research occurred between June 6 and December 6, 2021, in a protected area within the certified Cazones Plant-Producing Nursery (UPC 30033065/2016) in Cazones de Herrera, Veracruz, Mexico (20° 40’ N, 97° 28’ W, at an altitude of 10 m). The climate is tropical, warm, and subhumid, with an average annual rainfall of 1200 mm and an average yearly temperature of 25 °C. The experiment utilized plants from a certified seed-producing orchard (3033066/2016) at the Cazones nursery. The plants were germinated in plastic trays measuring 45 x 32 x 12 cm with a peat, perlite, and agrolite substrate in a 6:2:2 ratio (v:v:v). Each seed was sown individually, with the hilum facing down. When the plants had between two and four true leaves, they were transplanted into 120 mL tubes with the same substrate. Additionally, Osmocote Plus® fertilizer (15N-9P-12K) was added, which has a release period of 5 to 6 months.

Plant material and treatments

The study utilized three-month-old rootstock plants derived from seeds: 80 from Sour Orange (*Citrus aurantium* L.), 80 from Volkamer Lemon (*C. volkameriana* Pask.), and 80 from Citrange C-35 (*C. sinensis* L. × *Poncirus trifoliata* L.). The plants measured 21.26 cm and 1.78 mm, 27.14 cm and 2.03 mm, and 30.67 cm and 2.05 mm in height and stem diameter, respectively. Subsequently, they were transplanted into 4 L black polyethylene bags.

Four substrates were used in the experiment (Table 1). The first substrate was used as a control, which consisted of river valley soil (RV) and tepetzil (Tz) obtained from the region and used by the Cazones nursery. River valley soil is typically found in flood plains and has a lower silt content and a higher sand percentage. This soil contains goethite as the primary mineral (Arce and Rivera, 2018). Tepetzil has a discontinuous crystalline structure and high porosity due to the presence of clays (Vizcarra-de los Reyes, 2020). To increase the total porosity of the control, pine bark (PB) was added to substrates two, three, and four at 10, 20, and 30 %, respectively (Altland *et al*., 2014).

Table 1. Substrates used for the growth of three citrus rootstocks under nursery conditions.

Substrate	Components	Proportion (v:v)
1	C (RV:Tz)	3:1
2	C:PB	9:1
3	C:PB	8:2
4	C:PB	7:3

C: control; RV: river valley soil; Tz: tepetzil; PB: pine bark.

Management

During the transplanting process, the roots of the plants were trimmed to standardize their size and facilitate their placement into the bags using number 2 pruners (FELCO®, Switzerland). To prevent the spread of diseases, both the tool and the roots were disinfected using quaternary ammonium salts (1 g L^{-1}) (Timsen Biologics). Osmocote Plus® fertilizer (15N-9P-12K) with a 5–6 month release (2 g per plant) was applied. The pine bark used in this study was sourced from *Pinus patula* Schiede ex Schltdl. et Cham. and was composted for six months.

Four agrochemical applications were carried out during the research, as established by the Cazones Nursery. These included the application of 1) Raízal 400® (a root growth stimulant) at a concentration of 2 g L^{-1}, 15 days after transplanting; 2) DAP® [$(NH_4)_2HPO_4$, 18N-46P-00K, 2 g L^{-1}]; 3) Nitrofoska® (12N-8P-16K+3MgO, 2 g L^{-1}) applied 90 days after transplanting; and 4) Humic + N® (13N-7P-7K, 2 mL L^{-1}; Nasa Agro Organics) applied 150 days after transplanting. To avoid competition with the main shoot, lateral shoots were periodically removed. Irrigation was applied manually every four days using a graded container: 100 mL per plant in the first month, 350 mL per plant in the second month, and 600 mL per plant from the third to the sixth month.

Study variables

Plant height (cm) was measured from the surface of the soil of the stem to the apex, while diameter was measured at 10–15 cm above the soil surface every 28 days, starting from the first month after transplant until the end of the six-month experiment. Plant height and stem diameter were measured using a measuring tape (Truper® FH-8M, Mexico) and a caliper (Truper® Digital calibrator, Mexico), respectively.

Before the experiment, the physical characteristics of the substrate, including grain size, apparent density (Ad), true density (Td), total porosity (TP), and electrical conductivity (EC), were determined. Additionally, the chemical properties of the substrate, including pH and cation exchange capacity (CEC), were evaluated at the beginning and end of the research. These evaluations were conducted at the Soil Physics and Plant Nutrition laboratories of the Soil Science Program at the College of Postgraduates in Texcoco, State of Mexico, Mexico.

The grain size was determined on the four substrates using 500 g per sample and seven sieves with the following mesh sizes (mm): 6.36, 4.76, 3.36, 2, 1, 0.5, 0.25, and the receiver. The TP was determined by measuring the mass of water required to saturate a soil sample of a known total volume. The Ad was determined using the probe method, and the Td was determined using the water pycnometer method (Teixeira *et al.*, 2017); pH, EC, and CEC were measured using standard methods. The pH was measured using a potentiometer with a substrate-to-distilled-water ratio of 1:2 (v:v). EC was measured using a conductometer with the extract and saturation method, while CEC was measured using the ammonium acetate method (Page *et al.*, 1983).

Experimental design

A factorial arrangement A × B was utilized, where factor A represented the three rootstocks and factor B represented the four substrates. The substrates included three incorporating pine bark at 10, 20, and 30 %, and a control without pine bark. Each of the 12 resulting treatments had 20 repetitions (240 experimental units), distributed completely at random. The experimental unit consisted of one plant of each rootstock (described earlier) in a black, 4 L polyethylene bag. Analyses of variance and mean tests were conducted (Tukey, $p \leq 0.05$) for the variables plant height (cm) and stem diameter (mm). The data were processed using R-4.2.1® software.

RESULTS AND DISCUSSION

Physical characteristics of the substrates before the experiment

Grain size

The substrates used in the experiment exhibited varying grain sizes (Table 2), resulting in different porosity levels. This, in turn, directly affects the availability of water and oxygen for the roots of the established plants.

Table 2. Physical characteristics of the four substrates used to assess the effects of different ratios of pine bark on the development of citrus rootstocks, measured before the experiment.

Substrate*	Grain size (%) Mesh number							Receiver	Ad	Td	TP
	6.36	4.76	3.36	2	1	0.5	0.25		($g\ cm^{-3}$)		(%)
1	4.3	2.1	10.4	9.8	7.1	8.4	8.9	49.0	1.26	2.4	46
2	2.2	1.7	7.4	8.3	9.0	7.3	7.3	56.7	1.23	2.3	48
3	2.8	1.5	7.9	9.7	9.9	7.3	7.5	53.2	1.19	2.2	50
4	3.3	1.3	8.5	9.0	10.4	8.0	8.4	51.1	1.05	2.1	54

RV: river valley soil; Tz: tepetzil; PB: pine bark; Ad: apparent density; Td: true density; TP: total porosity. *Substrate 1: control, RV:Tz, 3:1 (v:v); substrate 2: C:CP, 9:1 (v:v); substrate 3: C:CP, 8:2 (v:v); substrate 4: C:CP, 7:3 (v:v); *n* = 4.

The addition of pine bark was projected to reduce the weight of particles in the receiver from substrate 1 to substrate 4 by 10 to 30 %. However, this trend was only observed from substrates 2 to 4, with substrate 1 having the lowest percentage in the receiver. This is because all meshes included a higher percentage of tepetzil particles, indicating that the pine bark particles were smaller. Schäfer and Lerner (2022) state that for container vegetable production, substrates should consist of particles between 3.5 and 8 mm. Smaller particles promote a greater release of ions into the solution and increase electrical conductivity.

The following results were obtained for coarse (≥ 2 mm), medium (0.5–2 mm), and fine particles (≤ 0.5 mm in weight) (Khamare *et al.*, 2022). Coarse particles: substrate 1 (17.3 %), substrate 2 (14.6 %), substrate 3 (14.8 %), and substrate 4 (16.4 %); medium particles: substrate 1 (16.9 %), substrate 2 (17.3 %), substrate 3 (17.2 %), and substrate 4 (19.4 %); and fine particles: substrate 1 (16.8 %), substrate 2 (11.3 %), substrate 3 (12.2 %), and substrate 4 (13.1 %). Given the lack of specific recommendations for citrus and the results of this study, the percentages generated could serve as a reference for developing the three rootstocks in nursery conditions.

Apparent (Ad) and true (Td) densities

According to Martínez and Roca (2011), the apparent density for plant production in pots should not exceed 0.75 g cm^{-3}. The values obtained for Ad in the substrates evaluated in this study exceeded the limit, possibly due to the inclusion of valley soil, known for its small particles. However, these values decreased with the addition of pine bark, as demonstrated in substrates 2 and 4. Additionally, the total porosity values increased (Table 2). The apparent density of a substrate depends on its particle size. An increase in apparent density can cause salinity and compaction in the substrate (Soto-Bravo and Betancourt-Flores, 2022).

According to Martínez and Roca (2011), the density of organic materials is around 1.45 g cm^{-3}, while minerals have a density of 2.65 g cm^{-3}. Values within this range are considered optimal. For the present study, the values vary from 2.1 to 2.4 g cm^{-3} (Table 2).

Total porosity (TP)

There are no specific recommendations regarding the total porosity of the substrate used in citrus plants. However, it has been suggested that for potted ornamentals and horticulture, values should range from 70 to 80 % (Sánchez-Cardozo and Díaz-Barrera, 2019). These values have been determined on peat, vermiculite, and perlite substrates. Fields *et al.* (2021) noted that pine bark TP varies depending on particle size. Substrates with particles ≤ 16 mm, ≤ 6.3 mm, and >12.6 mm show 78, 79, and 81 % TP, respectively. However, the values obtained (Table 2) are lower than those reported, possibly due to 50 % of the samples being composed of valley soil, which consists of small particles. On the other hand, substrate 1 (control) had a higher percentage of tepetzil particles in all meshes but had the lowest porosity percentage. This indicates that incorporating pine bark improves this parameter. Based on the observed response and the satisfactory development of the three rootstocks used, which were adequate for grafting four months after transplant, we can conclude that they require a 46 to 54 % TP to develop in a greenhouse environment.

Electrical conductivity (EC)

Furlani *et al.* (2009) recommend EC values of 2–2.5 dS m^{-1} for citrus rootstock growth. Bataglia *et al.* (2005) compared two fertilization management systems (fertigation and slow-release fertilization) in citrus rootstocks with a pine bark and vermiculite substrate. They found that values increased from 2 to 5 dS m^{-1} throughout the growth period due to salt accumulation from fertilization. The study shows a decrease in EC from the start to the end of the experiment for all substrates (Table 3), indicating that adding pine bark reduced EC. However, there were no significant effects on the development of the three rootstocks. To avoid toxicity problems, substrates should have a low EC and controlled nutrient concentration (Bataglia *et al.*, 2005).

Chemical characteristics of the substrates

pH

Arce and Rivera (2018) state that the optimal pH range for producing citrus rootstocks in pots ranges from 5.5 to 6, which maximizes nutrient availability. A slight increase in pH values for all substrates (Table 3) was registered at the end of the experiment, which can be attributed to irrigation, fertilization, and management. Regarding the incorporation of pine bark, no defined tendency was observed. Therefore, we can claim that it did not affect the pH of the substrates during the evaluation period. However, the pH values are above the range indicated as optimum for nutritional availability. This may be related to 50 % of the sample being composed of valley land, which characteristically has a neutral pH (Arce and Rivera, 2018). During plant development, substrate variations may occur due to management practices such as irrigation, fertilization, and differences between species (Schäfer *et al.*, 2008). It can be concluded that these pH values (Table 3) do not limit the development of the three rootstocks under nursery conditions in greenhouse environments.

Table 3. Chemical characteristics and electrical conductivity of four substrates used to assess the effects of different ratios of pine bark on the development of citrus rootstocks, at the beginning and the end of the experiment.

Rootstock	Substrate*	pH	EC (dS m^{-1})	CEC ($cmol_c$ kg^{-1})
		Before the experiment		
	1	7.69	3.06	16.5
	2	7.70	3.13	21.7
	3	7.70	3.86	20.7
	4	7.70	2.34	22.7
		After the experiment		
Sour Orange	1	7.92	2.55	20.71
	2	7.92	2.35	19.61
	3	7.95	2.18	22.30
	4	8.00	1.71	23.20
Volkamer Lemon	1	8.04	2.41	18.58
	2	8.05	2.35	20.12
	3	8.05	1.96	22.30
	4	7.93	1.98	23.73
Citrange C-35	1	7.89	3.54	20.18
	2	7.98	2.26	19.09
	3	7.96	2.29	18.05
	4	7.95	2.03	25.28

RV: river valley soil; Tz: tepetzil; PB: pine bark; EC: electrical conductivity; CEC: cation exchange capacity. *Substrate 1: control, RV:Tz, 3:1 (v:v); Substrate 2: C:CP, 9:1 (v:v); Substrate 3: C:CP, 8:2 (v:v); Substrate 4: C:CP, 7:3 (v:v); $n = 4$.

Cation exchange capacity (CEC)

The substrates generally had optimal CEC values, as Schäfer *et al.* (2008) reported, with values greater than 20 $cmol_c$ kg^{-1}. However, some exceptions existed, such as substrate 2 in Sour Orange, substrate 1 in Volkamer Lemon, and substrates 2 and 3 in C-35 (Table 3). The final CEC values were higher than the initial values, indicating that management practices positively impacted this variable. Altland *et al.* (2014) noted that the variation in results between substrates can be attributed to differences in the distribution of pine bark particle sizes. They evaluated the CEC in different particle sizes of pine bark and found that as the percentage of coarse particles (> 2 mm) decreases, CEC values also decrease, obtaining CEC values ranging from 21.3 to 46.5 $cmol_c$ kg^{-1} in pine bark. This coincides with the findings of this investigation, where substrates 2, 3, and 4 had the lowest percentages of particle size > 2 mm and the greatest CEC.

Plant height (cm) and stem diameter (mm)

Statistical differences ($p \le 0.05$) were observed for the plant height and stem diameter variables for the rootstock factor (Table 4). This finding is consistent with Girardi *et al.* (2007), who reported that Volkamer Lemon exhibits greater growth under

Table 4. Plant height and stem diameter of three citrus rootstocks grown in four substrates with different ratios of pine bark under nursery conditions.

Rootstock	Plant height (cm)	Stem diameter (mm)
Volkamer Lemon	118.05 a	7.8 b
Citrange C-35	108.56 b	8.2 a
Sour Orange	79.69 c	6.8 c
HMSD	4.28	0.23

*Means with different letters in each column indicate significant statistical differences (Tukey, $p \leq 0.05$). HMSD: honest minimum significant difference. $n = 20$.

nursery conditions. Volkamer Lemon showed greater plant height than C-35, which was superior to Sour Orange. Regarding stem diameter, C-35 surpassed Volkamer Lemon, superior to Sour orange (Table 4). According to Albrecht *et al.* (2020), C-35 and Volkamer Lemon reach the recommended stem diameter for grafting (5 to 6 mm) faster. This may be due to the higher number of stomata in both varieties (data not shown), which promotes photosynthesis (Xiong and Flexas, 2020).

Between months two and three, the three rootstocks displayed a significant increase in height (Figure 1). There was no significant effect on the four substrates during the rootstock development process. However, in substrate 4, Volkamer Lemon (124.1 cm for plant height and 7.9 mm for stem diameter) and Citrange C-35 (110.5 cm for plant height and 8.4 mm for stem diameter) exhibited the most growth. In substrate 1, Sour Orange showed the least growth, with a plant height of 84.5 cm and a stem diameter of 6.9 mm (Figures 1 and 2). Meanwhile, Volkamer Lemon displayed the most growth and consistent development throughout the evaluation period.

The growth dynamics of the tested rootstocks were similar to those of the 'Cravo' rootstock when grown in a pine bark-based substrate (de Almeida *et al.*, 2012). However, they were not similar to the Swingle Citrumelo, which exhibited the most growth during months four and five after transplanting (Sauer-Liberato *et al.*, 2021). The three rootstocks grown in all substrates reached the recommended diameter for grafting (5 to 6 mm) four months after transplanting, as previously indicated (Albrecht *et al.*, 2020). Transplanting is one of the most challenging stages in a nursery, as the roots are not fully functional in the first few weeks; the substrate plays a crucial role in preventing water stress. Among the citrus varieties evaluated, Volkamer Lemon and C-35 exhibited the most growth, reaching the suggested diameter for grafting in a shorter time than Sour Orange. This could reduce production costs.

Arrieta-Ramos *et al.* (2014) conducted a study on the effect of root malformation on the growth of Citrange Carrizo, Swingle Citrumelo (C.P.B. 4475), and Volkamer Lemon in an open environment. The substrate used was a mixture of river valley soil, vermicompost, and agrolite in a 3:1:1 ratio (v:v:v). At the time of transplanting, the plants were four months old. Height and stem diameter were evaluated when the plants were 10 months old. Volkamer Lemon reached a height of 86 cm and a stem

Agrociencia 2024. DOI: https://doi.org/10.47163/agrociencia.v58i3.2959
Scientific article

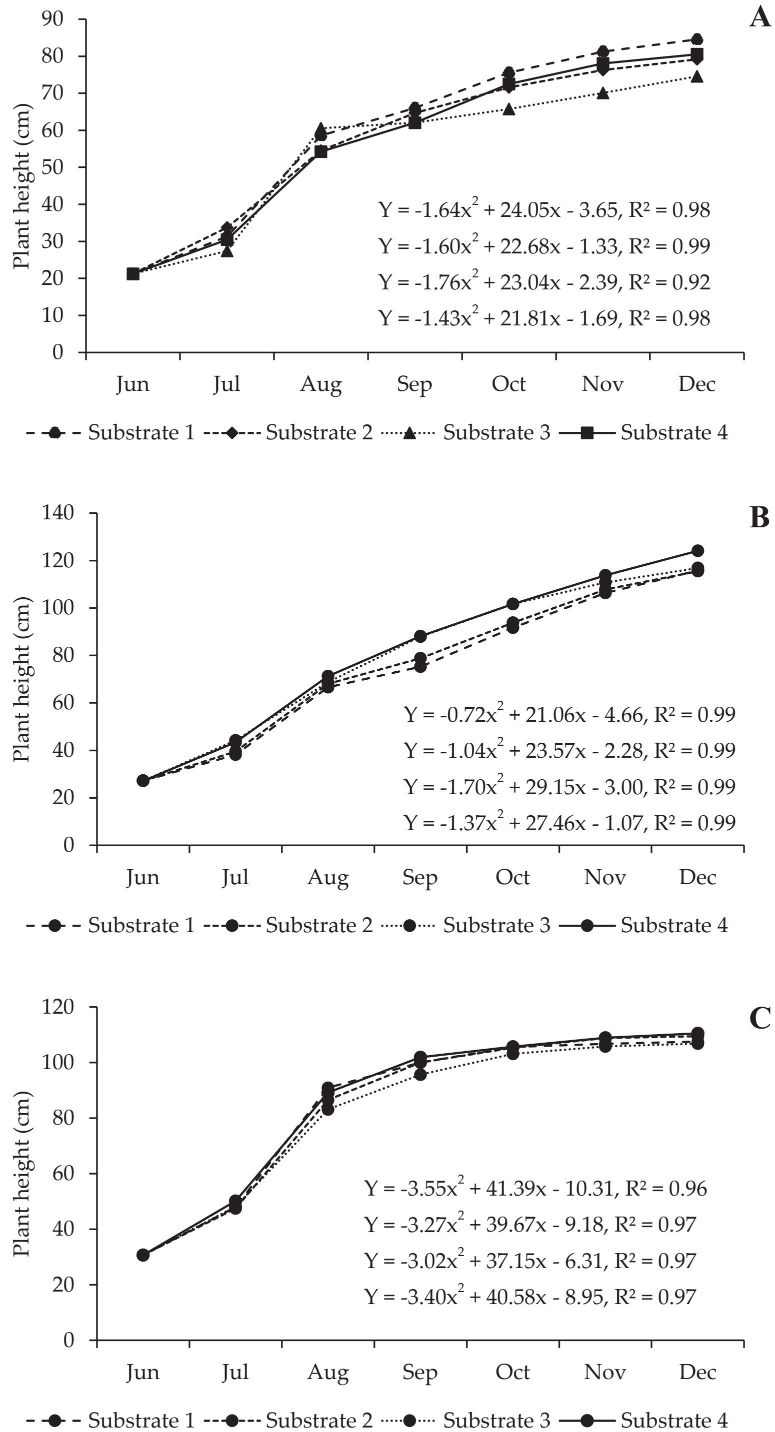

Figure 1. Growth changes of citrus plants grown in four substrates with different ratios of pine bark under nursery conditions. A: Sour Orange; B: Volkamer Lemon; C: Citrange C-35. Substrate 1: control, RV:Tz, 3:1 (v:v); Substrate 2: C:CP, 9:1 (v:v); Substrate 3: C:CP, 8:2 (v:v); Substrate 4: C:CP, 7:3 (v:v). RV: river valley soil; Tz: tepetzil; PB: pine bark. *n* = 20.

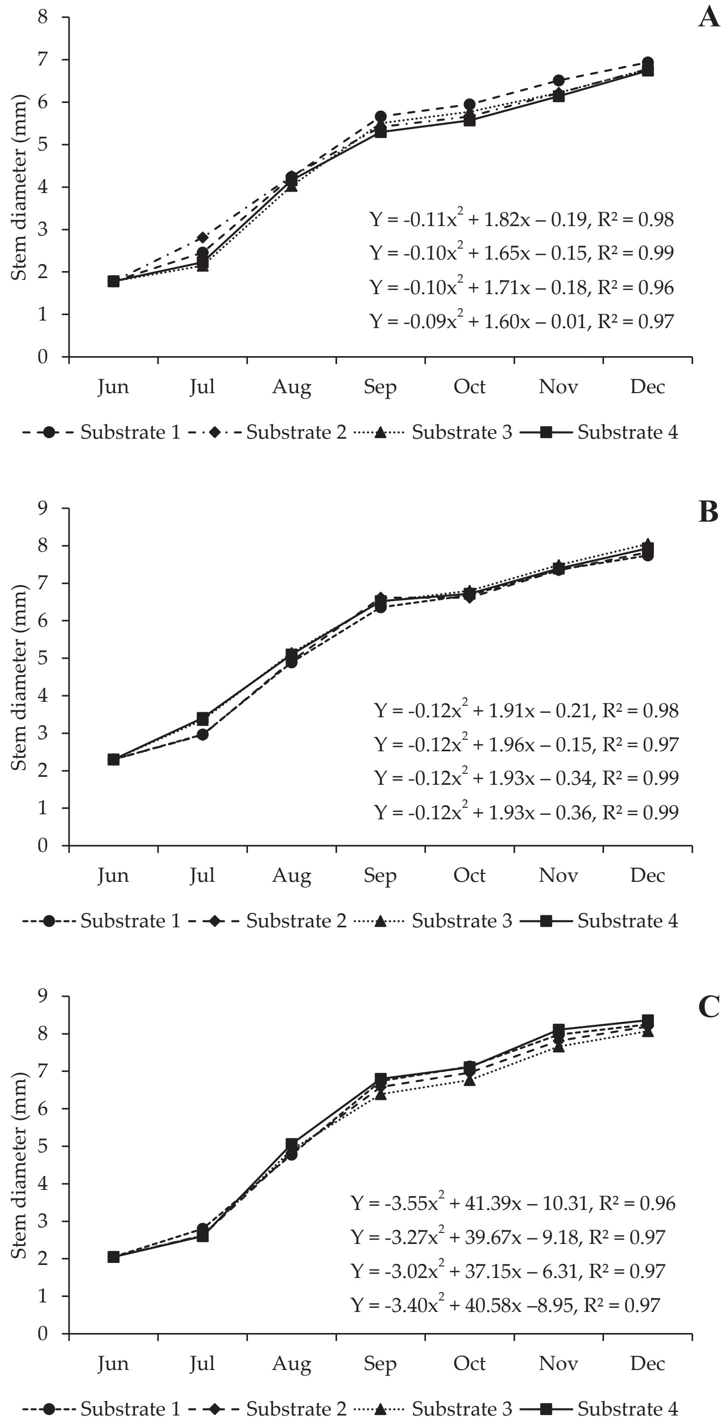

Figure 2. Stem diameter changes of citrus plants grown in four substrates with different ratios of pine bark under nursery conditions A: Sour Orange; B: Volkamer Lemon; C: Citrange C-35. Substrate 1: control, RV:Tz, 3:1 (v:v); Substrate 2: C:CP, 9:1 (v:v); Substrate 3: C:CP, 8:2 (v:v); Substrate 4: C:CP, 7:3 (v:v). RV: river valley soil; Tz: tepetzil; PB: pine bark. $n = 20$.

diameter of 7.5 mm. In our study, six months after transplanting, Volkamer Lemon reached a height of 124 cm and a diameter of 7.9 mm. This indicates that the plants obtained were suitable for grafting four months prior. The results demonstrate the significance of substrate effects, management, and environmental conditions on plants grown in greenhouse environments.

Arce and Rivera (2018) evaluated the effect of substrates and fertilizer on Citrange Carrizo and Citrumelo Swingle rootstocks. They used five substrates for their growth: 1) Promix and sand in a 1:1 ratio (v:v) (control); 2) Promix + sand + coconut fiber; 3) Promix + sand + coffee compost; and 4) Promix + sand + rice husk. The latter three substrates were in a 1:1:1 ratio (v:v:v). After six months, the 'Swingle' plants ranged from 31.1 to 49 cm and had a stem diameter of 3 to 4.25 mm, while Carrizo reached a plant height between 40.3 and 66.7 cm and stem diameters between 2.66 and 4 mm. These results are lower than those reported here. The substrate composed of rice husk had a negative influence on the growth of both rootstocks. 'Carrizo' showed the best development in substrate 3, while 'Swingle' did not exhibit significant differences in any substrate except for rice husk. This highlights the importance of assessing the physical and chemical characteristics of substrates for each rootstock.

The analysis of plant height (cm) and stem diameter (mm) means in the interaction of the studied factors (Rootstock × Substrate) showed that Volkamer Lemon had greater growth than C-35 and Sour Orange in all substrates, specifically in substrate 4. Conversely, Citrange C-35 in substrate 4 had the greatest stem diameter (Table 5). Sour

Table 5. Plant height (cm) and stem diameter (mm) of three citrus rootstocks for (Rootstock × Substrate) interaction, grown in four substrates with different ratios of pine bark under nursery conditions.

Rootstock × Substrate*	Plant height (cm)	Stem diameter (mm)
VL in S1	115.8 ab	7.7 b
VL in S2	115.5 ab	7.8 b
VL in S3	116.9 ab	8.0 b
VL in S4	124.1 a	7.9 b
C-35 in S1	107.5 b	8.3 b
C-35 in S2	109.5 b	8.2 b
C-35 in S3	106.8 b	8.1 b
C-35 in S4	110.5 b	8.4 a
NA in S1	84.5 c	6.9 c
NA in S2	79.2 c	6.8 c
NA in S3	74.6 c	6.8 c
NA in S4	80.5 c	6.7 c
HMSD	12.0	0.65

LV: Volkamer Lemon; C-35: Citrange C-35; AO: Sour Orange; S: substate; RV: river valley soil; Tz: tepetzil; PB: pine bark. *S1: Control, RV:Tz, 3:1 (v:v); S2: C:CP, 9:1 (v:v); S3: C:CP, 8:2 (v:v); S4: C:CP, 7:3 (v:v). Means with different letters in the same column are statistically different (Tukey, $p \leq 0.05$). HMSD: honest minimum significant difference. $n = 20$.

Orange had the least height and stem diameter, regardless of the substrate. Sauer-Liberato *et al.* (2021) found that Swingle Citrumelo (*Citrus paradisi* Macf. × *Poncirus trifoliata* L.) had a plant height of 106.8 cm and a stem diameter of 8 mm after five and a half months of being transplanted into 4 L polyethylene bags. The substrate was composed of varying proportions of peat, vermiculite, and rice husk. Similar results were obtained in this investigation with Volkamer Lemon, which had a plant height of 124 cm and a stem diameter of 7.9 mm six months after transplanting. The observed differences in rootstock height are attributed to the species, as evidenced by the growth dynamics of the three rootstocks (Figures 1 and 2).

CONCLUSIONS

The growth of Volkamer Lemon, Citrange C-35, and Sour Orange trees was enhanced in substrates with 46 to 54 % total porosity. After four months of transplanting, the trees were suitable for grafting. Adding pine bark at 10, 20, and 30 % of the substrate improved its apparent and real physical densities, electrical conductivity, total porosity, and cation exchange capacity. Under nursery conditions, Volkamer Lemon, Citrange C-35, and Sour Orange trees can grow in substrates with pH values ranging from 7.7 to 8.05.

ACKNOWLEDGEMENTS

The authors thank the National Humanities, Science and Technology Council (Consejo Nacional de Humanidades, Ciencia y Tecnología - CONAHCyT) for providing the funds for A.G.P.-C's Master's Degree.

Additionally, the authors thank the Cazones Nursery for providing the necessary resources to conduct this research in a greenhouse environment.

REFERENCES

Albrecht U, Bodaghi S, Meyering B. 2020. Influence of rootstock propagation method on traits of grafted sweet orange trees. HortScience 55 (5): 729–737. https://doi.org/10.21273/hortsci14928-20

Altland JE, Locke JC, Krause AR. 2014. Influence of pine bark particle size and pH on cation exchange capacity. HortTechnology 24 (5): 554–559. https://doi.org/10.21273/horttech.24.5.554

Arce S, Rivera D. 2018. New media components and fertilization to accelerate the growth of citrus rootstocks grown in a greenhouse. Horticulturae 4 (2): 10. https://doi.org/10.3390/horticulturae4020010

Arrieta-Ramos BG, Villegas-Monter A, Rodríguez-Mendoza MN, Luna-Esquivel G. 2014. Desarrollo en vivero de portainjertos de cítricos con malformación de raíz. Revista Chapingo Serie Horticultura 20 (1): 29–39. https://doi.org/10.5154/r.rchsh.2012.06.034

Barra PJ, Inostroza NG, Mora ML, Crowley DE, Jorquera MA. 2016. Bacterial consortia inoculation mitigates the water shortage and salt stress in avocado (*Persea americana* Mill.) nursery. Applied Soil Ecology 111: 39–47. https://doi.org/ 10.1016/j.apsoil.2016.11.012

Bataglia OC, Quaggio JA, Ferreira de Abreu M, Ronchini-Boaventura PS. 2005. Nutrient uptake and leaching on citrus nursery production in substrate with two fertilizer management programs. Acta Horticulturae 697: 281–284. https://doi.org/10.17660/ActaHortic.2005.697.34

Ceccagno H, Dutra-de Souza PV, Schäfer G, Demari-Avrella E, Sidnei-Fior C, Schwarz SF. 2019. Potential of *Pinus* sp. needles for use as substrate conditioners in the production of 'Trifoliata' rootstock in greenhouses. Revista Chapingo Serie Horticultura 25 (1): 5–16. https://doi.org/10.5154/r.rchsh.2018.02.003

Correa-Moreno DL, Martínez MF, Acosta G. 2022. Sustratos para la producción de portainjertos en ambiente protegido. *In* Martínez MF, Murcia-Riaño N, Barreto-Rojas JA, Acosta-Herrera GH, Jaramillo-Laverde A, Correa-Moreno DL, López-Galé Y, Rodríguez-Mora D, Kondo T, Palacios-Joya L, Beltrán-López HD. (eds.), Bases Tecnológicas para la Producción de Material de Siembra de Alta Calidad de las Especies Cítricas para Colombia. Corporación Colombiana de Investigación Agropecuaria (AGROSAVIA): Mosquera, Colombia, pp: 87–105. https://doi.org/10.21930/agrosavia.manual.7405682

de Almeida LVB, Sales-Marinho C, De Almeida-Muñiz R, Cordero de Carvalho AJ. 2012. Disponibilidade de nutrientes e crescimento de porta-enxertos de citros fertilizados com fertilizantes convencionais e de liberação lenta. Revista Brasileira de Fruticultura, Jaboticabal 34 (1): 289–296. https://doi.org/10.1590/S0100-29452012000100038

Fascella G. 2015. Growing substrates alternative to peat for ornamental plants. *In* Asaduzzaman M. (ed.), Soilless Culture: Use of Substrates for the Production of Quality Horticultural Crops. Intech Open: London, UK, pp: 47–51. https://doi.org/10.5772/59596

Fields JS, Owen JJS, Altland JE. 2021. Substrate stratification: Layering unique substrates within a container increases resource efficiency without impacting growth of shrub rose. Agronomy 11 (8): 1454. https://doi.org/10.3390/agronomy11081454

Furlani PR, Zanetti M, Bataglia OC. 2009. Citrus nursery production in soilless culture. Acta Horticulturae 843: 255–260. https://doi.org/ 10.17660/ActaHortic.2009.843.33

Girardi EA, Mourão F de AA, Kluge RA. 2007. Effect of seed coat removal and controlled-release fertilizer application on plant emergence and vegetative growth of two citrus rootstocks. Fruits 62 (1): 13–19. https://doi.org/10.1051/fruits:2006044

Haase DL, Bouzza K, Emerton L, Friday JB, Lieberg B, Aldrete A, Davis AS. 2021. The high cost of the low-cost polybag system: A review of Nursery Seedling Production Systems. Land 10 (8): 826. https://doi.org/10.3390/land10080826

Khamare Y, Marble SC, Altland JE, Pearson BJ, Chen J, Devkota P. 2022. Effect of substrate stratification without fine pine bark particles on growth of common nursery weed species and container-grown ornamental species. HortTechnology 32 (6): 491–498. https://doi.org/10.21273/horttech05113-22

Martínez PF, Roca D. 2011. Sustratos para el cultivo sin suelo. Materiales, propiedades y manejo. *In* Flórez RVJ. (ed.), Sustratos, Manejo del Clima, Automatización y Control en Sistemas de Cultivo sin Suelo. Editorial Universidad Nacional de Colombia: Bogotá, Colombia, pp: 37–77.

Page AL, Miller RH, Keeney DR. 1983. Methods of soil analysis, part 2: Chemical and microbiological properties. Soil Science Society of America: Madison, WI, USA. https://doi.org/10.2134/agronmonogr9.2.2ed

Sánchez-Cardozo J, Díaz-Barrera L. 2019. Evaluación de sustratos elaborados a partir de residuos celulósicos para la propagación de flores ornamentales y hortalizas. Bioagro 31 (1): 45–54.

Sauer-Liberato EM, Leonel S, Souza JMA, Napoleão GM. 2021. Substrate mixing formulations for citrus nursery management. Nativa 9 (5): 500–507. https://doi.org/10.31413/nativa.v9i5.12777

Schäfer G, de Souza PVD, Koller OC, Schwarz SF. 2008. Physical and chemical properties of substrates to cultivate seedling of citrus rootstocks. Communications in Soil Science and Plant Analysis 39 (7–8): 1067–1079. https://doi.org/10.1080/00103620801925547

Schäfer G, Lerner BL. 2022. Physical and chemical characteristics and analysis of plant substrate. Ornamental Horticulture 28 (2): 181–192. https://doi.org/10.1590/2447-536X.v28i2.2496

Shafqat W, Jaskani MJ, Maqbool R, Khan AS, Ali Z. 2019. Evaluation of citrus rootstocks against drought, heat and their combined stress based on growth and photosynthetic pigments. International Journal of Agriculture and Biology 22 (5): 1001–1009.

Soto-Bravo F, Betancourt-Flores A. 2022. Evaluación de metodologías para determinar las características físicas de un sustrato de fibra de coco. Agronomía Costarricense 46 (2): 29–45. https://doi.org/10.15517/rac.v46i2.52044

Soto-Plancarte A, Santillán-Mendoza R, Fernández-Pavía SP, Ploetz RC, Freeman S, Ortega-Arreola R, Osuna-Ávila P, Velázquez-Monreal JJ, Rodríguez-Alvarado G. 2015. Mango nurseries as sources of *Fusarium mexicanum*, cause of mango malformation disease in central western Mexico. Phytoparasitica 43 (4): 427–435. https://doi.org/10.1007/s12600-015-0471-4

Teixeira PC, Kangussu-Donagemma G, Fontana A, Gerlades-Teixeira W. 2017. Manual de métodos de análise de solo (Third edition). Embrapa: Brasilia, Brazil. 574 p.

Urák I, Hartel T, Gallé R, Balog A. 2017. Worldwide peatland degradations and the related carbon dioxide emissions: the importance of policy regulations. Environmental Science and Policy 69: 57–64. https://doi.org/10.1016/j.envsci.2016.12.012

Vizcarra-de los Reyes M de los A. 2020. Lecciones para la recuperación de saberes tradicionales: Las tapias de la región de Tepeyahualco, México. Journal of Traditional Building. Architecture and Urbanism 1: 434–446.

Xiong D, Flexas J. 2020. From one side to two sides: the effects of stoma distribution on photosynthesis. New Phytologist 228 (6): 1754–1766. https://doi.org/10.1111/nph.16801

VOLUME 58, NUMBER 3 | APRIL 1 - MAY 15, 2024 | MEXICO